

ALMA MATER STUDIORUM
UNIVERSITA' DI BOLOGNA

SCUOLA DI INGEGNERIA E ARCHITETTURA
Sede di Forlì

Corso di Laurea in
INGEGNERIA MECCANICA
Classe L-9

ELABORATO FINALE DI LAUREA
in
Tecnologia Meccanica

MIXED ALLOY CHIP EXTRUSION

CANDIDATO

Gianmarco Santoro

RELATORE

Prof. Dr-Ing. Lorenzo Donati

CORRELATORI

Prof. Dr-Ing. Dr-Ing. A. Erman Tekkaya

Ing. Johannes Gebhard

Ing. Felix Kolpak

Anno Accademico 2017/2018

Abstract

Il seguente lavoro di tesi è stato svolto presso il dipartimento “IUL” (Institut für Umformtechnik und Leichtbau, Technische Universität Dortmund); le relative sperimentazioni sono state compiute nei laboratori del dipartimento.

Lo scopo della tesi è quello di analizzare ed ottimizzare il processo di riciclo diretto dei trucioli, il materiale di scarto delle lavorazioni alle macchine utensili. Questo processo, già studiato sotto diversi aspetti, è noto come Chip Extrusion. Tale metodo di riciclo dell'alluminio secondario consiste estrudere direttamente i trucioli, senza rifonderli, ottenendo profili con qualità simili a quelle delle estrusioni con billette standard. In particolare, si vuole ottenere profili con buone caratteristiche utilizzando trucioli di differenti leghe di alluminio, con forme e dimensioni diverse. Si procederà classificando diverse tipologie di trucioli, per poi compattarli a freddo – a temperatura ambiente – in billette pronte da estrudere. La lavorazione tramite deformazione plastica a caldo – ad alta temperatura – indicherà parametri di processo utili per poter realizzare prodotti finali con ottime proprietà estetiche-strutturali. Questo processo è molto interessante a livello industriale, dove i trucioli di leghe differenti vengono accumulati insieme dopo le operazioni alle macchine utensili, tuttavia vi sono ancora diverse difficoltà che rendono la realizzabilità del processo nelle industrie complicato.

La lavorazione dell'alluminio secondario comporta un abbondante risparmio di energia nella trasformazione di questo materiale, presentando un risparmio energetico del 95% rispetto alla produzione dello stesso da minerale –Bauxite– da cui si ricava l'alluminio primario. Come presentato dalle varie ricerche sul Chip Extrusion, vi è un ulteriore risparmio energetico nell'estrudere gli scarti di lavorazione direttamente, senza rifonderli, in un'ottica ambientalista e di riciclo, principale motivazione della ricerca attuata.

Oltre ad annoverare le varie problematiche dell'estruzione partendo dallo stato dell'arte della stessa, e più in particolare del Chip Extrusion, la ricerca effettuata ha l'obiettivo di collaudare le ottimali combinazioni di leghe ed i relativi parametri di processo al fine

di ottenere i profili desiderati.

Parallelamente alle sperimentazioni è implementata una simulazione FEM -Finite Element Method- con software HyperExtrude e MatLab, i cui codici siano in grado di emulare processi di estrusione con differenti caratteristiche e parametri, che diano risultati simili ai dati verificabili sperimentalmente.

In qualità di relatore autorizzo la redazione della tesi in lingua straniera e mi faccio garante della qualità – anche linguistica– dell’elaborato.

Prof. Ing. Lorenzo Donati

A handwritten signature in black ink, appearing to read "Lorenzo Donati". It is written over two horizontal lines, with the first line being longer than the second.

In cooperation with:

Institut für Umformtechnik und Leichtbau, Technische Universität Dortmund.



Institute of
Forming Technology and
Lightweight Construction

Table of contents

<i>Introduction</i>	- 9 -
<i>1.1 ALUMINIUM</i>	- 11 -
<i>1.2 EXTRUSION PROCESS</i>	- 14 -
<i>1.2.1 Overview</i>	- 14 -
<i>1.2.2 The process</i>	- 16 -
<i>2.1 CHIP EXTRUSION -state of the art-</i>	- 27 -
<i>3.0 MIXED ALLOY CHIP EXTRUSION</i>	- 37 -
<i>3.1 Introduction</i>	- 37 -
<i>3.2 Aim & motivation</i>	- 38 -
<i>3.3 Experimentation & numerical analysis</i>	- 39 -
<i>3.3.1 Work plan</i>	- 39 -
<i>3.3.2 Classifying chips & Mixing</i>	- 40 -
<i>3.3.3 Compaction & extrusion</i>	- 44 -
<i>3.3.4 Tensile, Hardness tests & Microstructure analysis</i>	- 51 -
<i>3.3.5 Test data elaboration</i>	- 56 -
<i>3.3.6 FEM Simulation</i>	- 75 -
<i>4.1 OUTCOMES ANALYSIS & CONCLUSIONS</i>	- 84 -
<i>5.1 OUTLOOKS</i>	- 88 -
<i>References</i>	- 90 -

Introduction

The following thesis was elaborated at the IUL department (Institut für Umformtechnik und Leichtbau, Technische Universität Dortmund), the related experiments were carried out in the department's laboratories.

The aim of the investigation is to characterize the behaviour of billets composed of different aluminium alloys chips, shape and size. The billets were processed by plastic deformation in order to obtain useful parameters to make final products with good aesthetic-structural characteristics. This is made possible by direct recycle of chips with plastic deformation processes, in specific with a chip-based hot extrusion process. This technique is very interesting at an industrial level where the chips coming from various aluminium alloy machining procedures are accumulated together.

The classic secondary aluminium production process by re-melting already saves 95% of energy in comparison to primary aluminium production from mineral (Bauxite). As previously shown from several researches on Chip Extrusion, there is a higher energy saving through direct extrusion of chips and scraps pre-compacted in chip-based billets without re-melting.

The research has the objective of testing the optimal combination of process parameters for different mixes of alloys in order to obtain the desired profiles; at the same time a FEM (Finite Element Method) simulation is implemented with HyperExtrude and MatLab software. The code is expected to describe processes with different parameters and give results similar to the experimental ones.

1.1 Aluminium

Nowadays aluminium is the second most important metal for industrial application, after steel, with a world production of about 57.6 million tons per year that grows up at a rate of 0.3%. Italy is the second country in Europe in production, after Germany, with a growth rate of 7.5% in 10 years [20].

Aluminium can be created from Bauxite (primary aluminium), a mineral which contains 50–60% of AL_2O_3 (Aluminium Oxide), or by re-melting aluminium scraps (secondary aluminium). The energy required to produce secondary aluminium is about 5–10% the amount needed in primary aluminium process, but an average material loss of 20–50% cannot be avoided due to the high surface area to volume ratio of scraps contaminated by oxide, lubricant, etc. Moreover, melting can be skipped by direct chip extrusion, thus permit to save more energy and material. This is getting more attention due both to the increasing demand for the material and to the stricter governmental policies on climate change [21].

Aluminium alloys have attractive properties, which depend on purity and grain size of the material, as instance light weight, high mechanical strength, corrosion resistance, high electrical conductivity, workability, weldability, aesthetic qualities, non-magneticity, non-toxicity. These are the reasons why it is attractive to several engineering application, form electronical to aerospace, automotive and more.

Some average characteristics are:

- Density at 20°C [ρ]: 2,66–2,85 g/cm³
- Crystal Structure: FCC
- Brinell Hardness: 2,75
- Hardness Vickers: 50
- Melting point: 660°C
- Fracture strength [R_m]: 75–360 MPa
- Strength strain [ϵ]: 50–55%
- White-silver Aesthetic
- Young modulus [E]= 62–70 GPa

-
- Poisson ratio: 0.33

Aluminium can be mixed with several materials to realize different type of alloys, which are internationally classified as series:

- 1xxx: pure aluminium alloy with minimum 99% of Al on weight, for packaging and chemical application.
- 2xxx: [Avional] Al-Cu alloy, with 0.7–6.8% of Cu, after heat treatment has great mechanical properties, in high load mechanical and aerospace application.
- 3xxx: Al-Mn alloy, with 0.05–1.8% of Mn, is used in strain hardening processes, for pipelines and kitchen tools.
- 4xxx: Al-Si alloy, with 0.6–21.5% of Si, has low thermal dilatation, for high temperature applications.
- 5xxx: [Peraluman] Al-Mg alloy, with 0.2–6.2% of Mg, has high corrosion resistance and low weight, for naval applications.
- 6xxx: [Anticorodal] Al-Si-Mg alloy, with 1% of Si and Mg, is the most used aluminium alloy covering the 90% of the actual commercial demand, it has great workability qualities and it could reach high mechanical properties, for example after T6 thermal treatment. It is the most important alloy to product profiles by extrusion processes.
- 7xxx: [Ergal] Al-Zn-Mg alloy, with 0.8–12% of Zn, similar to the Avional, has good mechanical properties, for high solicited parts.
- 8xxx: Al-Li (or other elements), are mixed aluminium alloys.
- 9xxx: experimental aluminium alloys.

The indication of the mechanical and thermal treatment completes the designation:

- F: raw, no special control has been performed.
- O: annealed, is the lowest strength, highest ductility temper.
- W: solubilized, is applied to homogenize the microstructure.

- H: work hardened, plus a number which indicates the grade of work hardening.
- T: indicates the types of thermal treatment, plus a number which specifies its grade; the two most relevant are:
 1. T4: solution heat treated, and naturally aged to a substantially stable condition.
 2. T6: solution heat treated then artificially aged, to attain the best mechanical properties.

Figure 1.1.1 shows usual thermal cycle in an extrusion.

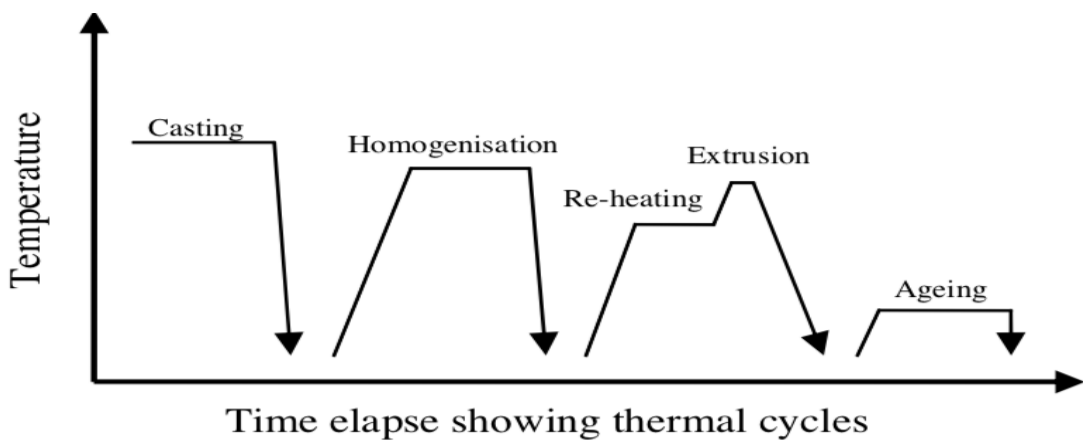


Fig. 1.1.1 Thermal cycle of a typical extrusion, T6 tempering^[1]

Aluminium alloys can be divided in non-heat treatable alloys (3, 4, 5xxx series) and treatable (2, 6, 7xxx series) and in two families: for foundry and for plastic deformation processes.

In extrusion process the most used aluminium alloy is 6xxx series, since it has great workability and high mechanical properties, due to thermal treatment with aging which creates Mg_2Si precipitates, where Mg and Si are under 1,5% on weight.

1.2 Extrusion process

1.2.1 Overview

Manufacturing processes can be divided into:

1. Forming, such as casting, sintering of materials powder;
2. Plastic deformation, like rolling, extrusion, forging;
3. Machining, like cutting, turning, milling;
4. Treatment, such as thermal treatments, galvanization, electromagnetic forming;
5. Jointing, as welding, bolting, riveting.

The processes of plastic deformation can be additionally divided into two categories:

- I. Bulk processes such as forging, extrusion, rolling and drawing.
- II. Metal sheet deformation processes such as bending, deep drawing and stretching.

These processes can also be classified according to the working temperature:

- I. Hot processes: working temperature is higher than the recrystallization temperature of the material, i.e. 0.4÷0.5 times the melting point of the material and over.
- II. Cold processes, working temperature is lower than the recrystallization temperature.

In hot processes the working temperature changes the flow stress of the material, hence the resistance to deformation is lower compared to cold processes.

Plastic deformation is convenient for high production volumes so that the cost of the tools can be divided on the entire fabrication. The requirement of high metallurgical integrity also makes forming processes appropriate. Design and optimization of plastic deformation procedures require a good knowledge of mechanical properties such as metal flow stress, heat transfer mechanism, and also technological data on the lubrication, working temperature and tools design.

Nowadays extrusion is one of the most relevant system for light metal alloys forming. Figure 1.2.1 shows two complex-shapes aluminium profiles.



Fig. 1.2.1 complex-shapes aluminium extruded profiles ^[33]

Extrusion can be carried out at room temperature or at high temperatures, depending on the alloy and method in question. In the majority of the cases hot processes are preferred, which work at a temperature over the recrystallization of the material, so tools are maintained in a range of 350°C to 580°C, as to reach less working pressure due to lower flow stress of the material.

Figure 1.2.2 shows the classic steps of extrusion process.

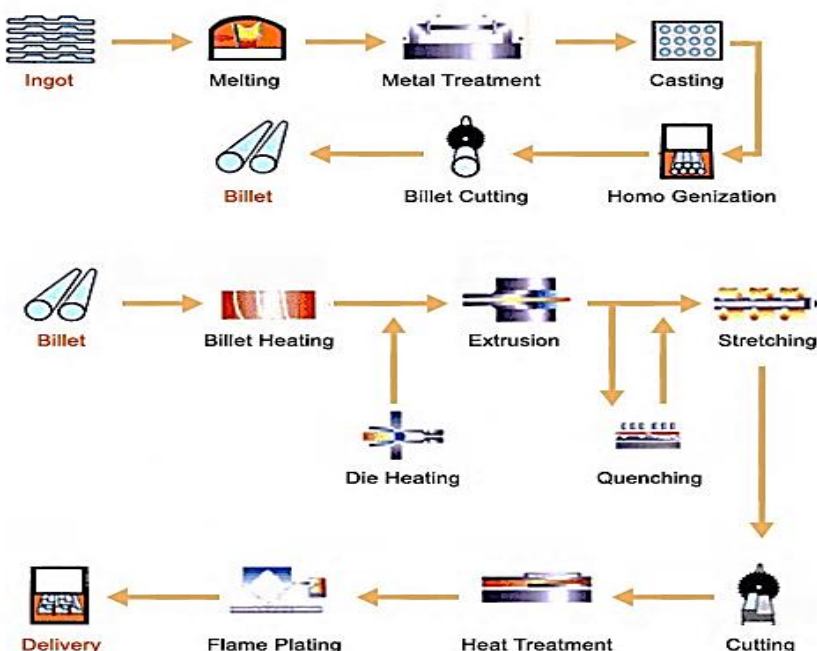


Fig. 1.2.2 Classic Al-extrusion process phases ^[3]

1.2.2 The process

Extrusion technology permits the production of medium and big batches of constant-cross-section profiles, characterised by complex shapes, geometry, limited tolerances on dimensions and aesthetic qualities perfectly following the philosophy of “Design for Assembly” [22].

Figure 1.2.3 shows a typical extrusion hydraulic press and its components.

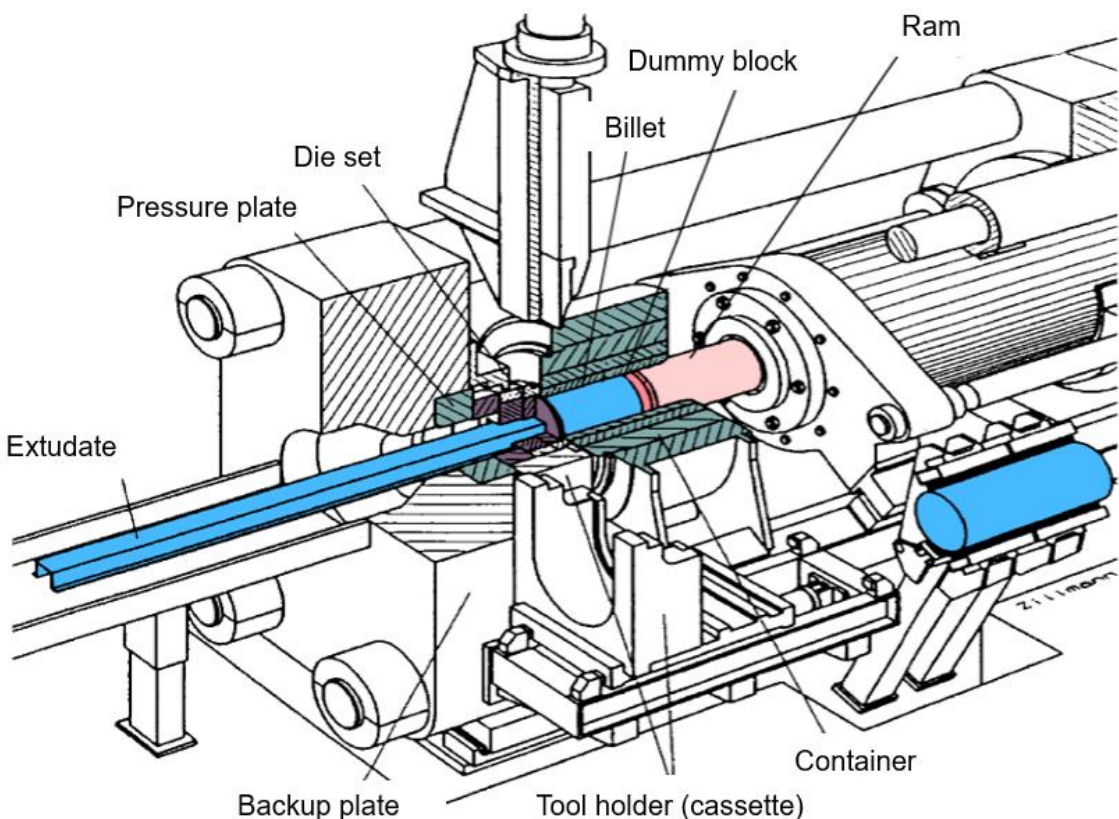


Fig. 1.2.3 schematic diagram of an extrusion press [32]

In this process a piston strongly loads a billet which squeezes through a die resulting in the final shape of the artefact.

Figure 1.2.4 shows two direct extrusions processes, one for continuous profile usually produced with a flat-face die and one for hollow sections profiles typically made with a port-hole die.

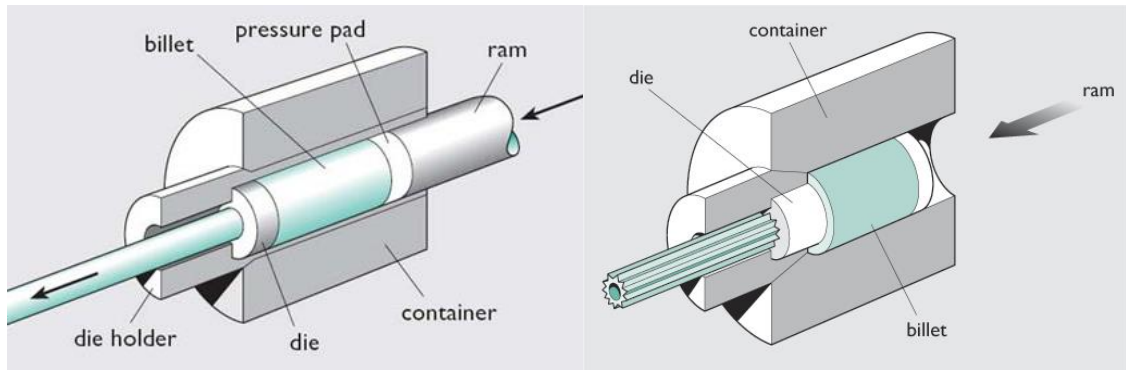


Fig. 1.2.4 direct extrusion of profile with full and hollow sections ^[5]

This technology can be performed in two ways: by direct extrusion (also known as forward) and indirect extrusion (or backward). The first one is the most performing as far as industrial functions are concerned, it will be better examined in this paper.

Figure 1.2.5 displays direct and indirect extrusion processes. Figure 1.2.6 explains the different loads involved by hydraulically or mechanically driven ram on the billet through an intermediate dummy block, in the two processes.

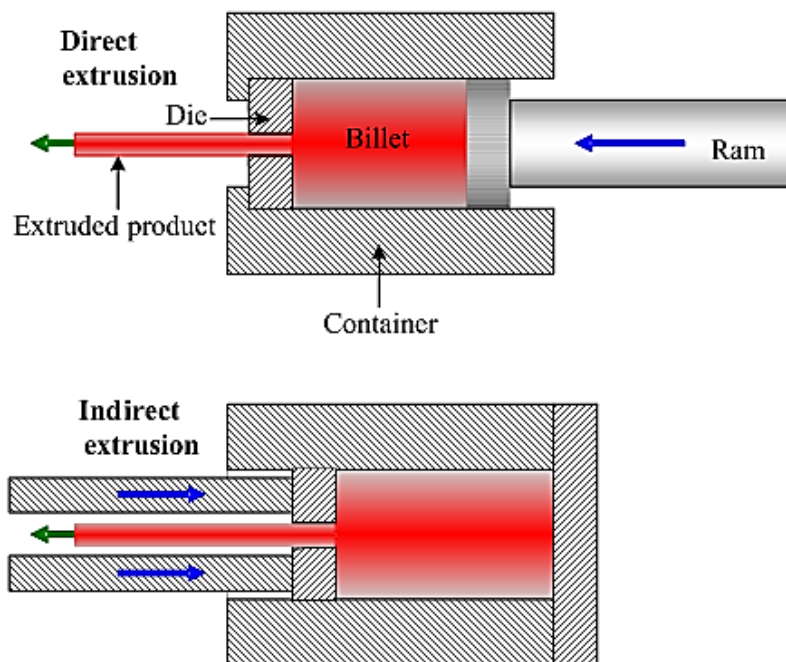


Fig. 1.2.5 Direct & Indirect extrusion ^[6]

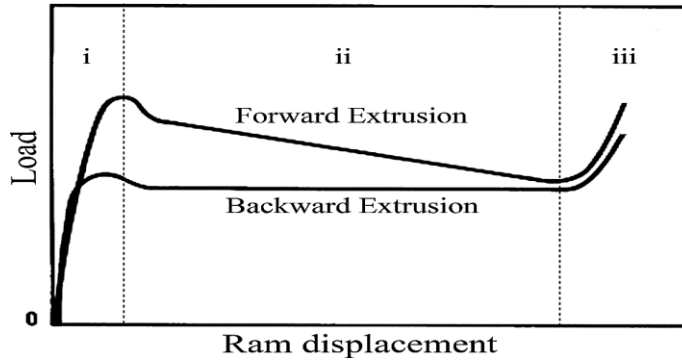


Fig. 1.2.6 Load vs Ram in Forward and Backward extrusion [7]

The typical load–ram stroke history can be divided into 3 stages:

- I. In the direct extrusion process the load initially grows very fast in order to overcome friction in the container, then a further increase occurs when the plasticization process starts.
- II. From this point on there is a constant work used for the deformation of the billet and another work that decreases with the stroke to overcome the friction and the shear stress in the container in the dead metal zone. Figure 1.2.7 displays Dead Metal zone.
- III. Continuing to extrude up to touch the die, the load would have a new increase as the extrusion material tends to flow mostly in the radial instead the axial direction.

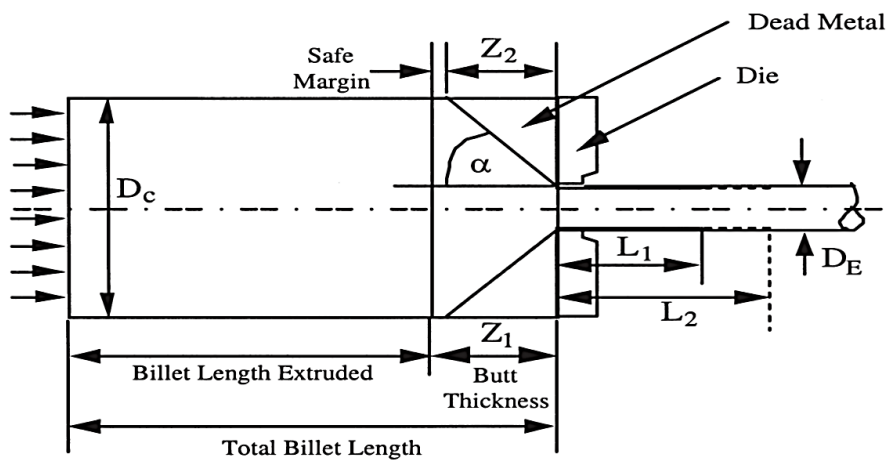


Fig. 1.2.7 Dead Metal zone and other parameters [8]

Normally, the industrial processes are “billet to billet”, when the piston reach the end of the stroke a new billet is loaded in order to have a continues profile

extruded as long as the runout table placed after the die, that normally is circa 60 meters long, as showed in Figure 1.2.8.



Fig. 1.2.8 Extruded profiles on table^[9]

Between a billet surface and another a certain amount of impurities and oxides accumulates, especially in hot processes, because of oxidation, lubricant, etc. This leads to a low-quality welding part in the edge, which will be discarded at end of the procedure. Usually this part is elongated due to the tendency of aluminium to stick to the tool steel and container, consequently the material velocity is higher in the centre of the billet.

The extrusion tooling includes die, mandrel, dummy block, ram head, the welding chamber of the die and auxiliary tooling such as container and ram. The die is the most important component in an extrusion machine, which is the most stressed part due to several factors: high loads, low-cycles fatigue, creep, high temperature gradients, etc, hence it has to be continually replaced.

Figure 1.2.9 shows a die assembly diagram.

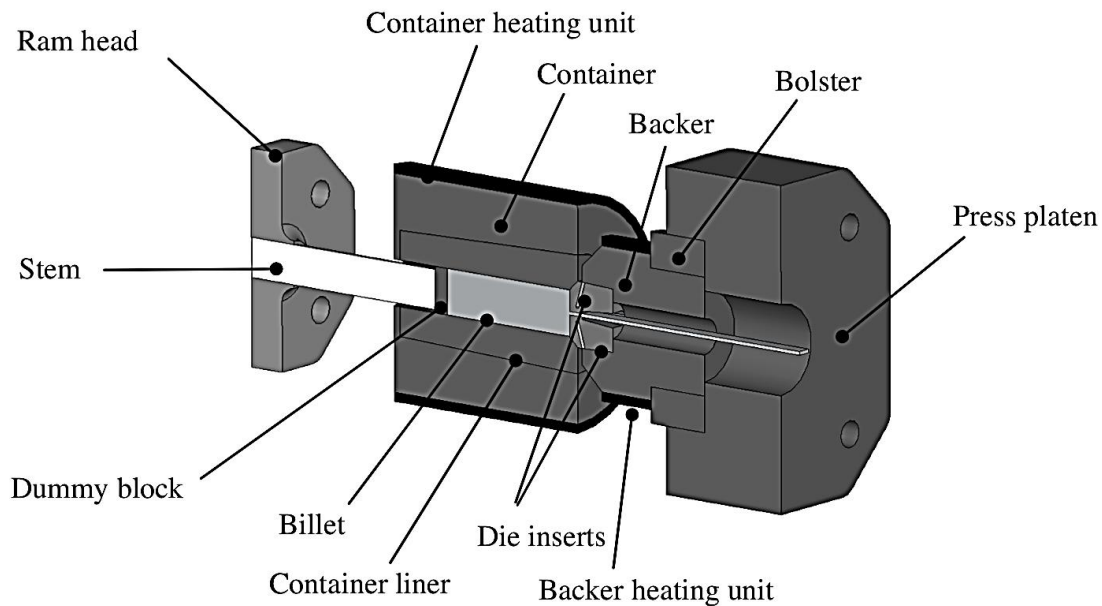


Fig. 1.2.9 A typical die tooling assembly ^[1]

There are different types of dies according to the kind of extruded profile:

- Flat-face die: is a simple die with the required shape of the extruded, it is used for solid section profiles.
- Port-hole die: similar to bridge and spider die, is composed by a welding chamber, where the welding process happens leading to the presence of longitudinal seam weld lines on the profile, and a matrix allowing to produce semi-hollow and hollow profiles.

Figure 1.2.10 illustrates these dies, figure 1.2.11 a solid and a hollow profile.



Fig. 1.2.10 porthole die, spider die and bridge die ^[10]

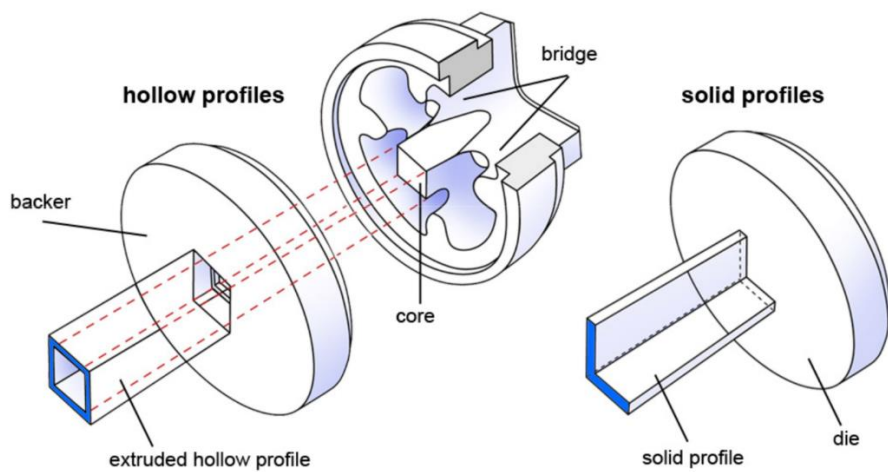


Fig. 1.2.11 port-hole die & flat-face die [11]

Process parameters depend on:

- Shape of the profile;
- Material stress flow [$\bar{\sigma} = \bar{\sigma}(\bar{\varepsilon}, \dot{\varepsilon}, T)$];
- Friction at the material–tool interface;
- Billet container vs profile section areas ratio;

Shape and ratio depend on the kind of billet used and customer necessity, thus are fixed variables. The shear friction depends on lubricant conditions and it is calculated by the relation $\tau = \mu\sigma_n$ (Coulomb friction) or, when normal stress is higher than yield stress of the material, $\tau = m\bar{\sigma}/\sqrt{3}$ (sliding friction or shear friction model or Tresca model) where friction factor is equal to 1 for non-lubricant extrusion and $0.1 \leq m \leq 0.4$ in lubricant extrusion (usually with molten glass).

Figures from 1.2.11 to 1.2.14 give some examples.

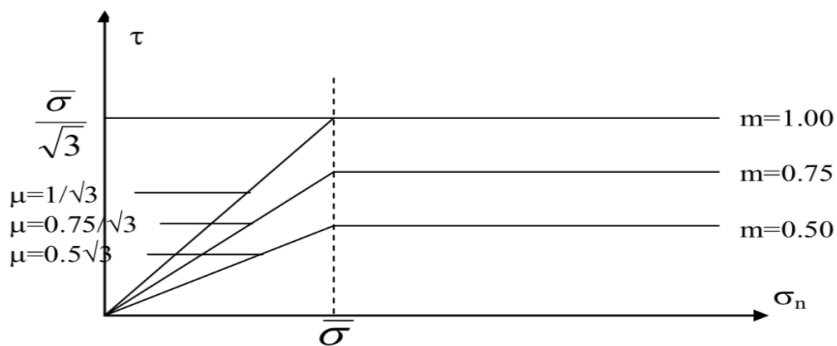


Fig. 1.2.11 m factor dependence on pressure [12]

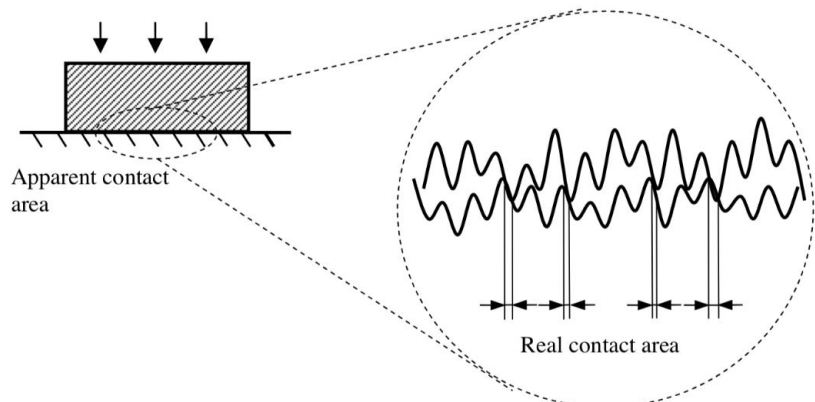


Fig. 1.2.12 Contact area model in Coulomb situation ^[1]



Fig. 1.2.13 A full plastic contact condition ^[1]

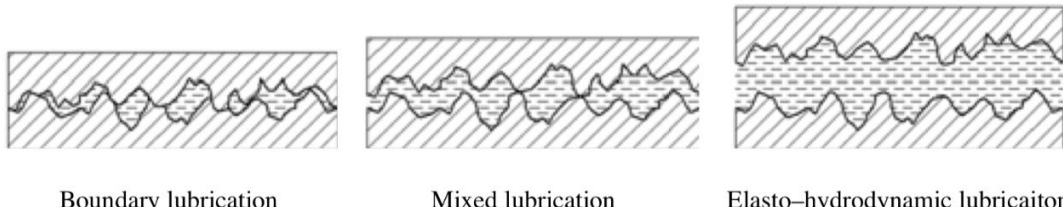


Fig. 1.2.14 Lubrication regimes ^[1]

The metal stress flow is function of preheating temperature and tools temperature, strain, strain rate (depending on ram speed), kind of die, type of material and its microstructure. An approximated formula for the extrusion pressure required is $p = a \ln \frac{A_{in}}{A_{out}} + b$ where p is pressure at the stroke, A_{in} is the cross-section area of the billet section, A_{out} is the cross-section area of the profile section, a is an index of the die complexity and b is constants of the lubricant working conditions.

Through induction heating, heat is developed in the surface of the billet; the penetration depth depends on the frequency used and also on the permeability and electrical conductivity of the alloy. Induction heating gives a very uniform

temperature distribution around the billet circumference. Uniformity of heating in gas furnaces depends on the type of furnace and heat transfer. The heat is not developed internally but is transferred to the billet surface by radiation and convection. This can cause large temperature gradients.

A complex thermal distribution arises when hot extrusion process starts, which is caused by:

1. Deformation in the area in front of the die;
2. Friction between billet and container and by shearing at the dead metal zone;
3. Heat conduction to the tooling and billet;
4. Heat generation by friction through the die.

Figure 1.2.15 displays billet temperature profile, figure 1.2.16 shows the process window that allows not to incur into different problems.

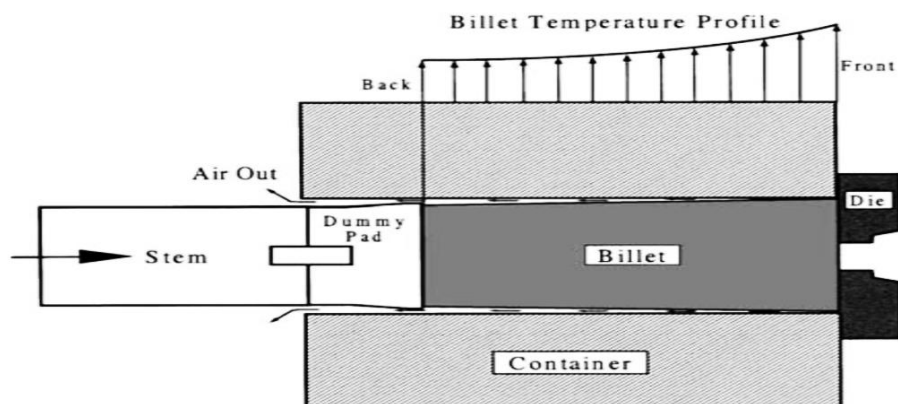


Fig. 1.2.15 Temperature distribution on the billet [8]

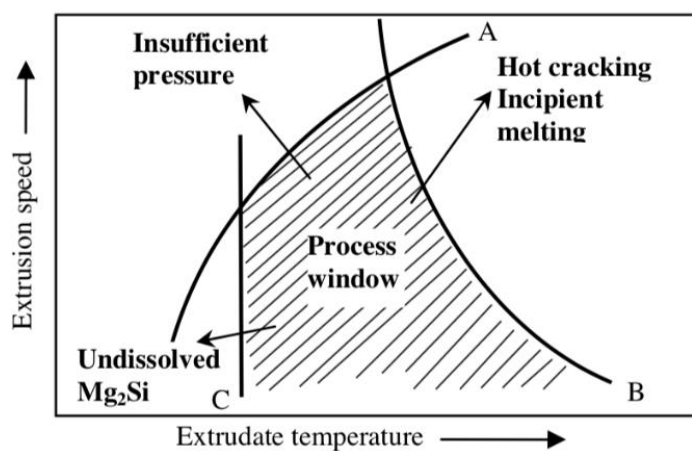


Fig. 1.2.16 Speed-Temperature process window [1]

Different flow patterns are possible, as figure 1.2.17 shows:

- S: homogeneous flux, there is not friction between billet and container.
- A & B: there is friction in both container and die interfaces and an extended dead-metal zone is formed.
- C: Flow pattern C is obtained with billets having inhomogeneous material properties.

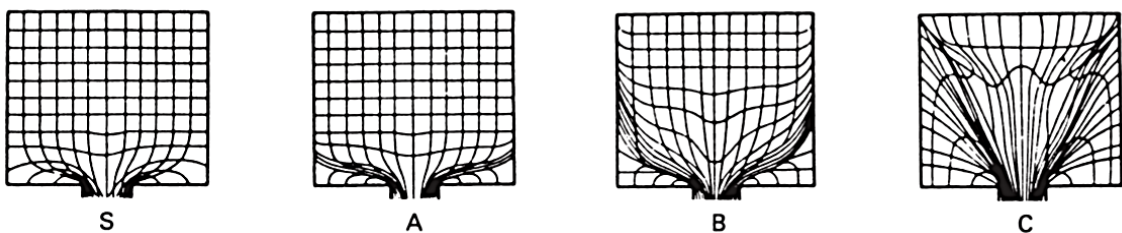


Fig. 1.2.17 Different flow patterns [8]

The alloy microstructure: grains orientation and size, usually clearly separated by distinct boundaries, depend on the thermo-mechanical transformation undertaken. The phenomena which change the microstructure are:

1. Geometric Dynamic Recrystallization: grains deform principally in extrusion direction, so they are thin in radial direction (deformation texture). This leads to an anisotropic extruded material: higher strength in extrusion direction. In the shear zone the deformation is higher compared to the core zone, which allows the formation of coarse grain due to recrystallization on the profile surface (peripheral coarse grain zone).

Figures 1.2.18 shows a schematic structure alteration process.

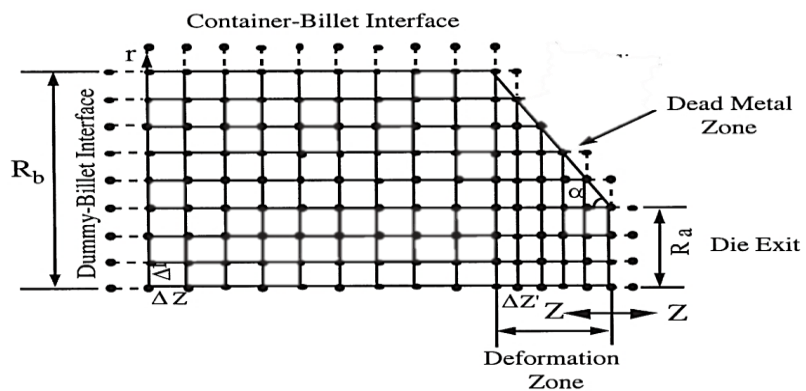


Fig. 1.2.18 Reticular deformation process [1]

2. Dynamic Recrystallization: During the extrusion plastic deformation, a certain part of the energy creates some reticular crystallographic defects, usually dislocations, as it happens in strain hardening where dislocation moves interaction with other dislocation or physical obstacles, in figure 1.2.19.

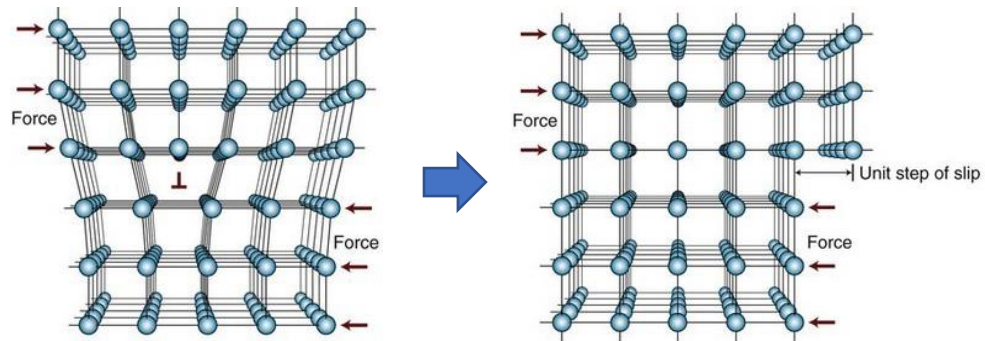


Fig. 1.2.19 Dislocation process ^[13]

3. Static Recrystallization: similar to the dynamic, is a nucleation starting from the core of the material and zones with high dislocation density, it could be avoided by ensuring rapid cooling of the profile after the die.
4. Recovery: a reorganization of defects after extrusion.
5. Grain Growth: the last part of energy stored during process makes big grain grow up incorporating the small ones as shown in figure 1.2.20.

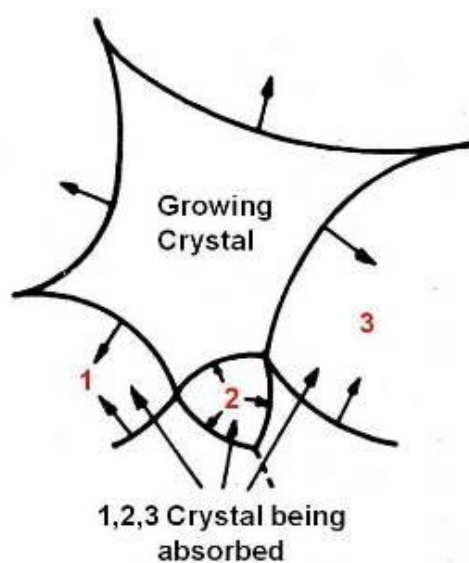


Fig. 1.2.20 Grain Growth ^[14]

It is important to highlight that microstructure, strain hardening, grain size, solid solution, dispersion and precipitation strengthening are the direct responsible of the mechanical properties of the processed material as shown in figure 1.2.21.

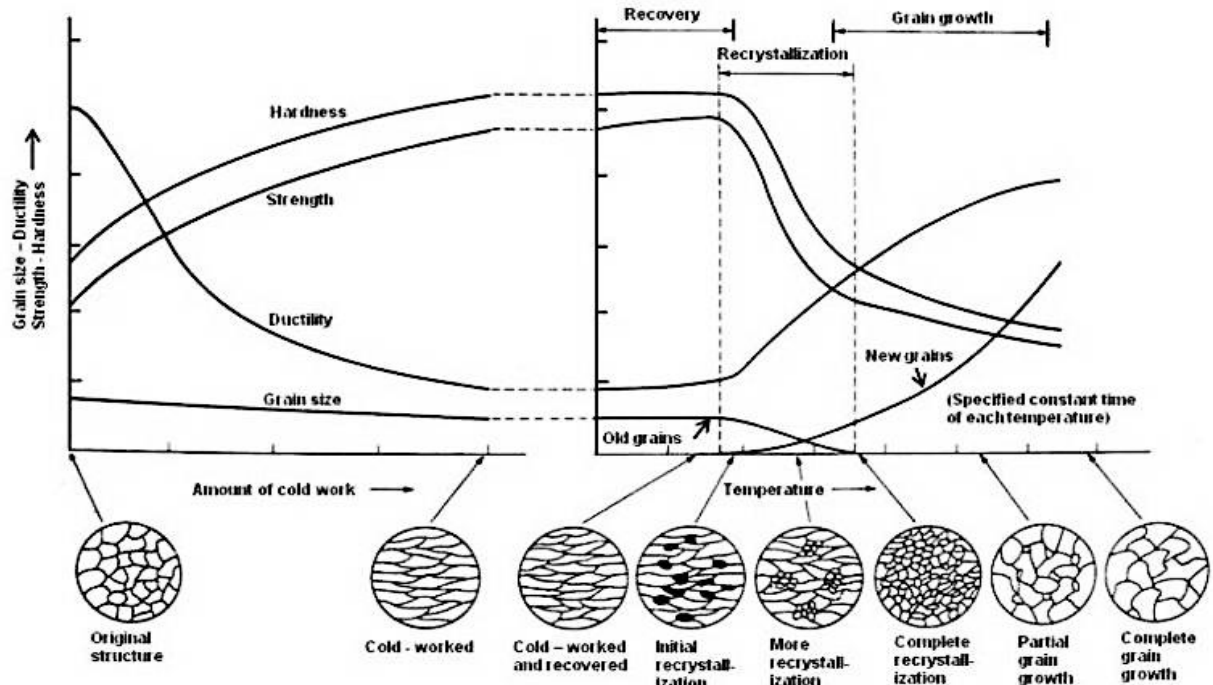


Fig. 1.2.21 Schematic effects on properties and microstructure. [14]

2.1 Chip Extrusion -state of the art-

A reduction of CO₂ emissions is becoming gradually more important to prevent global warming caused by polluting gas. A decrease in energy consumption in every field of industrial processes, as well as transportation and production engineering, is necessary.

In manufacturing technology, normally, the major amount of energy is used to produce the primary material instead of cutting and forming processes.

In this case, aluminium could be made from first melting after mining, by refining Bauxite ore into aluminium oxide and subsequently electrolyse to transform oxides in pure aluminium; or secondary material, made from melting scraps after recycling, which needs 90% less energy compared to primary material production.

In case of hot extrusion, approximately 90–93% of the energy used is needed for the material production, 3–7% for thermal treatment, and only 1% for the forming process^[1]. These data indicate that from an economic and ecologic point of view, increasing the recycling of aluminum alloy machining chips into finished products by direct hot extrusion is a favorable approach to intensify the energy efficiency and to overcome the problem of material loss due to oxidation during re-melting, up to 20–25%^[17]. On the other hand, the mechanical properties of the chip-based products are often inhomogeneous during an extrusion process and inferior compared to those based on cast-billets. The use of hot extrusion to recycle aluminum scraps has many benefits compared to other solid-state recycling processes, as short process time and ability to produce complex geometries for industrial applications.

Figure 2.1.1 and fig. 2.1.2 show direct extrusion steps.

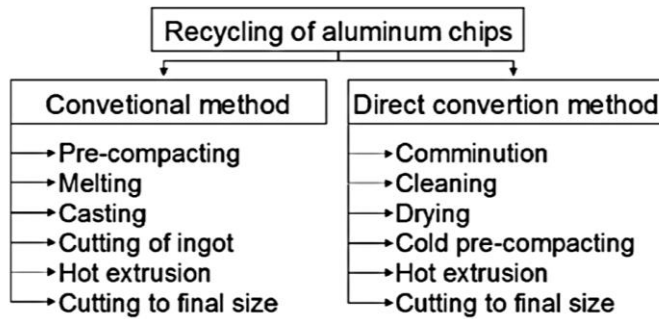


Fig. 2.1.1 Recycling methods conventional vs direct [15]



Fig. 2.1.2 Direct method steps [16]

This process was introduced as “direct conversion method”: metal scraps were separated according to their composition, than cleaned, chopped, compacted and hot extruded between 500°C and 550°C [34]. This technology enables the chips to be relatively quickly and easily recycled with low environmental impact and high recycling rate.

This method was investigated from many points of view: it was studied in different type of extrusion processes and the resulting profiles were compared with cast billets extruded products. The influences of extrusion process parameters on profiles qualities were examined, such as the die design, temperature of process, extrusion ratio, ram speed, shape of chips, surface area/volume ratio of the chips and kind of alloy treated, billet compaction procedure, welding mechanism problems like oxides breaking and resulting necessity (high pressure and strain acting on the chips, high deformation during the process, etc.), the prediction of the result by FEM codes, etc.

This innovative process of direct conversion of aluminium scraps by hot

extrusion of chip-based billet is rising good prospective for the future. Moreover, the whole process requires several intermediate operations (sorting, cleaning, drying, compacting, etc.) causing these technologies to be inadequate for the actual industrial necessities.

Scraps come from a big amount of waste material in machining operations cycles. Chips are characterised by irregular geometry with high surface/volume ratio, thus comports high presence of contaminants (i.e. lubricant fluids and oxide layers), low density, and non-uniform composition, causing this metal scrap recycling difficult.

The most used aluminium is AA-6060, which is a ductile alloy that often leads to adhesive wear and a continuous chip formation when machined.

In figure 2.1.3 are presented two examples of chips.

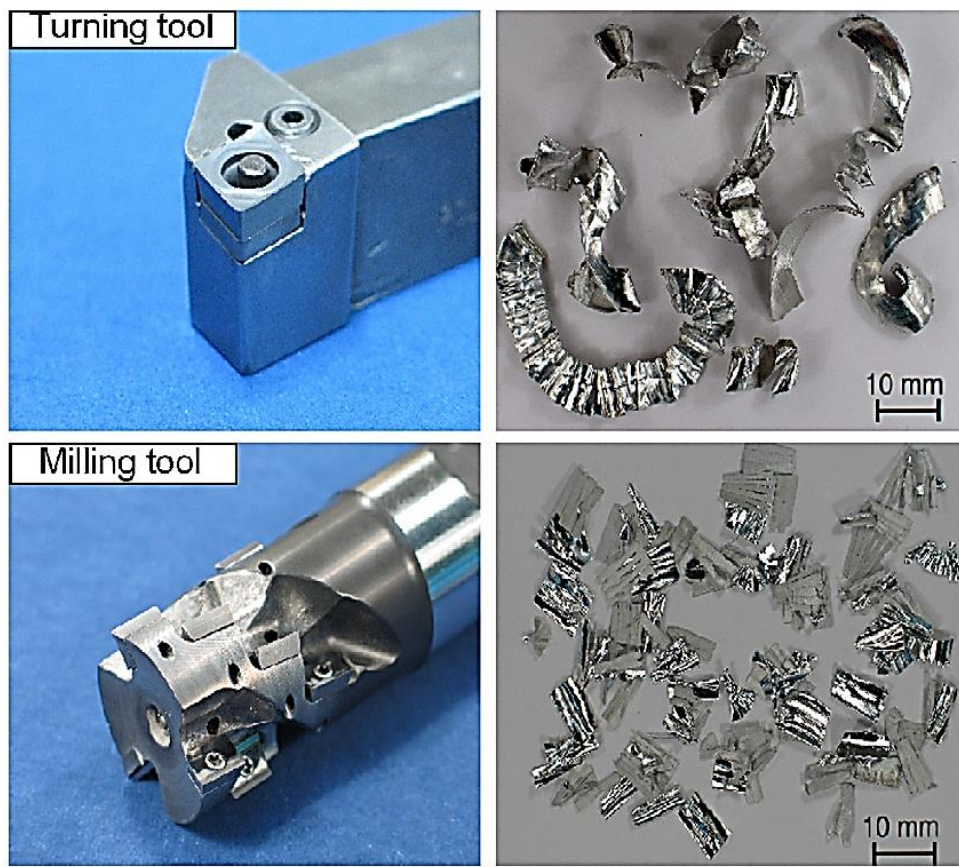


Fig. 2.1.3 Turned & milled chips. [15]

To reach sound bonding of the virgin chips material and therefore favorable mechanical properties of the chip-based products is necessary that surface

oxides layers fracture [17]. This is caused by large plastic deformation and high compressive stress due to some critical factors: shear, pressure, temperature and strain affecting the chips during the extrusion process, and also by chips size and compaction parameters, shape of the die, extrusion rate, pre-heating temperature and in/out cross-section ratio.

Consequently, to ensure welding between chips, two criterions must be fulfilled:

1. Oxide layer must be broken down to allow metal to metal contact [17].

It is possible to use a pressure-time-flow criterion to determinate if extrusion welding take place: chip welding = $\int_{L_1}^{L_2} \frac{p}{\sigma} dl \geq \text{Cost}$ where p is the normal pressure, σ is the effective stress, L_1 is the point where oxides start to break and L_2 is where compressive strain go to zero, thus L_1-L_2 is circa the path from the end point of mandrel to the die exit (Fig. 2.1.4).

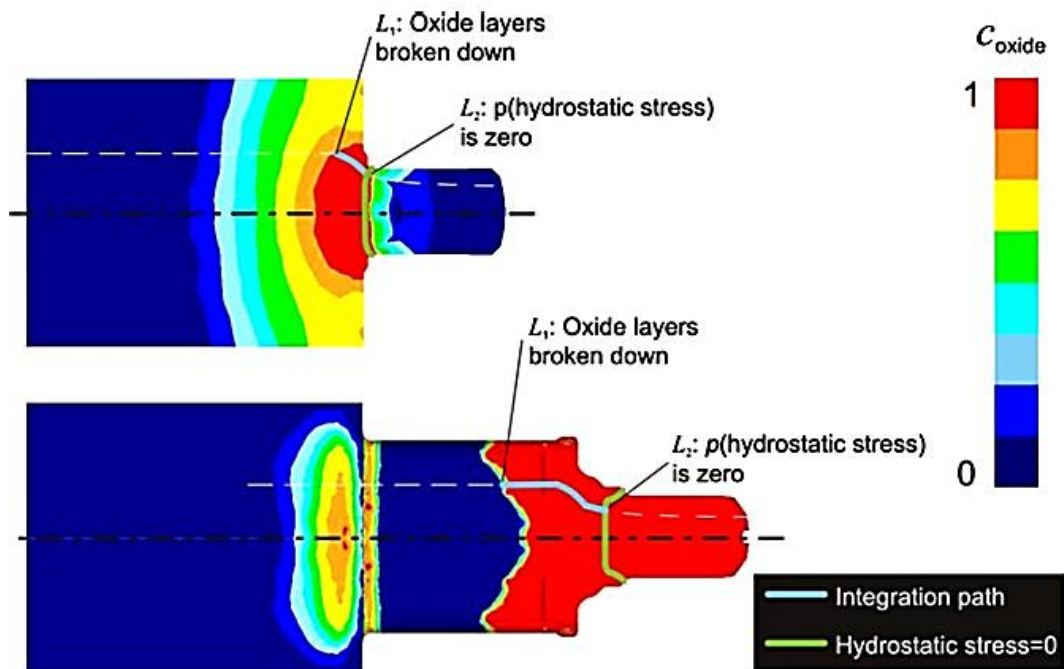


Fig. 2.1.4 Integration path in flat-face die & porthole die [17]

2. The shear stress level must be greater than a constant value to maintain a sufficient welding quality: $C_{cr} = \frac{\tau}{\tau_{critical}} > 1.0$ [17].

Fig. 2.1.5 shows plastic strain and strain rate during an extrusion stroke.

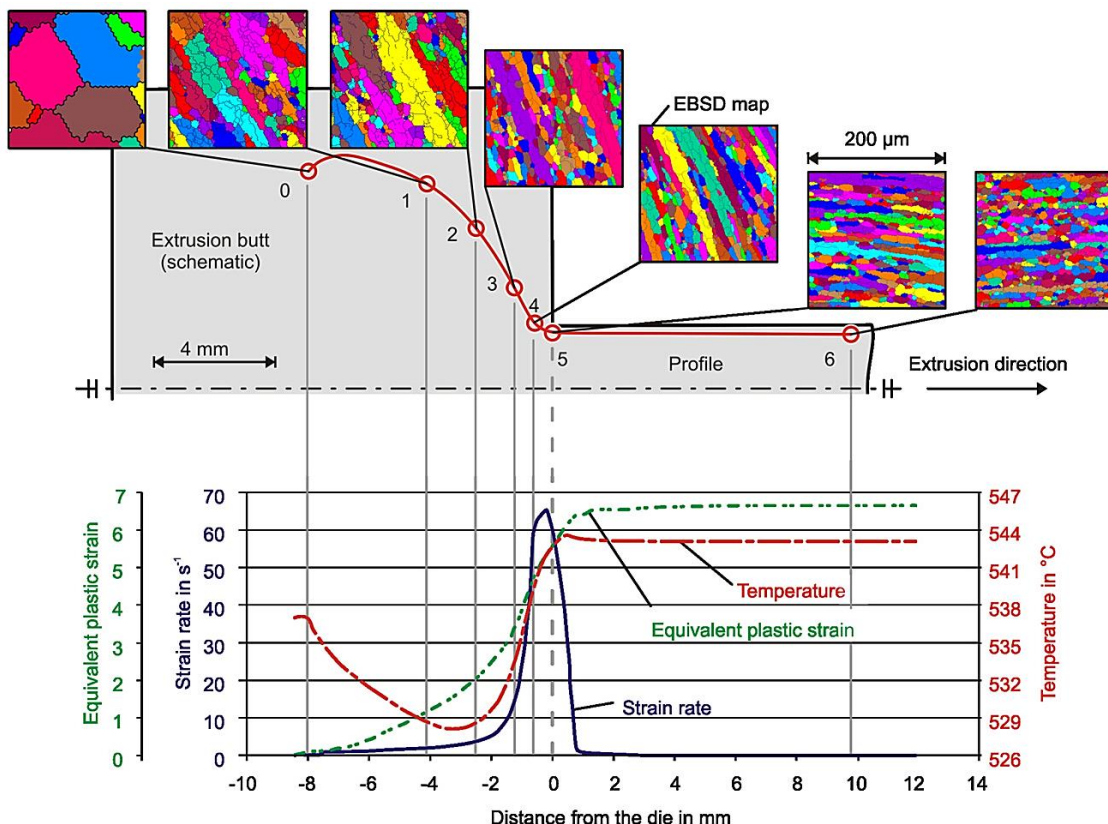


Fig. 2.1.5 Process parameters history during extrusion [18]

For instance, the deformation route of the flat-face die does not assure sound chip bounding under an extrusion ratio of 8.7 circa, where the true strain can be calculated as $\varepsilon = \ln\left(\frac{A_{in}}{A_{out}}\right) = \ln(R)$.

On the other hand, porthole and iECAP (integrated Equal Channel Angular Pressing -Fig. 2.1.6-) dies provided condition for superior bounding quality related to a high amount of pressure and strain affecting the chips [16]. In particular, extrudates by iECAP die have superior mechanical properties (ductility) in accordance with the microstructure showing fine uniform grains.

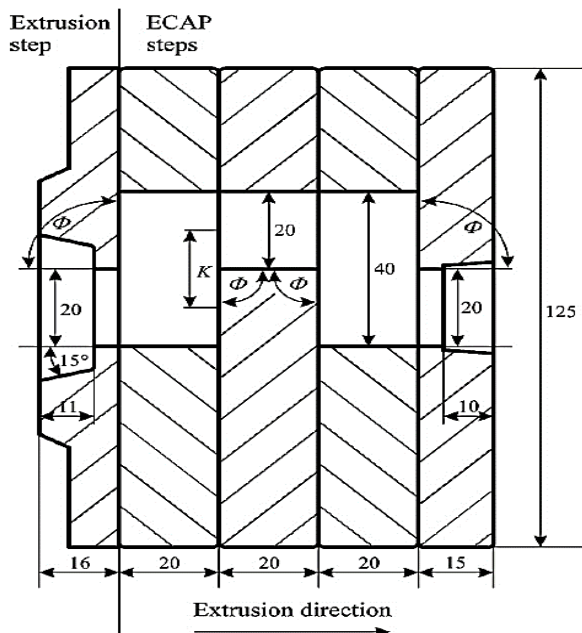


Fig. 2.1.6 iECAP tools ^[19]

The first step in chip extrusion process is collecting chips, shredding, cleaning and drying them, if necessary. The oil emulsion can be removed from the chips by a chemical method or a thermal method, such as using acetone.

The size of chips allows an incremental oxide density with a decrease chip dimensions, thus chip-based extrudates tend to form micro-cracks visible on the fracture surface of the tensile specimens in addition to micro-voids at the expense of ductility and strength. On the other hand, a high amount of oxides has an advantageous suppression of grain growth during extrusion since grain can grow only where oxide layers are broken during the process. However, the process can be independent on the chip geometry: different kind of chips lead to a homogenous extruded if a critical value of pressure-strain-temperature is accomplished.

For example, higher ram speed leads to a decreasing strength and ductility due to higher deformation temperature, but slow speeds lead to adhesion effects, such as stick-slip effect.

Consolidation of chip-based billets, considering chip geometry, is processed by a press which load up chips into a container with the diameter of the desired billet (Fig. 2.17).

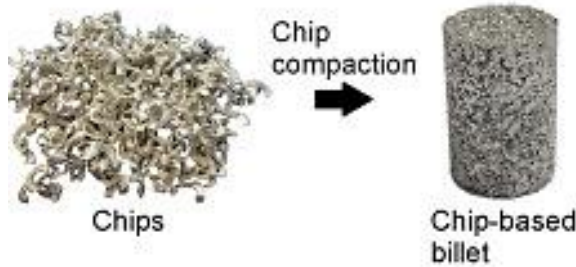


Fig. 2.1.7 chip-based billet [19]

In the direct extrusion of scarp, the influence of the pre-compaction is a negligible step to guarantee high pressure and strain level inside the die, but the problem of the inclusion of the air inside of the profile could considerably affect the quality [19].

Usually a cold-compacted billet has a density of 2.1 g/cm^3 which corresponds to 78% of the theoretical aluminium density. Using four-layer compaction is possible to reach 7.5% higher density but the mechanical properties of the profiles do not change, in comparison to single compaction ones [16]. The compaction method has influence for low extrusion ratio, for example, under ratio of $R=6.25$ only with hot compaction and hot extrusion the required sound bounding is achieved. Whereas for R bigger than 25 a cold compaction of the chip-based billets is sufficient [16].

The similar problematic of seam weld formation, in case of hot extrusion with porthole dies, can be used as a reference for the analysis of chip welding. Indeed, in the chip extrusion technology, the problem of the low-quality seams between a billet and another is not present because, for a nice product, good sound bounding and elimination of porosity must be present between every chip surface. These properties are the directly responsible of the mechanical properties of the extrudates.

In literature, some specific conclusions were attained:

- Usually surface quality is enough using chips of the same alloy.
- Using SiC particles as mixing materials inside the billet causes a damage of the surface in many points, as shown in figure 2.1.8. [15].

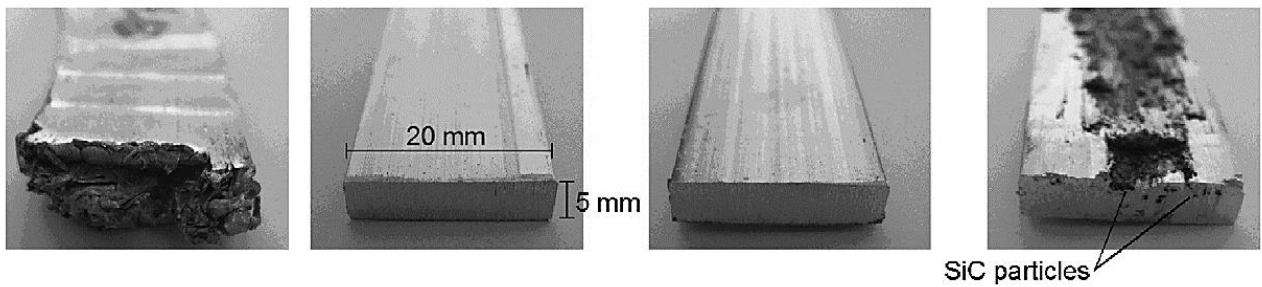


Fig. 2.1.8 Profile damaged during extrusion with SiC particles [15]

- The use of a porthole die lead to a fracture strain of 26% that is 80% higher ductility compared to profiles extruded through flat-face die (Fig. 2.1.9) [17].

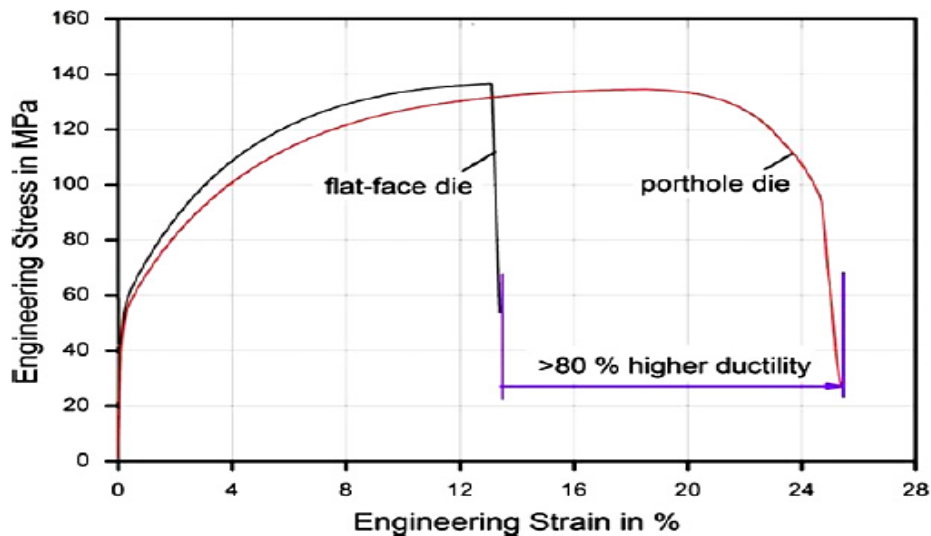


Fig. 2.1.9 Chip-based extruded by flat-face and porthole dies. [17]

- Using billets made of AA-6060 chips, with the same shape, can lead to similar mechanical and microstructural properties as using of conventional cast aluminium billets (Fig. 2.1.10) [19].

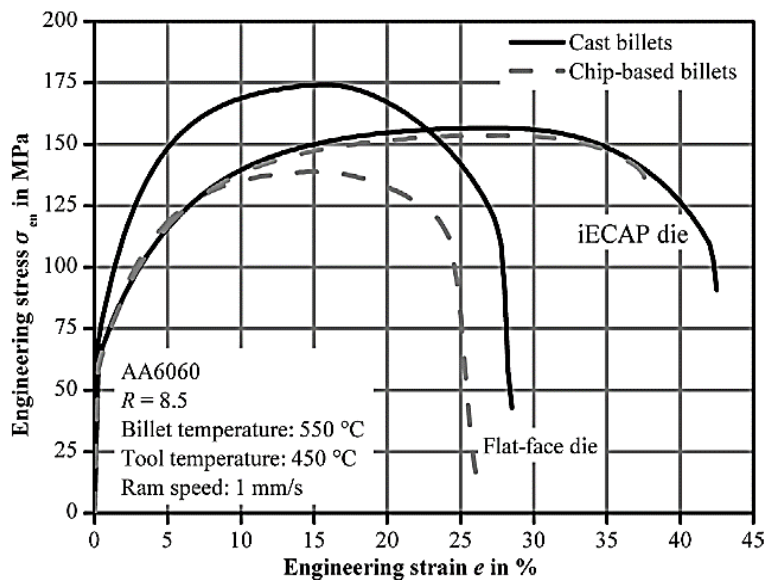


Fig. 2.1.10 Cast vs chip-based billets [19]

- Chip processed by hot extrusion with subsequent forward cold extrusion to product cans have the same properties of the cast material extruded and a finer grain microstructure ^[35].
- Compression test specimens indicate anisotropic behaviour of chip-based extrudates depending on die design.
- In some tests shafts based on chip extrudates through the flat-face die delaminated during compression tests.
- Well implemented FEM codes can be used to optimize the process parameters, die design and predict the profile results.

Fig. 2.1.11 shows an example of FEM result ^[17].

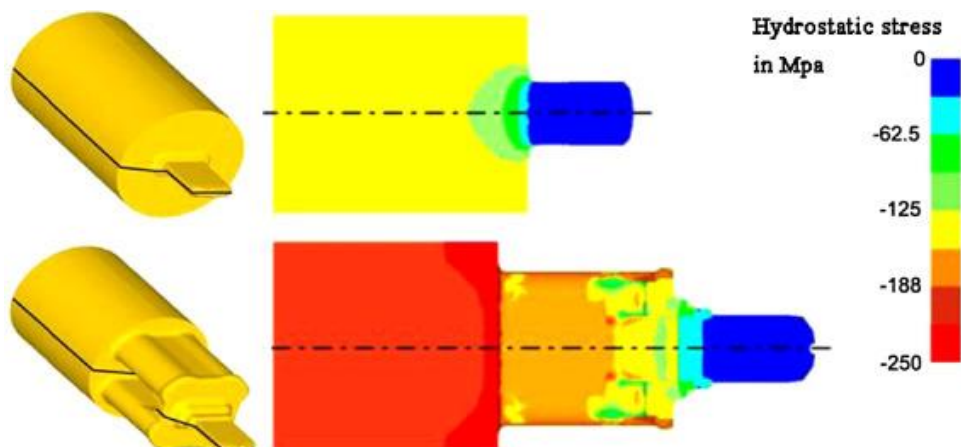


Fig. 2.1.11 Simulation of the hydrostatic stress during extrusion [17]

The new process of direct recycling of mixed aluminium alloy was investigated in IUL. Pins of AA-1050 chips of AA-6060 were mixed and compacted in 1:1 weight ratio billet. The extrusion was carried out with a two feeders porthole die at 450°C with 1mm/s ram speed and billets were preheated for 6 h at 550°C. A deteriorating effect of the cooling lubricant on the mechanical properties was observed. The lubricant-free profile revealed an intermediate character between AA6060 and AA1050 ^[36].

We want to proceed further on these testing in order to find the possible mixture of alloys allowing good aesthetic-mechanical properties and the respective process parameter due to obtain these products cheaper and in an industrial implementable way.

3.0 Mixed alloy chip extrusion

3.1 Introduction

Several researches have been carried out about chip extrusion, currently some focused also on mixed material extrusion. As instance:

- Scraps of AA-6060 with AA-1050 where mixed and extruded.
- Mixture of aluminium chips reinforced with SiC particles, as shown in the previous chapter.
- Billet of mixed aluminium and copper chips extrusion.

Until this paper, none extended the research to the behaviour of different aluminium alloy chip extrusion, mixed in various percentages and shapes, with an industrial approach.

Figure 3.1.1 shows some of the chips used for the experimentation.



Fig. 3.1.1 The different chips used in the experimentation

3.2 Aim & motivation

The investigation has the purpose of optimizing the chip extrusion process using the same chips discarded by industries.

In manufacturing industries, the chips are all collected together in big boxes after the machining works, as rejected material which will be sent to recycle sites for re-melting. Chips are usually only sorted by the main material, i.e. steel, aluminium, copper, etc. Size, width, length, thermal and mechanical history and the other elements inside the alloys of chips can vary a lot, depending on the rough piece processed and the cutting parameters (velocity, cutting depth, etc). The optimization of the industrial chips extrusion is very interesting both for an ecological and economical point of view and for industrial necessities. As shown in literature, with the chip extrusion direct recycling method is possible to save 3-4% more energy than the total saved by the second aluminium re-melting system. Additionally, a 20% circa of material loss due to oxidation is preserved. Finally, chip extrusion technique can perform good quality results in terms of mechanical properties. In some cases, the strength is higher than cast-extrudates because the oxide layers between chip can stop the process of grain growing, during extrusion, leading to higher performances in term of tensile strength. It is also possible to reach very smooth surfaces, therefore nice aesthetic characteristics.

3.3 Experimentation & numerical analysis

3.3.1 Work plan

The main steps we planned to develop the research are:

1. Collect chips divided by type and classify them.
2. Clean chips from lubricant, impurities and other possible discard materials.
3. Dry the cleaned chips into oven at low temperatures and evaluate the amount of chips.
4. Mix chips in a strategic way in order to get useful parameters during the extrusions.
5. Cold compaction of mixed chip into billets, calculation of the density and the expected length of the outcome profiles.
6. Hot extrusion of billets by porthole die and flat-face die with the same matrix shape to have comparable profiles.
7. Evaluation of the extruded profiles by surface characteristics. Cutting specimens for tensile, hardness Vickers 10 tests and microscopy analysis after Baker etching to evaluate chip bounding, grain size, impurities, etc.
8. Design the CAD model of tools, use dies geometries for HyperExtrude simulation and implement MatLab code to evaluate the results.
9. Analysis of the results from the tests taking into account all the process parameters and the problems in extrusion profiles, such as air inclusion, worse surface parts, peeling, etc. Compare simulation results with the experimental ones, checking the correspondences and differences.
10. Discuss outlooks.

3.3.2 Classifying chips & Mixing

The chips were selected from the accumulation box (Fig. 3.3.2) of the Machining Department “Institute of Machining Technology”. Initially, these chips were mixed together in an inhomogeneous way, thus we divided them in different boxes sorted by the size, length, width, thickness, and classified by type. Due to the impossibility of sorting them perfectly, we estimated the percentage of each kind of chips in every division-box.



Fig. 3.3.2 Accumulation box from IMT

We took an example of each chip and categorised them. There were 11 different kinds of chips, where the majority was composed by the 3 types below (Fig. 3.3.3).



Fig. 3.3.3 From left to right: Chip A, Chip B, Chip C

In each box of chips there was a minimum of 90% on volume of the principal chip-kind: chip A, B or C (Fig. 3.3.4). The 10% left was composed by some other kind of chips, of the 11 types categorized, impurities and extra material that were accidentally inside the accumulation box. The IMT department recognized the kind A and B as 6xxx series and the type C as 7xxx series. We proceeded further analysis to confirm the elements inside every chips type.

Kind of chip-groups	Info: main chip-type	Other chip-type (% on volume)	Density [g/l]	Tot. amount [g]	Accuracy
Chip A	small size, short, large, curved	other and impurities (1-2%)	380,2 ± 10%	7400	± 10%
Chip B	small size, like grains, short	long scraps (8%), chip 2 (3%)	287,4 ± 10%	6600	± 10%
Chip C	big size, elicoidal, thick	long straight (5%), other (5%)	152,4 ± 10%	5400	± 10%

Fig. 3.3.4 Principal chips info, zero-density, total amount

Once estimated the amount of chips, we decided the way to mix them for the billet compaction (Fig. 3.3.5):

Mixture, same [%] on weight	Number of billets
Chip A	8
Chip B	6
Chip C	6
Chip B+C	6
Chip A+B+C	5
Total	31

Fig. 3.3.5 Number and mixing chips into billets

After this phase, we started to clean up the chips from the lubricants, which are used during the machining processes, and from impurities which typically appear during logistic movements of the chips.

The content of acidity or basicity of lubricant oils is TAN (Total Acid Number) or TBN (Total Base Number) and is an important factor to select a good cleaning fluid. Furthermore, while main oils are composed by fat substances, the manufacturers add some solutions which allows oil to form emulsions with water. This is called saponification; the quantity of solution is indicated from a number following ASTM D 94. This number is evaluated by the ability of the oil to soap when they react with a basic (alkaline) solution, normally at high temperature ^[31].

We had chosen Wigol VR X 74S a degreasing fluid.

First, we set-up the workbench (Fig. 3.3.6) with the necessary tools: two metal

boxes 40x40cm, with an electric resistance, to heat the fluid inside up to the desired temperature, in our case we heated up to 60°C circa. We also used two tubs with a mesh where we could put the chips to wash.



Fig. 3.3.6 The workbench for the cleaning process

The cleaning process consisted in:

- Putting the chips into the mesh-tub and soaking them for 10 minutes in the first box with a homogenous solution of washing fluid, 10% and 90% of water.
- Washing the chips with running water.
- Another soak in the second bath-tub with the cleaning fluid for ten minutes.
- A further wash of the chips with running water.

At the end, we placed them into the containers (Fig. 3.3.7), ready for the oven.



Fig. 3.3.7 Cleaned chips in containers for the oven

This process took circa 25 minutes for each cycle of chip-washing. In every

cycle we treated about 2 litres of chips. It was important to refill the tub (Fig. 3.3.8) with some cleaning fluid every 5-10 cycles, considering the amount of oil emulsion on the surface of the fluid.



Fig. 3.3.8 The tub for cleaning process and the oven

Meanwhile we were carrying out the cleaning process, we started drying the chips which were already washed.

The oven was set up at 50 degrees in order not to incur in variations on chips microstructure and the recycle of the air was set on, from inside to outside, to eject humidity. Every box was thin, with large surfaces to spread all the chips and maximize the contact with the air. The chips remained in the oven for 24 hours circa to get completely dried. Once having dried all the chips, we have sifted them with a magnet to prevent and clean them from the presence of steel-based scraps which could damage the extrusion die tools.

3.3.3 Compaction & extrusion

The cold-compaction step was carried out with a hydraulic press (Fig.3.3.9), with maximum pressure of 150 bar circa. We used a cylindrical container made of hardened steel, with 60 mm of internal diameter and 250 mm of internal length, which corresponds to the length of the available stroke.



Fig. 3.3.9 The hydraulic press and the container

The compaction and the necessary number of strokes depended on the size of the chips and on the mixture: big-sized chips easily filled the volume inside the container, so that we had to repeat the compaction to complete a billet, figure 3.3.10 gives data on compaction.

Mixed chips:	Composition
A	100%
B	100%
C	100%
B + C	50%+50% on weight
A + B + C	33%+33%+33% on weight

Billet number	Weight [g]	N. strokes	Length [mm]	Ideal weight [g]	Density [%]	Profile Length [mm]
1	569	4	106	809	70	2107
2	593	4	111	847	70	2196
3	598	4	117	893	67	2215
4	598	4	119	908	66	2215
5	595	4	118	901	66	2204
21	605	4	113	863	70	2241
32	600	4	112	855	70	2222
33	585	4	110	840	70	2167
6	543	4	113	863	63	2011
7	606	5	110	840	72	2244
8	623	6	109	832	75	2307
9	620	5	111	847	73	2296
10	618	5	110	840	74	2289
22	604	5	108	824	73	2237
11	542	6	119	908	60	2007
12	602	7	118	901	67	2230
13	600	7	118	901	67	2222
14	623	8	118	901	69	2307
15	612	6	116	886	69	2267
23	685	8	130	992	69	2537
16	605	6	112	855	71	2241
17	603	6	110	840	72	2233
18	602	6	113	863	70	2230
19	604	6	111	847	71	2237
20	604	5	112	855	71	2237
24	602	5	112	855	70	2230
27	604	5	112	855	71	2237
28	603	5	112	855	71	2233
29	602	5	109	832	72	2230
30	605	5	107	817	74	2241
31	605	4	108	824	73	2241
Total (31)	19846	179	3737	28529	2299	73504
Average	601,39	5,42	113,24	864,50	69,67	2227,38
Max	685	10	130	992	75	2537
Min	542	4	106	809	60	2007

Fig. 3.3.10 Compaction parameters card

We decided to produce billet of 600g each. The products had a 113mm medium length, 60mm of diameter, and an average density of 70% (Fig. 3.3.11) supposing a 2,7 g/cm³ green density of aluminium. From the data sheet it is also visible the expected length after the extrusion for every billet, with a extrusion ratio of 34,2.

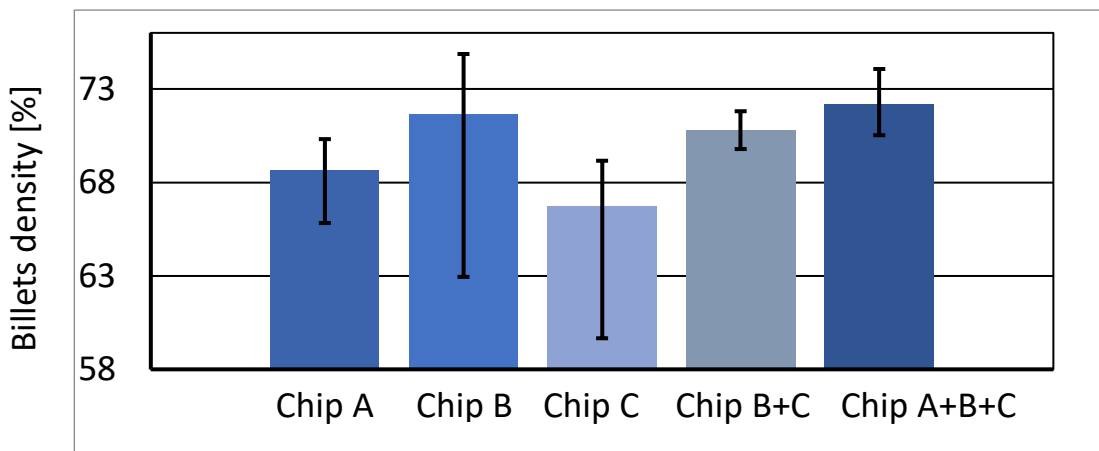


Fig. 3.3.11 Billets density [%]

The compaction set-up, observable in figure 3.3.12, is composed by the vertical ram and the container, locked by a moveable plate. The plate is moved by an hydraulic cylinder with maximum pressure of 150 Bar, that corresponds to 42kN of force on the chips.



Fig. 3.3.12 Compaction tooling set-up

Once compressed, we removed the plat from the bottom of the container and ejected the billet with a press stroke, as shown in figures 3.3.13.

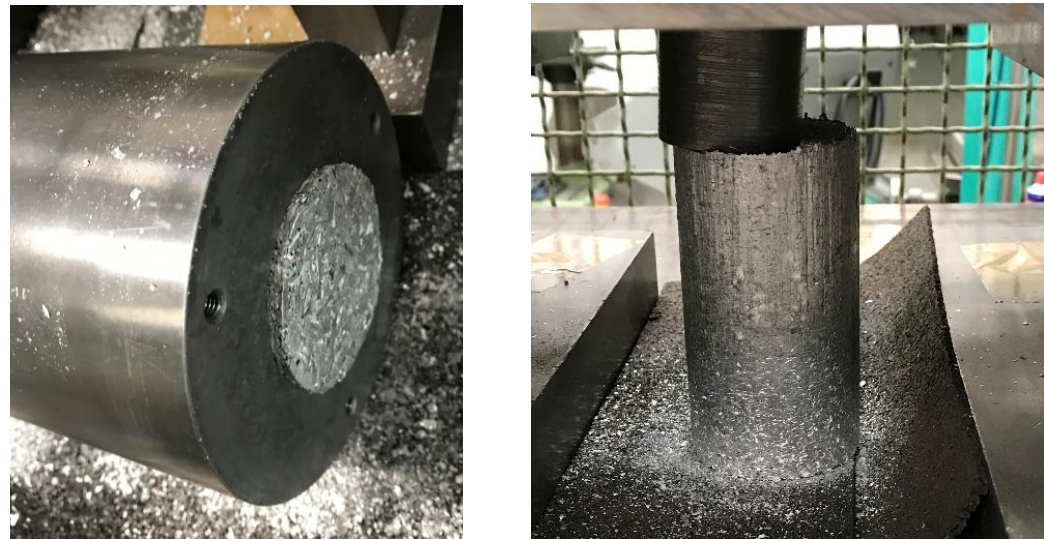


Fig. 3.3.13 Billet-removing procedure

The outgoing billets are easily handling, because the friction involved during the compression was enough to create micro-welding between chips. In some cases of lower pressure than ~ 90 bar, the density did not reach $\sim 67\%$, and the friction was not sufficient to create well-compacted billets.

Fig. 3.3.14 shows one billet based on chip C and one with a broken layer.

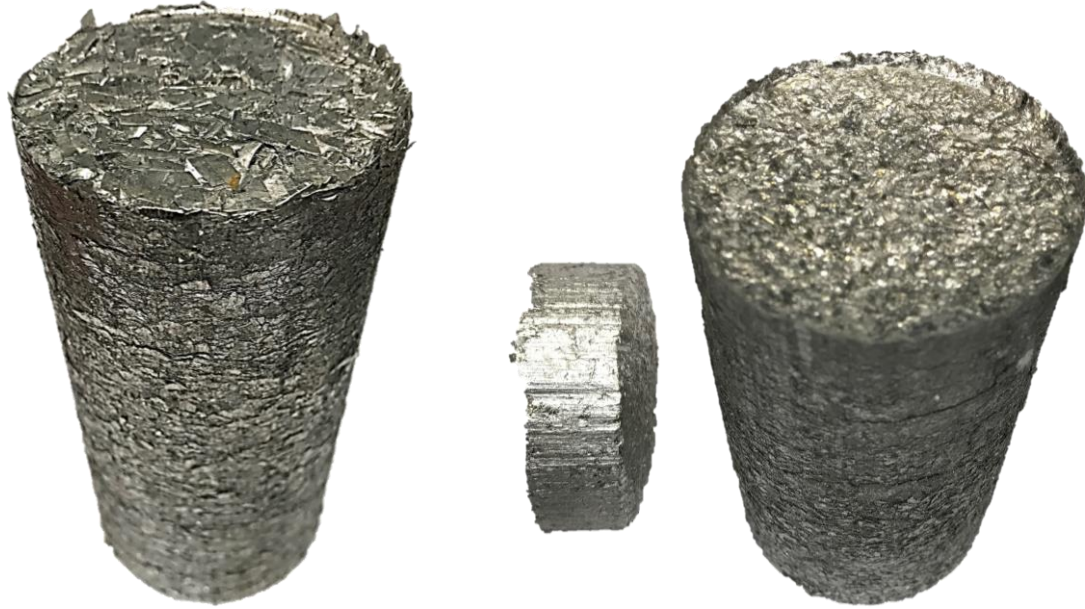


Fig. 3.3.14 Compacted billet and a billet with a broken layer

Once having compacted all the chips into billets, we started the extrusion process. We operated through a hydraulic extrusion press (Fig. 3.3.15).



Fig. 3.3.15 The extrusion press

We have chosen a simple cross-section of the profile to easily cut out samples from the extrudates for the tests. Moreover, to have comparable profiles and evaluate the die design influence on the results, we used two different dies with the same internal matrix. The shape selected was rectangular 20x5 mm (Fig. 3.3.16).



Fig. 3.3.16 Extrudates cross-section profile



Fig. 3.3.17 Two feeder port-hole die

We started the extrusion with the port-hole die presented above (Fig. 3.3.17). According to literature, the billets were heated up at 550°C for 5,5 hours for homogenizing the temperature inside the material. The extrusion was carried out at 450°C degrees with a ram velocity of 1 mm/s. Figure 3.3.18 shows the billets in the oven.



Fig. 3.3.18 The electric oven

We have extruded with the billet-to-billet method. First, we used an AA-6060 cast billet to fill the extrusion tools and guarantee a better outcome of the following chip-based billets. At the end a last cast billet completed the extrusion profile ejecting the whole chip-billets.

The cast-based extrudates were the reference for the analysis.

The extrusion force varied depending on the kind of billet processed, the figure 3.3.19 shows average values of extrusion force. The billets based on chip C required a higher level of force compared to the cast billet, whereas billets A and B needed lower force. The mixed chips shown intermediate values.

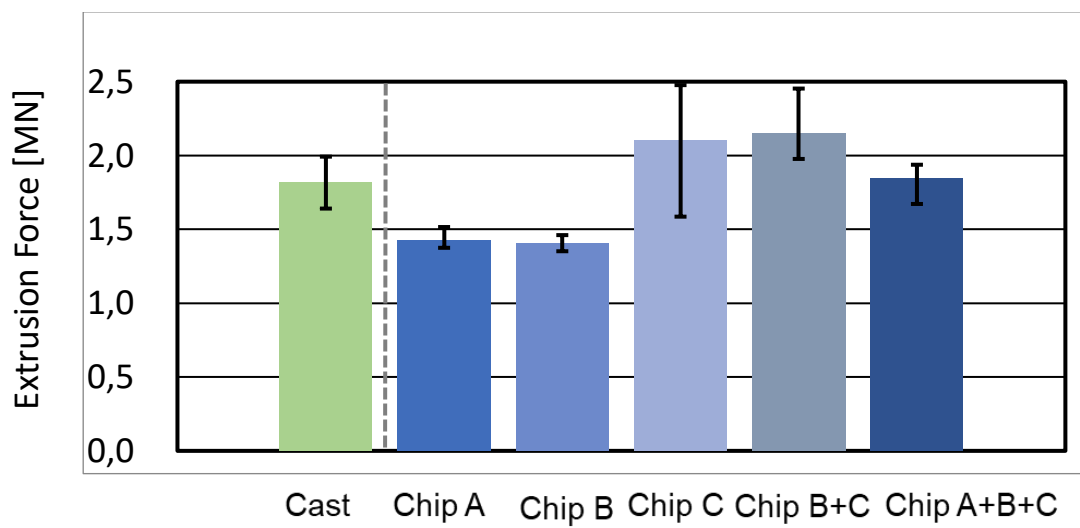
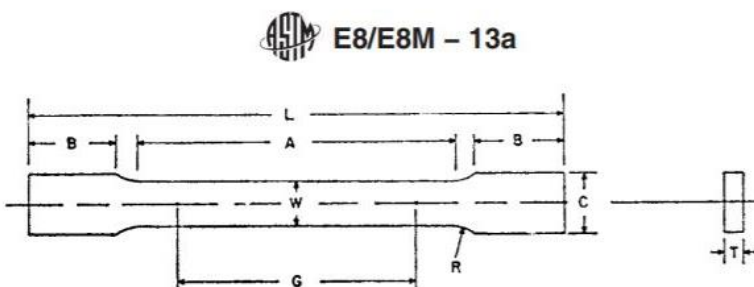


Fig. 3.3.19 Extrusion force depending on kind of billet processed

3.3.4 Tensile, Hardness tests & Microstructure analysis

We have carried out tests to classify and evaluate the quality of the profiles obtained by mixed-chip extrusion. We implemented the typical tensile, hardness and metallography analysis.

First, we cut out specimens from the profiles, with the following ASTM-B557M geometry (Fig. 3.3.20 & Fig. 3.3.21), using a CNC milling machine:



Dimensions		Standard Specimens	
		Plate-Type, 40 mm [1.500 in.] Wide	Sheet-Type, 12.5 mm [0.500 in.] Wide
	mm [in.]	mm [in.]	mm [in.]
G—Gauge length (Note 1 and Note 2)	200.0 ± 0.2 [8.00 ± 0.01]	50.0 ± 0.1 [2.000 ± 0.005]	
W—Width (Note 3 and Note 4)	40.0 ± 2.0 [1.500 ± 0.125, -0.250]	12.5 ± 0.2 [0.500 ± 0.010]	
T—Thickness (Note 5)		thickness of material	
R—Radius of fillet, min (Note 6)	25 [1]	12.5 [0.500]	
L—Overall length, min (Note 2, Note 7, and Note 8)	450 [18]	200 [8]	
A—Length of reduced section, min	225 [9]	57 [2.25]	
B—Length of grip section, min (Note 9)	75 [3]	50 [2]	
C—Width of grip section, approximate (Note 4 and Note 9)	50 [2]	20 [0.750]	

Notes:
 G—Gauge length (Note 1 and Note 2)
 W—Width (Note 3 and Note 4)
 T—Thickness (Note 5)
 R—Radius of fillet, min (Note 6)
 L—Overall length, min (Note 2, Note 7, and Note 8)
 A—Length of reduced section, min
 B—Length of grip section, min (Note 9)
 C—Width of grip section, approximate (Note 4 and Note 9)

Fig. 3.3.20 ASTM-B557M geometry for tensile specimens ^[11]



Fig. 3.3.21 Sample for tensile test

In our case the overall length was of 225 mm instead of 200 mm shown in directive.

We used a Zwick Roell Z250 testing machine for the tensile tests (Fig. 3.3.23). The number of specimens for every kind of extrudates was chosen by the

scattering characteristics of the superficial state, for example by the presence of bubbles, surface delamination, etc, with a minimum of 3 samples for each type. Every sample has been pushed to the breaking point where it is affected by the fracture strength (Fig. 3.3.22).

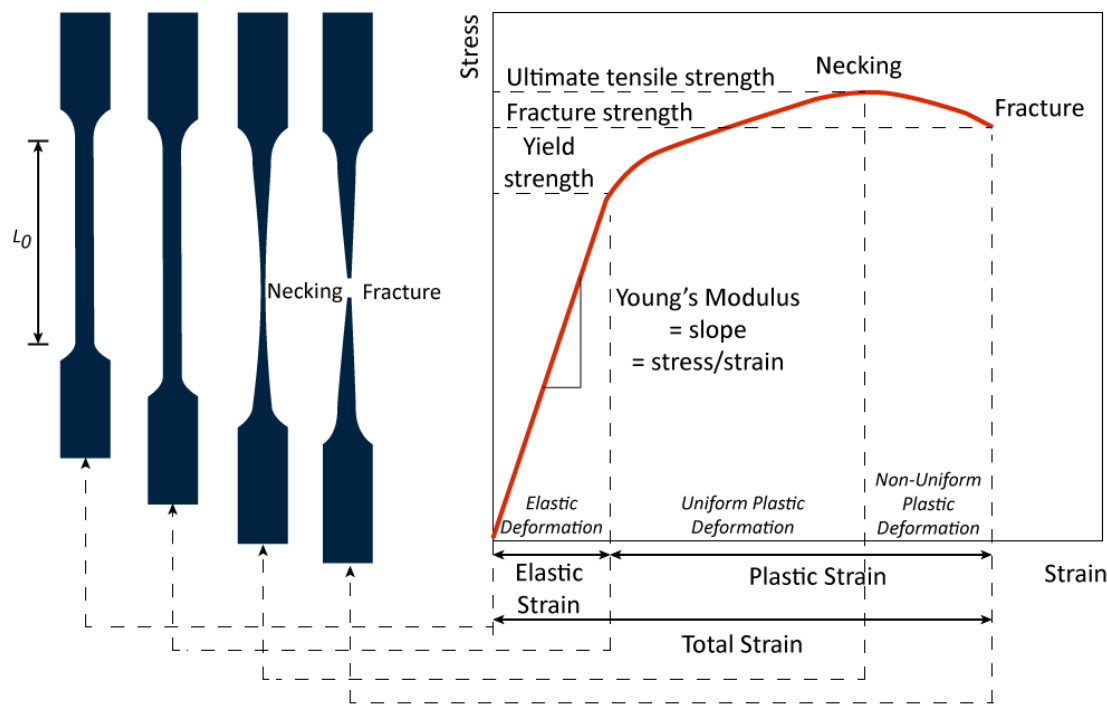


Fig. 3.3.22 The typical tensile test history [2]

At the end of the tests we obtained the stress-strain curves below (Fig. 3.3.24) and the values were elaborated and will be discussed in the chapter “Test data elaboration”. From these curves, we were able to extract important information, such as young modulus (E), ultimate tensile strength (R_m), yield strength (R_{p0,2}) and total strain [%].

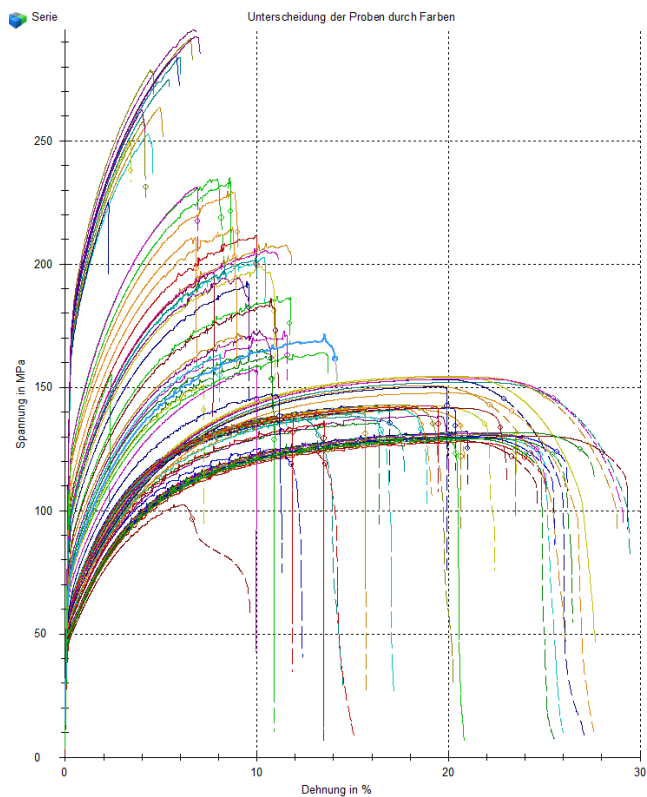


Fig. 3.3.23 The tensile test machine & Fig. 3.3.24 Stress-strain curves obtained by tests

We continued the examinations with Hardness Vickers 10 test, using a Wolpert machine (Fig. 3.3.25).

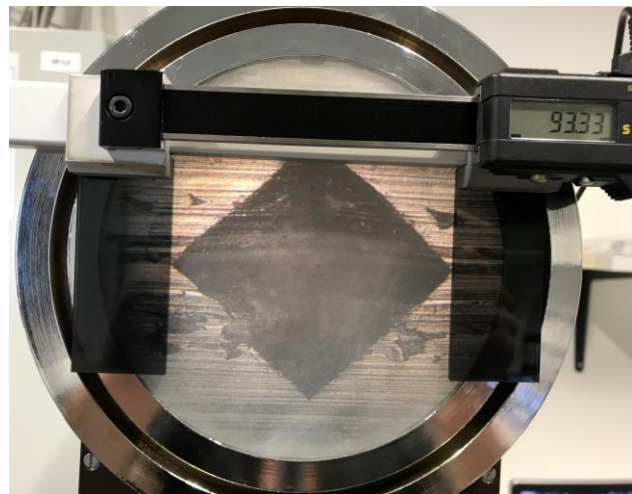


Fig. 3.3.25 Wolpert test machine & trace measurement after indentation

Hardness Vickers is an optical measurement system which follows ASTM E-384. It consists in using a diamond indenter, with a pyramid shape, to make an indentation which is measured (the diagonals) and converted to a hardness value. With this technique, we were able to evaluate the hardness of the material and to have information about the surface quality of the extrudates.

As last valuation, we proceeded with microstructure analysis to understand the chip bonding, grain size, presence of porosity, etc. The preparation for this analysis included:

1. Cutting both longitudinally and transversally parts of the profile to study the behaviour of the metal and the influence of the extrusion flow direction on microstructure.
2. Preparing a resin-hardener solution, we used EpoFix by Struers, to lock specimens (see figure 3.3.26).
3. Polishing the specimens to mirror-finish by using, step by step, finer abrasive grinding SiC paper. In order to get the smoothest surface, we also used as last phase with an Ammonia-solution on very low abrasive paper.
4. Etching the metal with Baker process. It consists in a chemical attack which permits to evaluate better the grain characteristic under polarized light.



Fig. 3.3.26 Specimen for microstructure analysis

Once completed the samples preparation, we could take pictures of the metal from an Axio-Zeiss optical microscope (Fig. 3.3.28). We have taken photos (x140) with white light and with polarized light. An example of the same piece is shown below, in both cases (Fig. 3.3.27).

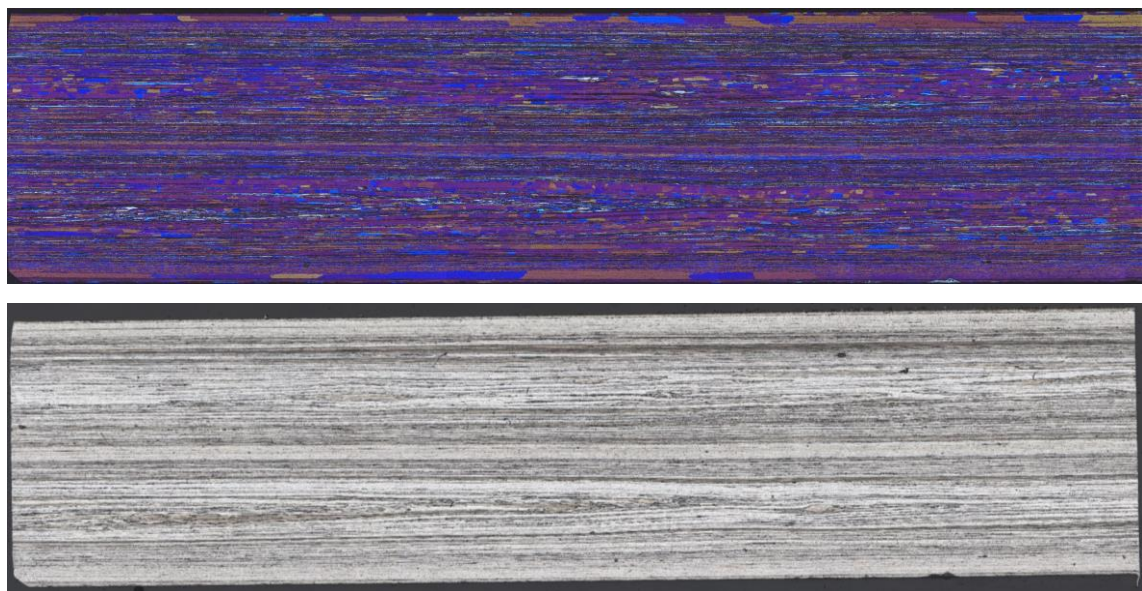


Fig. 3.3.27 Sample under polarized light -above- & white light -below- after Baker process

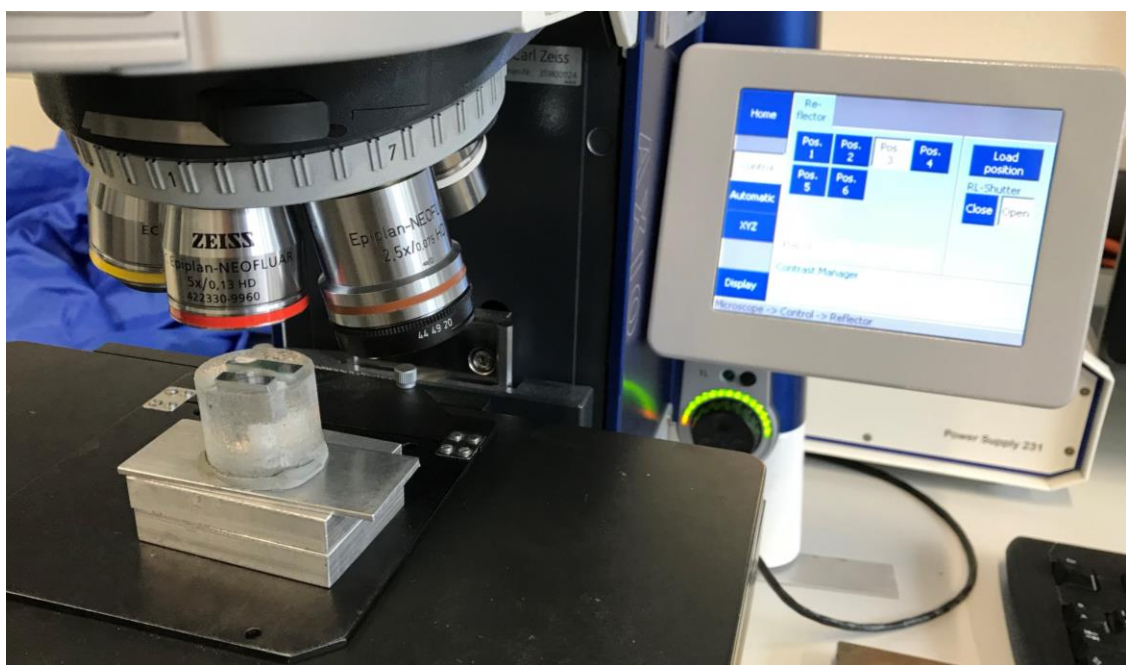


Fig. 3.3.28 Axio-Zeiss optical microscope

3.3.5 Test data elaboration

The information we have taken by analysis were elaborated to evaluate the behaviour of the different mixture-extrudates. For every kind of billets:

- We took photos of the surface, considering the different appearances along the profiles. As reference, in the following pages are visible two of the worse profiles extruded for each kind, to simply explain the issues involved during the process. There were parts with bubbles, just 0.5mm circa under the surface, peeling effect, delaminated parts, some very smooth and high-quality portions, etc.
- We took data from the tensile machine software (TestXpert) in form of excel-tables and created engineering stress-strain curves. We used all significant values from tests, deleting specimens which were broken outside of the gauge length. It was not possible to create real stress-strain diagrams because of the impossibility to estimate the quantity of porosity inside the samples.
- We have compared the Hardness Vickers values with the tensile results.
- From the microstructure analysis was visible the presence of the Peripheral Coarse Grain and the presence of the seam welding line due to the two feeders of the port-hole die. In some extrudates there were inclusions and porosities.

More on detail, kind by kind on the following pages.

CAST EXTRUDATES (AA-6060):

As previously described, the cast billet extrusion was used both to fill the tool, improving the chip-based extrusion, and to have a reference to compare the outcoming results.

The last cast-billet extruded was influenced by the previous chip-extrudates (Fig. 3.3.29.1), where superficial damages appear. In the second picture 3.3.29.2, the cast-extruded with smooth surface and homogenous characteristics along the profile, is shown.

It is affected by general good surface quality and no porosities appear.

The grain size grows from the middle, where the seam welding line is visible as region, to the edge (Fig. 3.3.29.3).

Fig. 3.3.29.4 displays the engineering stress-strain diagram with the values of all the specimens traded. The maximum strength was fewer than 160MPa and total strain was about 28% leading to a ductile behaviour.

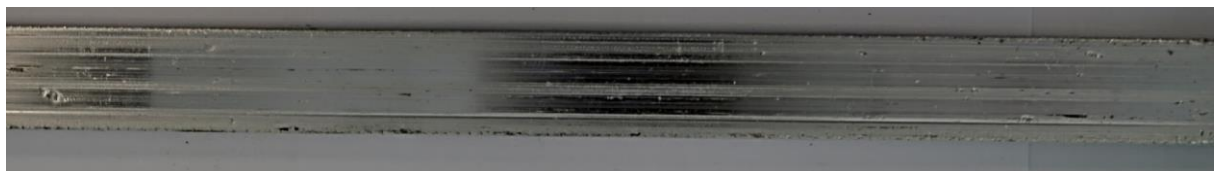


Fig. 3.3.29.1 Last cast extruded with imperfections



Fig. 3.3.29.2 Cast extrudates

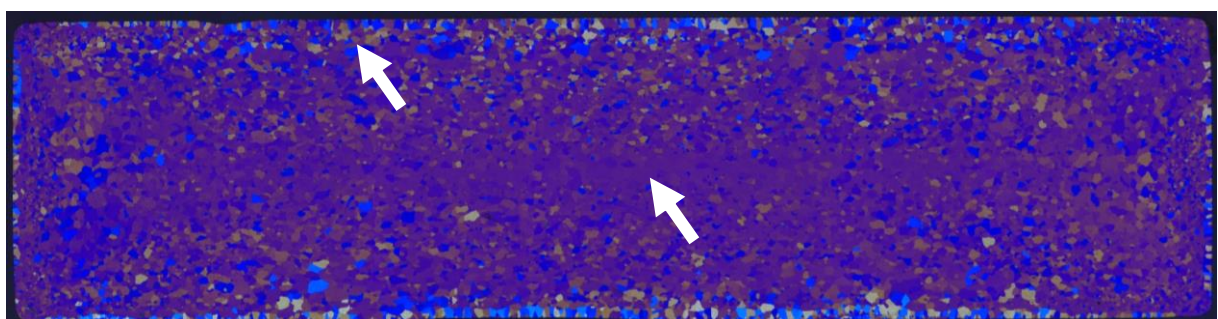




Fig. 3.3.29.3 Cross-section imagines at polarized & white light

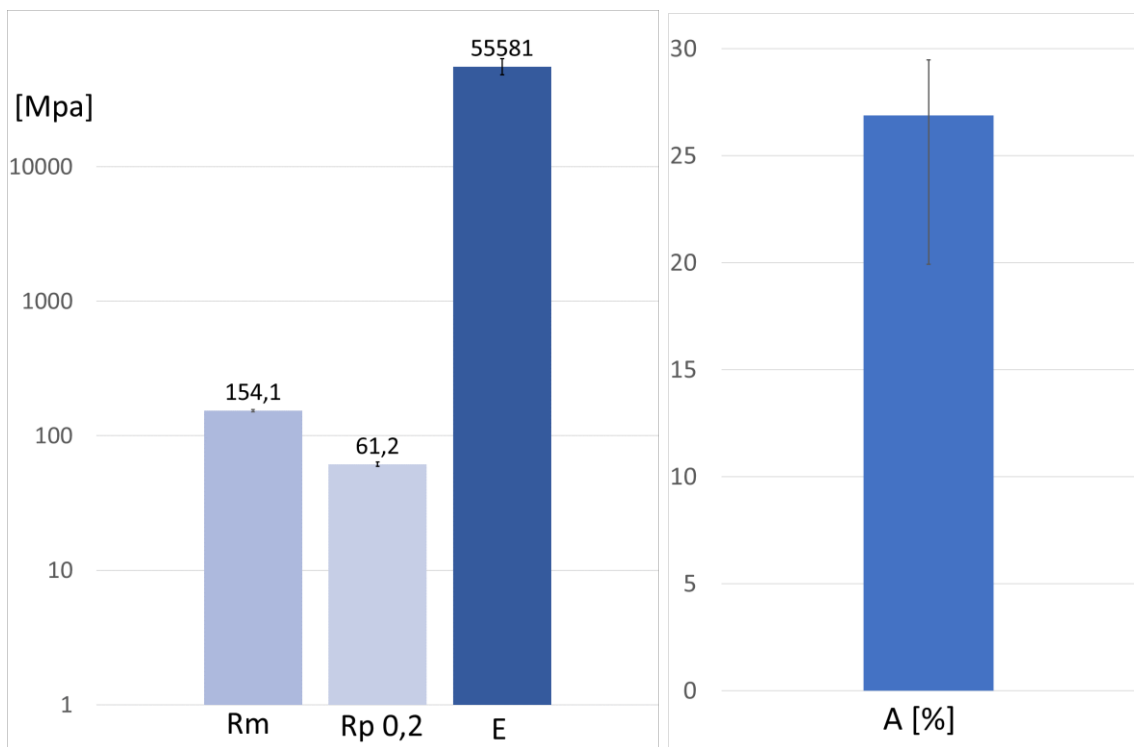


Fig. 3.3.29.4 R_m , R_p , E [Mpa] -logarithmic scale- & A [%]

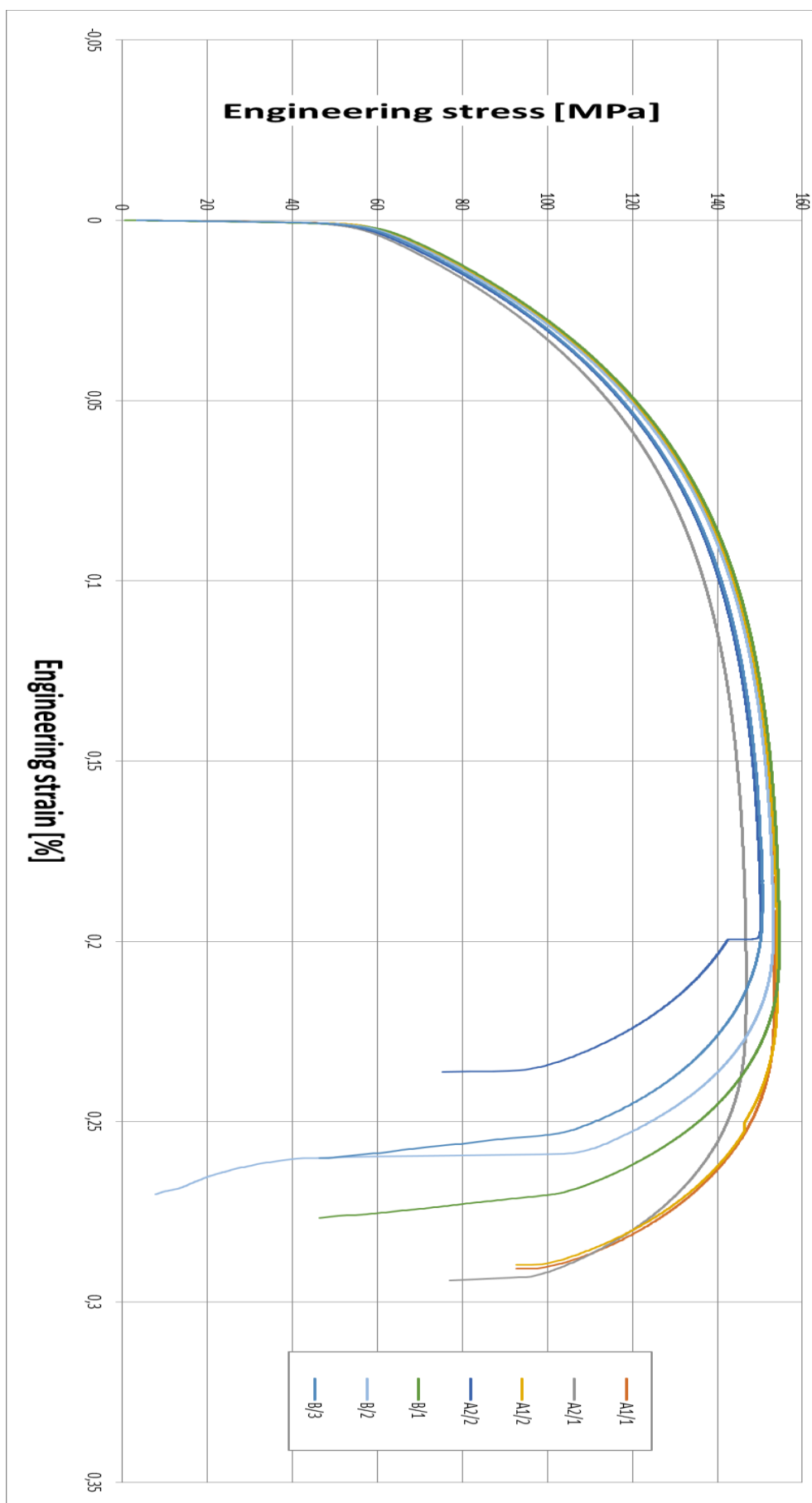


Fig. 3.3.29.5 Cast billets engineering stress-strain diagram

CHIP A EXTRUDATES (6xxx series, small size, curved):



This small-size chip leads to good aesthetic characteristic.

Some superficial bubbles arose, after the first billet extruded (Fig. 3.3.30.1), also some internal presence. In literature the problem of air-inclusion in chip extrusion process was studied and solved by different techniques. In our case the air remained inside the billet during the compaction and grew as volume due to the high temperature. For this reason, the quality along the profile varied, from zone with optimal qualities to zone with air inclusion. Anyway, general good-aesthetic characteristics appear.

In this case, is clearly visible the welding line, and the Peripheral Coarse Grain. A middle zone with lower density appears between the surface and the welding line, according to simulation results (see following chapter).

The stress and elongation were similar to the cast extruded.



Fig. 3.3.30.1 Bubble in the profile sub-surface

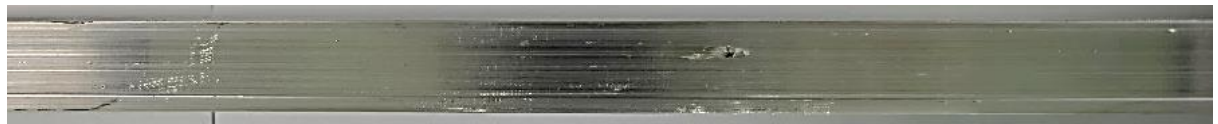


Fig. 3.3.30.2 Smooth surface with a damage



Fig. 3.3.30.3 Quality surface profile

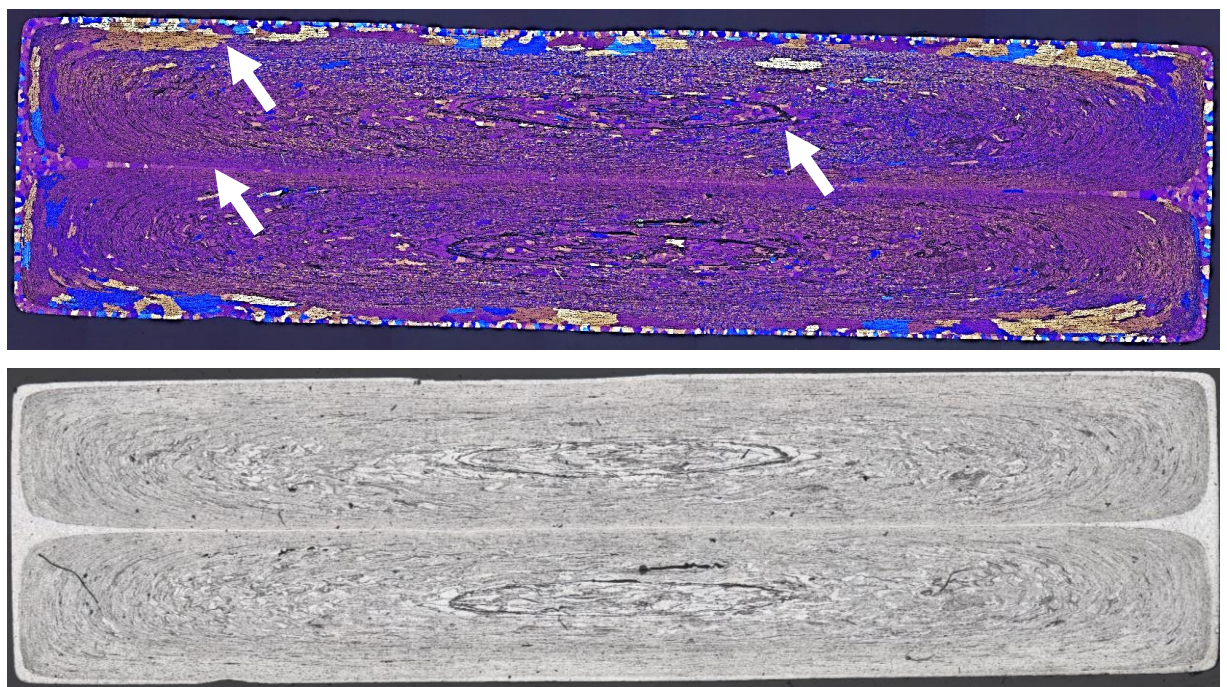


Fig. 3.3.30.4 Pictures after Baker process

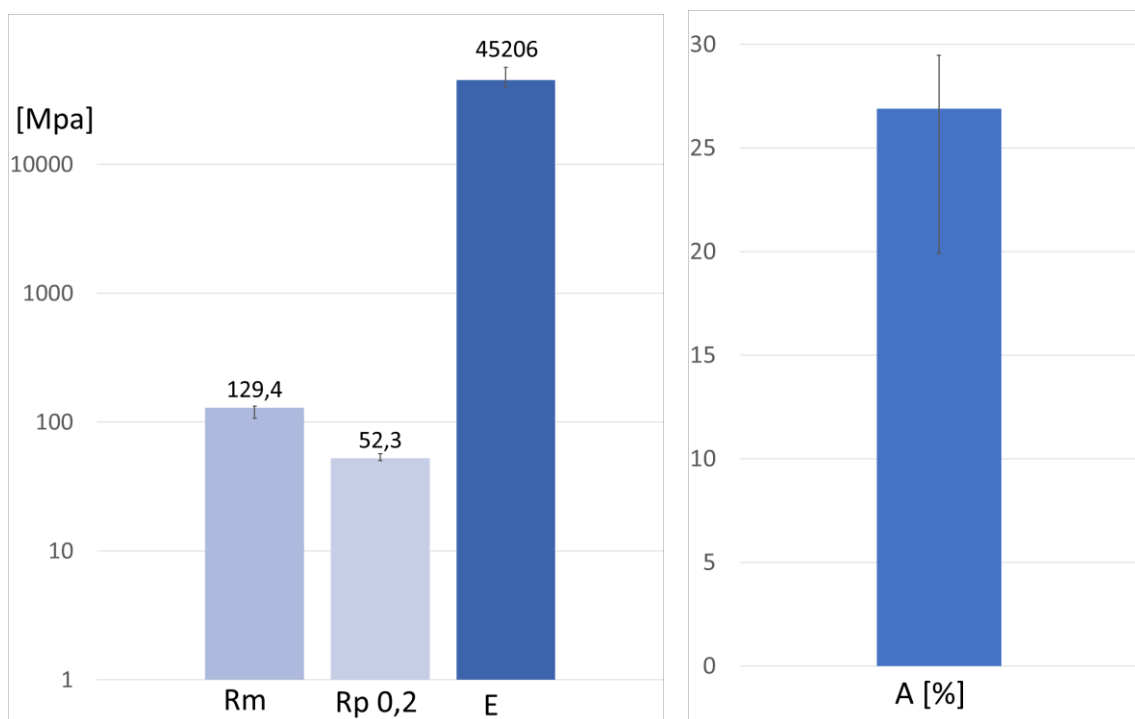


Fig. 3.3.30.5 R_m , R_p , E [Mpa] -logarithmic scale- & A [%]

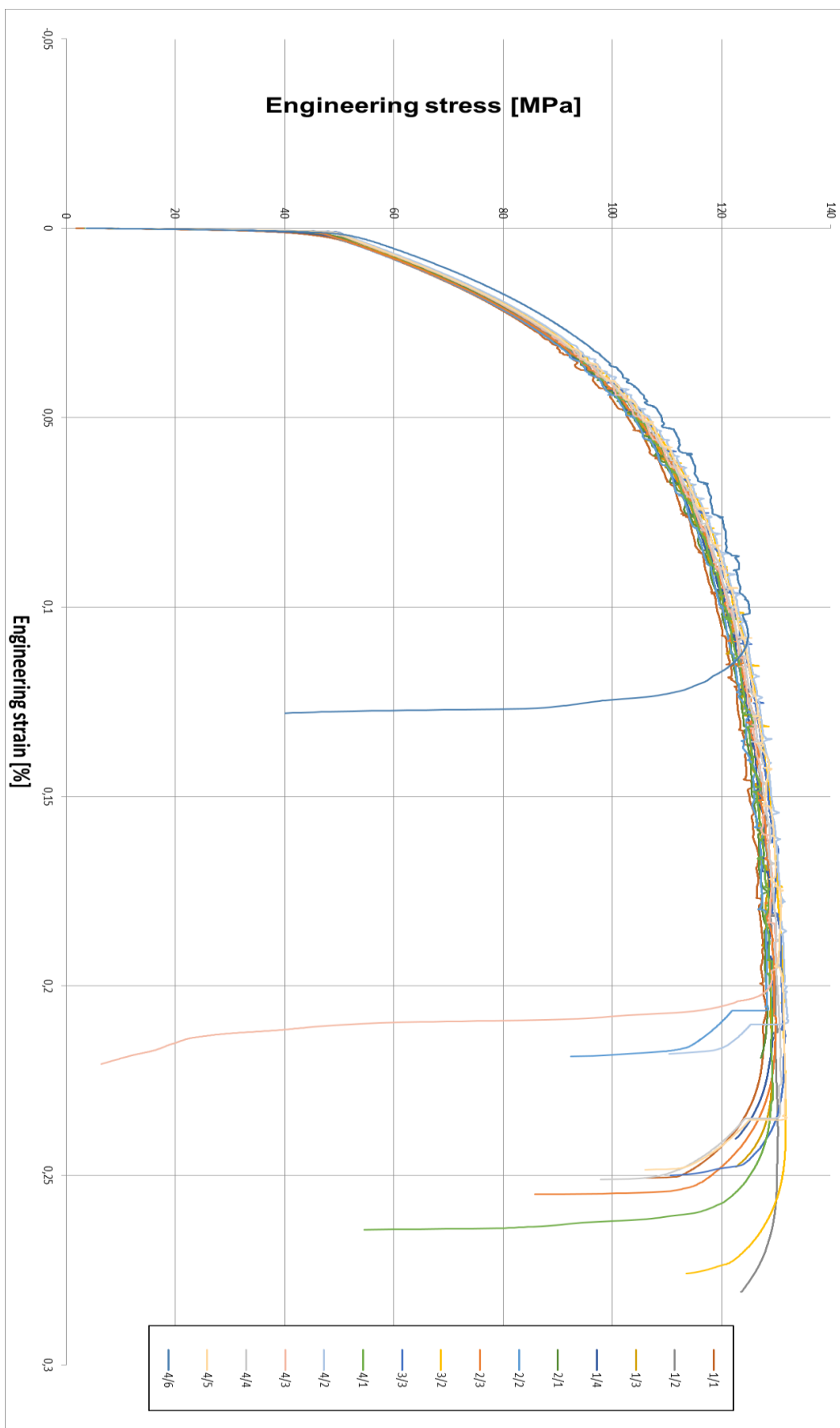


Fig. 3.3.30.6 Chip A billets engineering stress-strain diagram

CHIP B EXTRUDATES (6xxx series, small size, short):



This extruded has comparable properties to Chip A. Some superficial small air inclusions appear (Fig. 3.3.31.1).

The characteristic result homogenous along the profile.

Also in this case, the welding line and the Peripheral Coarse Grain are clearly visible.

The grains are finer and there is a zone with lower density which is visible in figure 3.3.31.3.

The maximum stress obtained was about 145 MPa and the elongation goes from 13 to 24 % with a high level of scattering.



Fig. 3.3.31.1 Chip B extruded with little air-inclusions

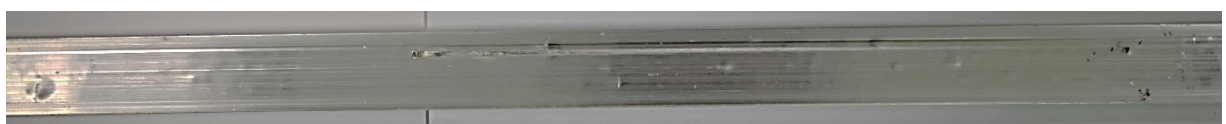


Fig. 3.3.31.2 Chip B extruded with some damages



Fig. 3.3.31.3 Chip B profile

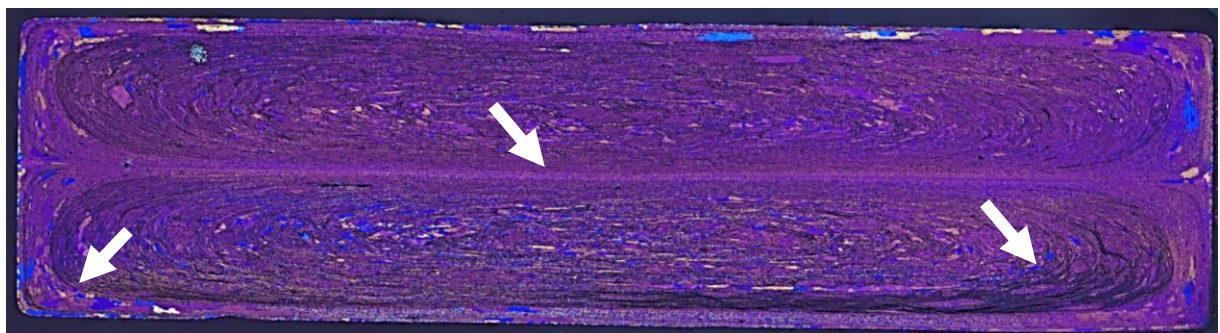




Fig. 3.3.31.4 Chip B cross section profile microscope pictures

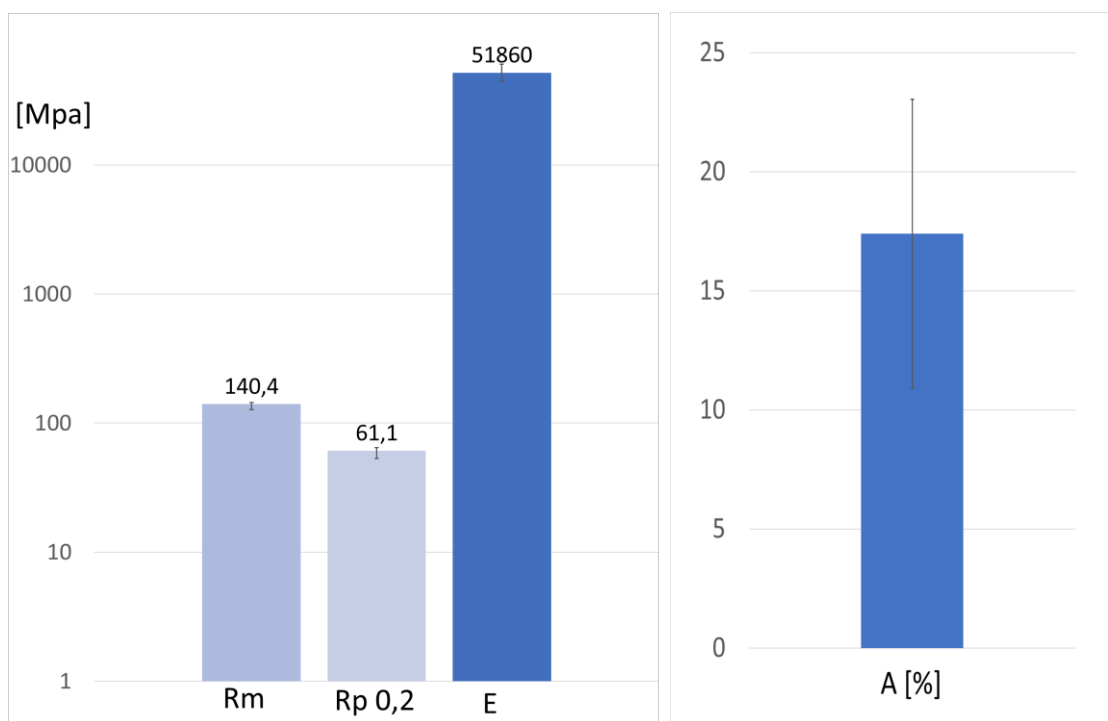


Fig. 3.3.31.5 Rm, Rp, E [Mpa] -logarithmic scale- & A [%]

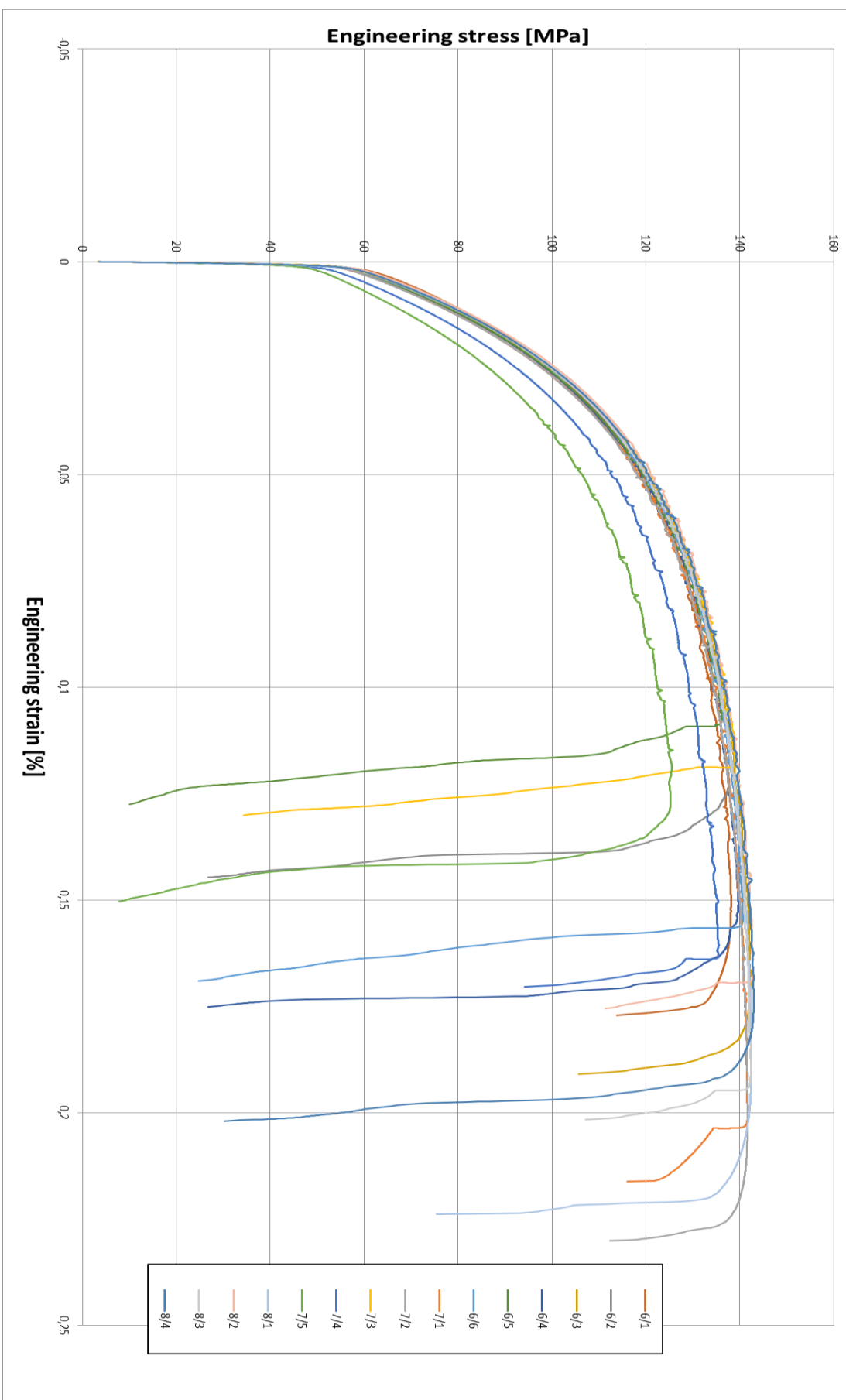


Fig. 3.3.31.6 Chip B engineering stress-strain diagram

CHIP C EXTRUDATES (7xxx series, big size, helicoidal, thick):



With this 7xxx series alloy the results had a very lower quality. There was a presence of delamination on the surface of the profile along the major amount of length, leading to very anaesthetic appearance. This kind of alloy needed different process parameters to obtain useful profiles.

In microscope pictures is evident the presence of big porosities and a grain size different point by point. Overall the seam weld line is not so evident. These reasons demonstrate that the required criterions were not satisfied, thus the chip bounding was not enough.

With this profile, the maximum stress measured was about 300 MPa, very higher level than the previous profiles. The behaviour was very fractile with a max elongation of 7%.



Fig. 3.3.32.1 Chip C profile with delamination



Fig. 3.3.32.2 Chip C profile



Fig. 3.3.32.3 The best part we achieved with chip C

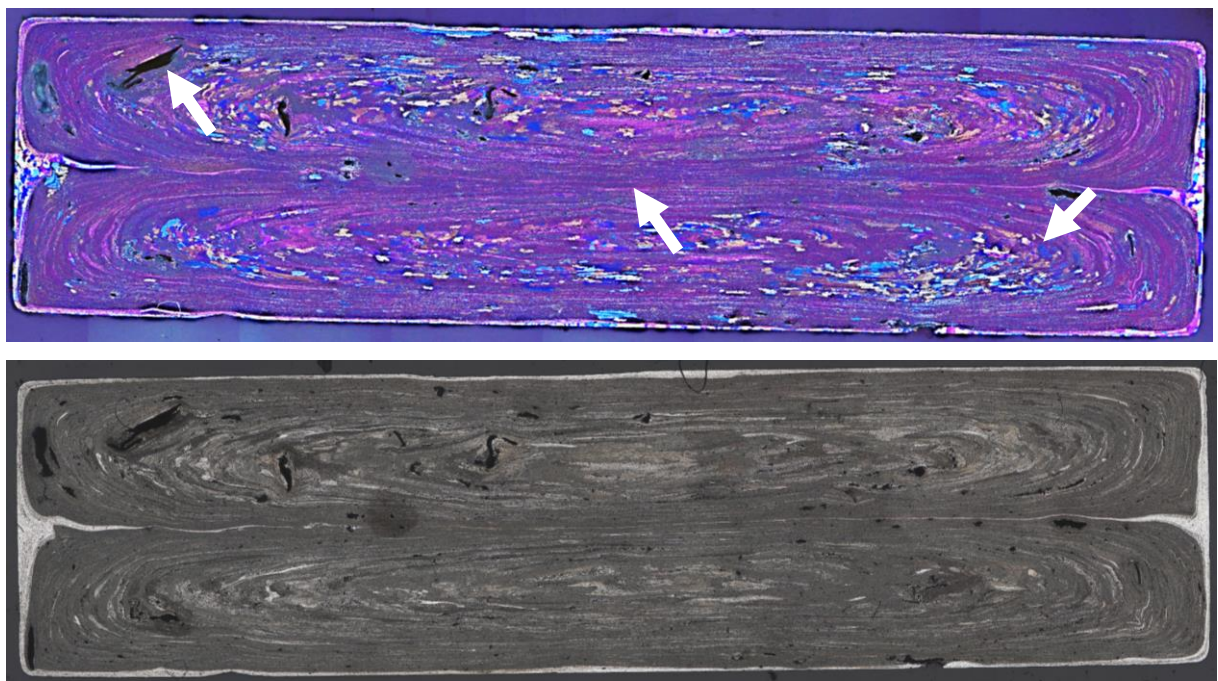


Fig. 3.3.32.4 Chip C microscope pictures

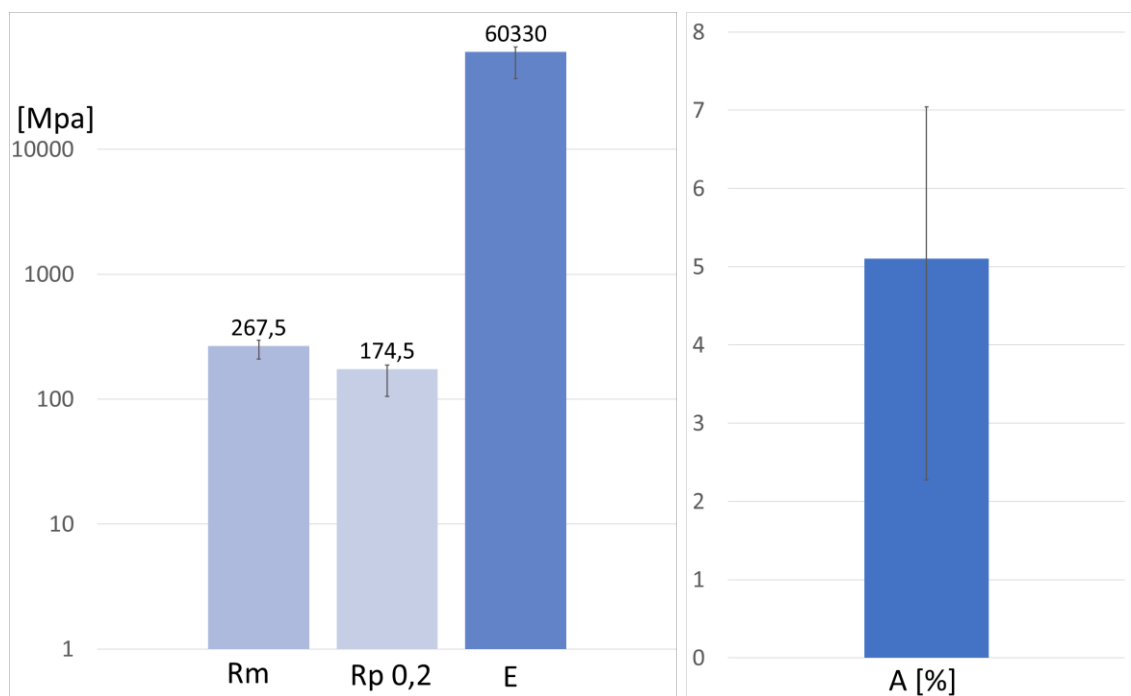


Fig. 3.3.32.5 Rm, Rp, E [Mpa] -logarithmic scale- & A [%]

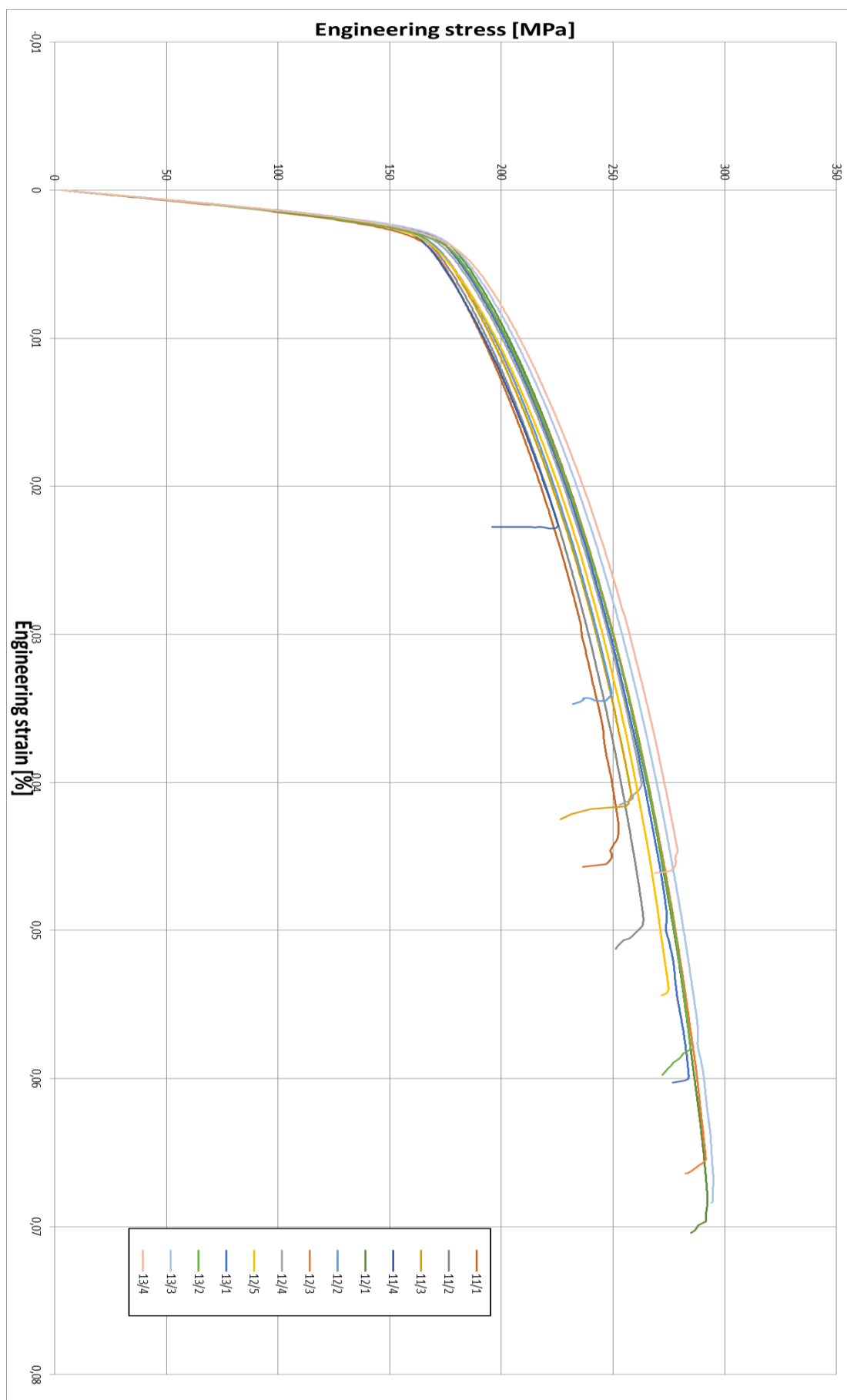


Fig. 3.3.32.6 Chip C engineering stress-strain diagram

CHIP B + C EXTRUDATES (mixture of 50% chip B and 50% chip C):

Mixing chip C and chip B the characteristics of the profiles started to improve. The delamination at the edges disappeared and the surface became smoother. The problem of air inclusion on the surface remained, but it went down as amount and grew as size.

In this case is possible to observe that the stress-strain curves assumed intermediate values between chip B and of chip C ones. The scattering of the values became more sensible in term of stress than of strain.



Fig. 3.3.33.1 Chip B + C profile



Fig. 3.3.33.2 Chip B + C profile

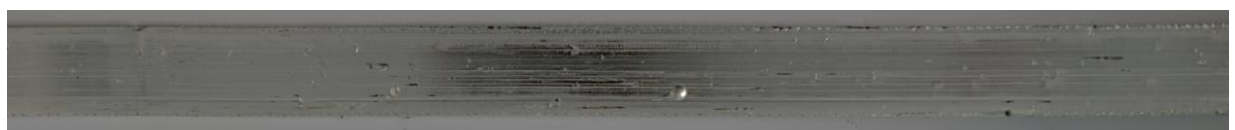


Fig. 3.3.33.3 Best result obtained with chip B + C mixture

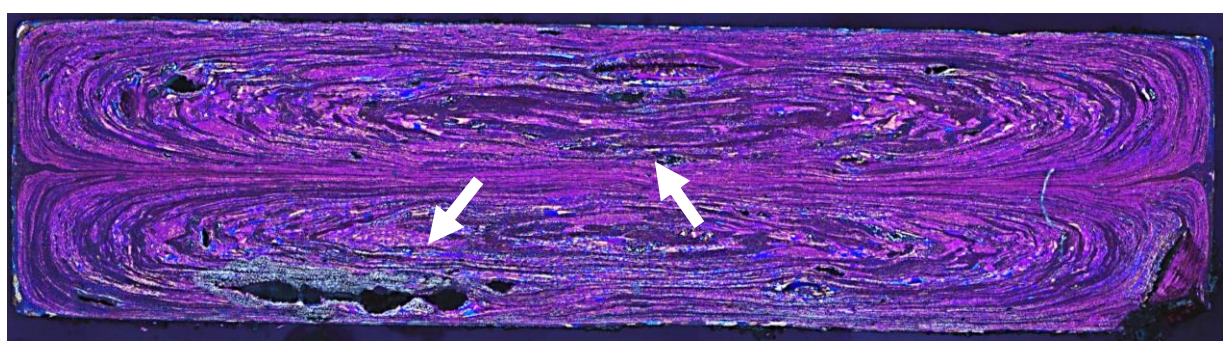




Fig. 3.3.33.4 Chip B + C cross section microscope pictures

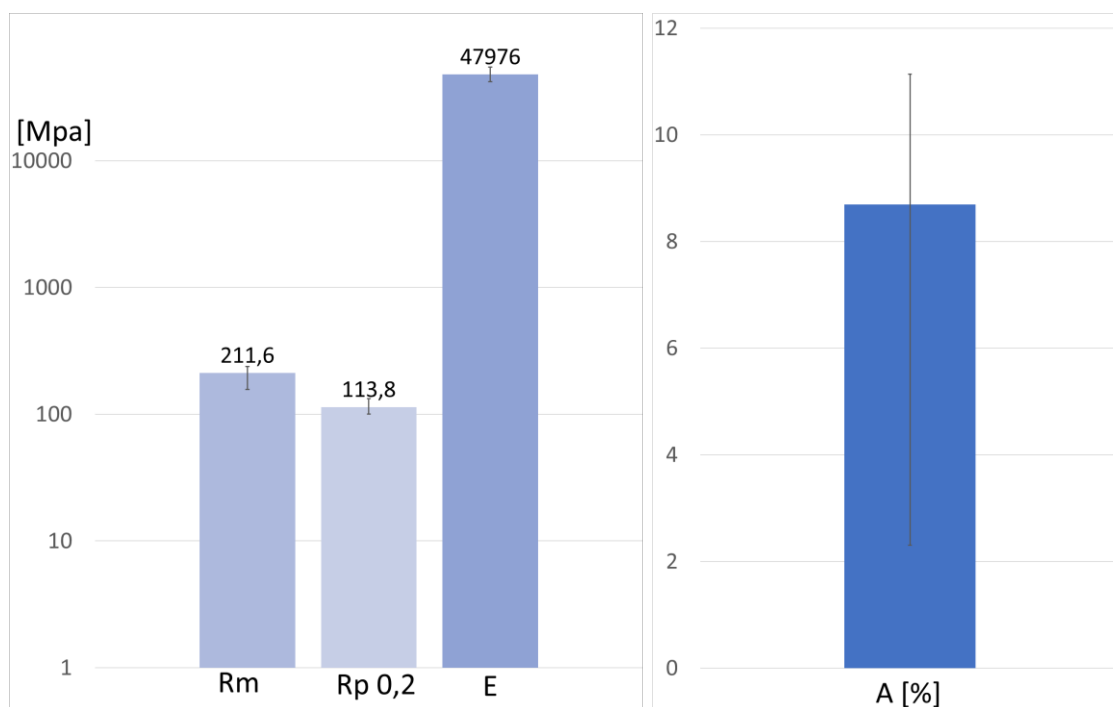


Fig. 3.3.33.5 R_m , R_p , E [Mpa] -logarithmic scale- & A [%]

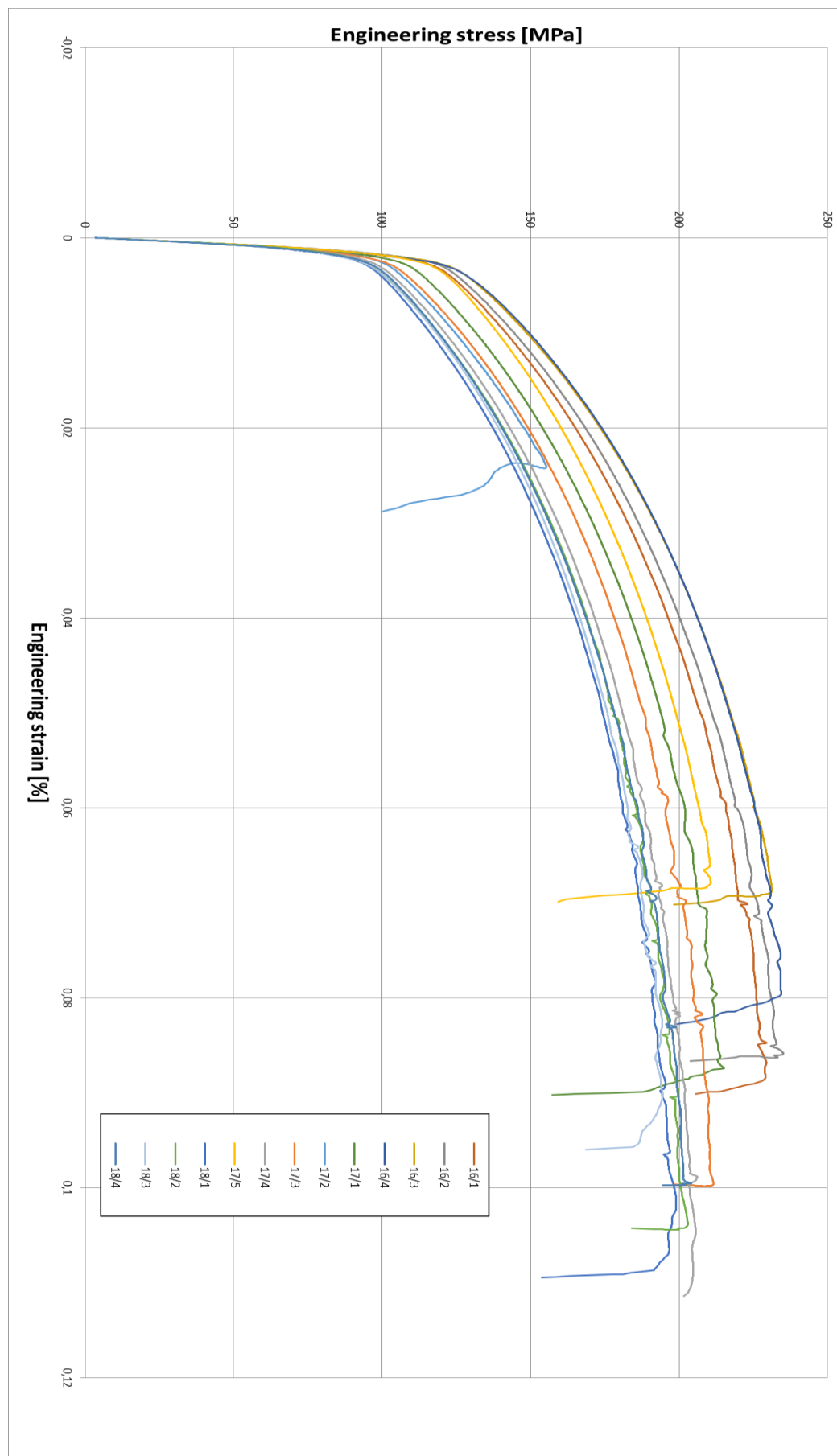


Fig. 3.3.33.6 Chip B + C engineering stress-strain diagram

CHIP A+ B+ C EXTRUDATES (mixture of chips: A 33%, B 33% and C 33%):

The quality still improved compared to the extruded based entirely on chip C. The porosities dropped down and surface became better.

Anyway, the general quality was not sufficient for aesthetic application but enough to structural ones.

The stress-strain diagram found values intermediate between chip B+ C and chip A. The range scattering of the stress-values was one more time bigger.



Fig. 3.3.34.1 Chip A+B +C profile

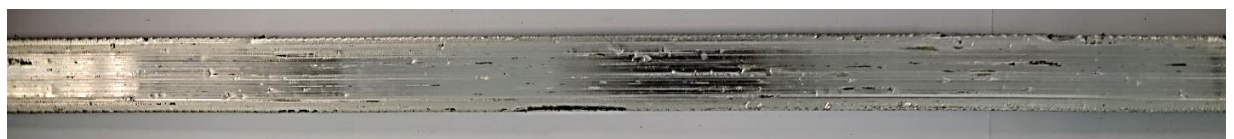


Fig. 3.3.34.2 Chip A+B +C profile



Fig. 3.3.34.3 Chip A+B +C best results

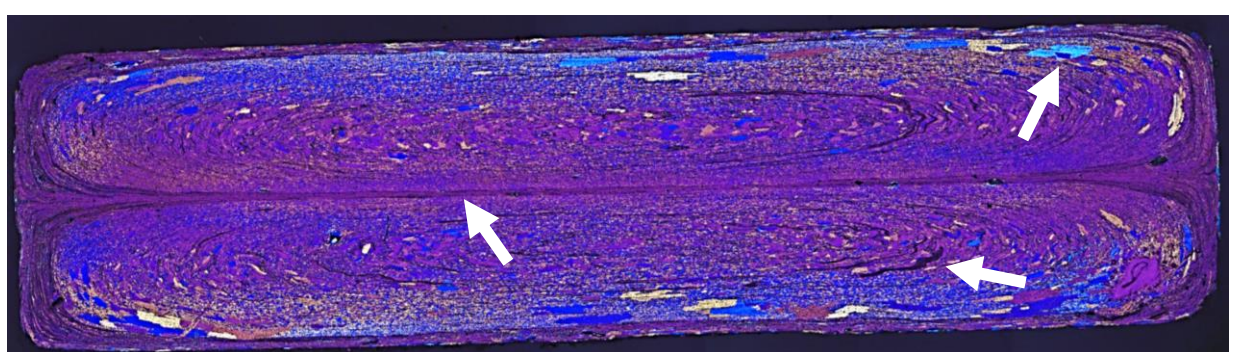




Fig. 3.3.34.4 Chip A + B + C microscope pictures

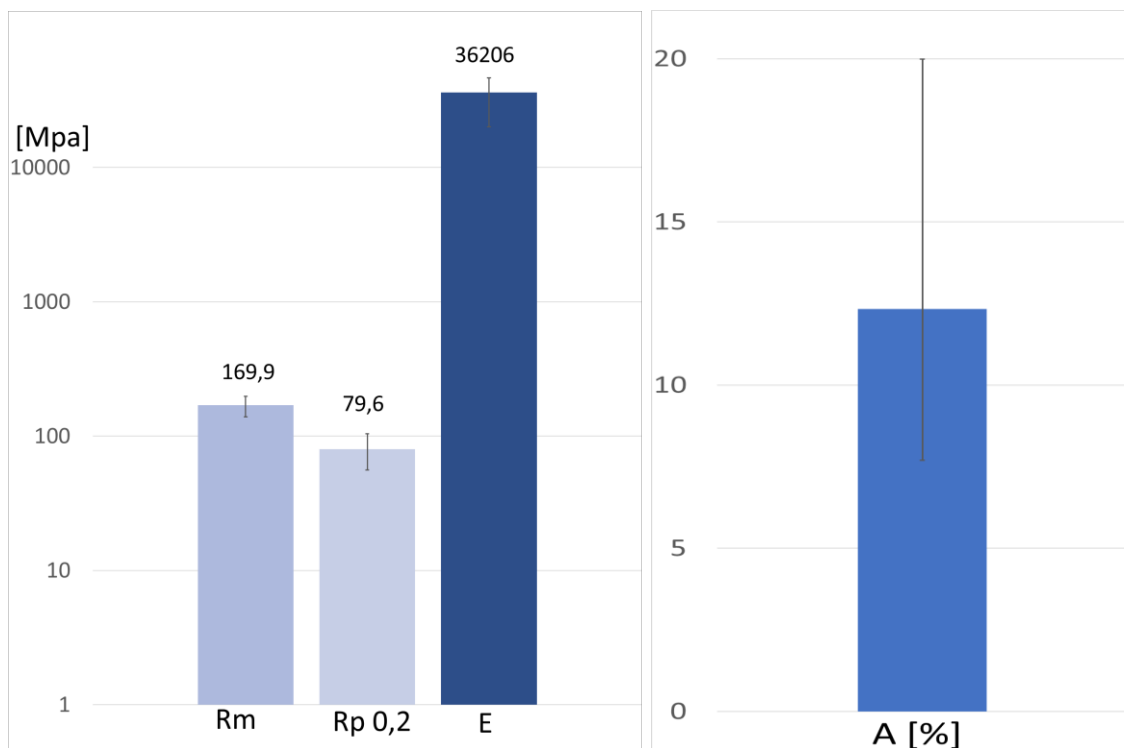


Fig. 3.3.34.5 Rm, Rp, E [Mpa] -logarithmic scale- & A [%]

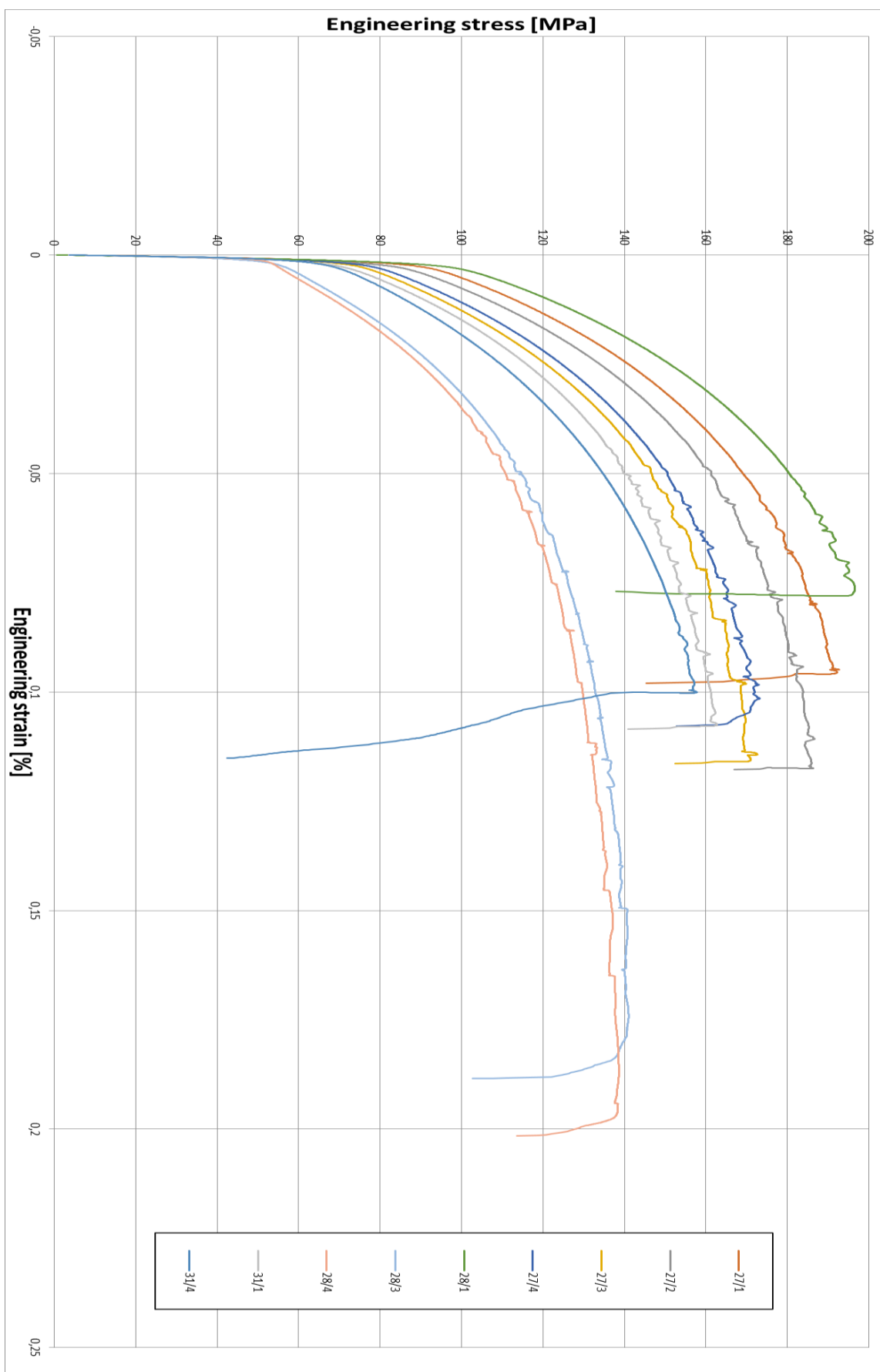


Fig. 3.3.34.6 Chip A + B + C engineering stress-strain diagram

3.3.6 FEM Simulation

During the experimental trials, we have implemented a simulation to validate the results. As starting point we measured our tools and designed the CAD models by CATIA program, both for flat-face and for port-hole dies. We will focus on the port-hole simulation. In figure 3.3.35 & Fig. 3.3.36 are visible respectively the feeder and the assembled die with the welding chamber and bearing path.

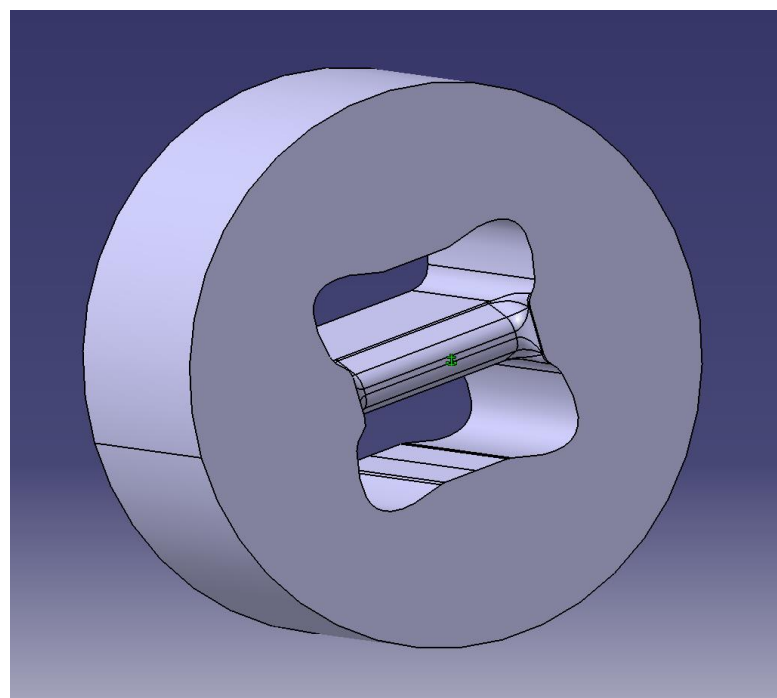


Fig. 3.3.35 The feeder of the port-hole die

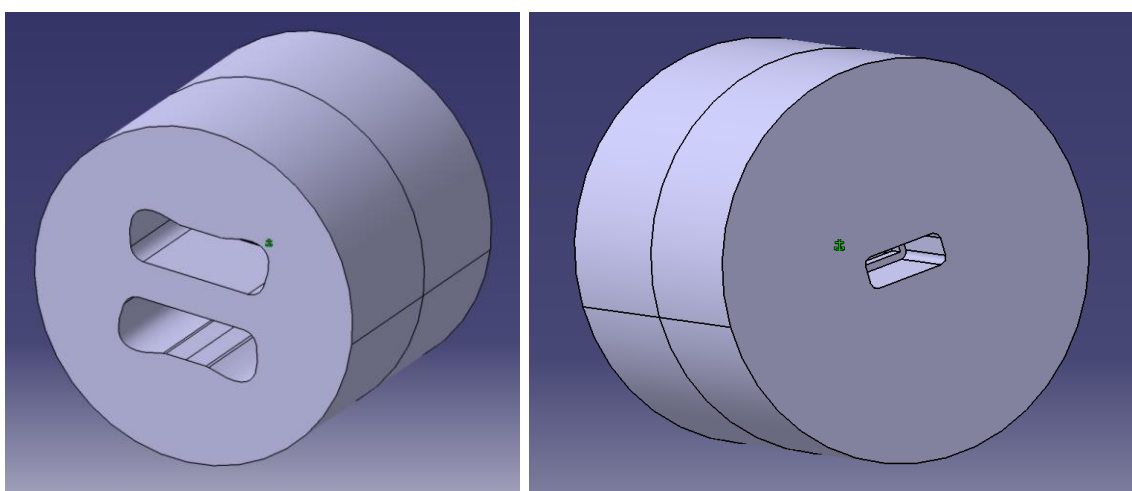


Fig. 3.3.36 The assembly of the port-hole die

With these CAD-geometries, we implemented the simulation of the extrusion process on HyperExtrude. This FEM-program is able to analyse steady-state problems, where a mesh fixed in space (Eulerian) is appropriate, since the process configuration does not change with time. We used a configuration with the same parameters used during the testing:

- Tool temperature: 450°C
- Preheating temperature: 550°C
- Ram speed: 1mm/s
- Container diameter: 66mm
- No lubrication

From the simulation we attained the results shown in the following figures.

The pressure goes from the maximum value, touching the dummy block, to zero at exit of the bearing path.

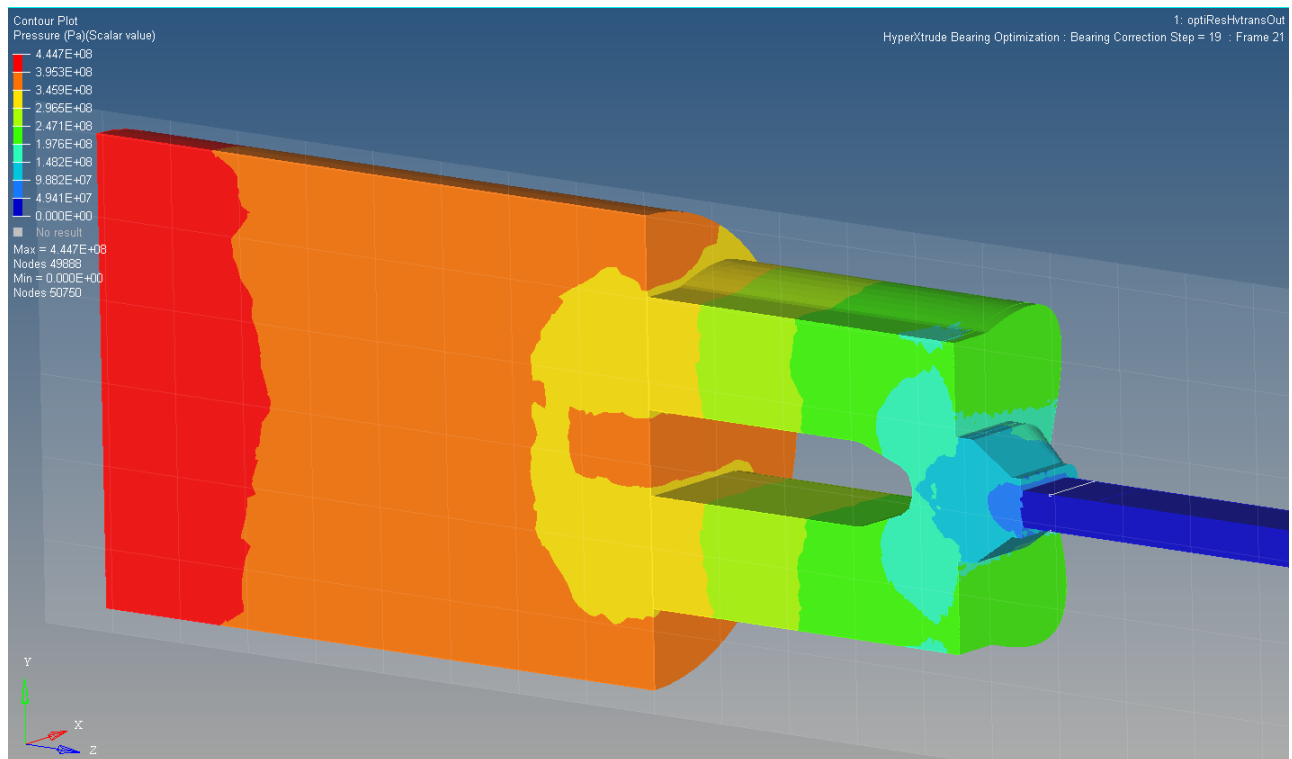


Fig. 3.3.37 The pressure involved in the material during extrusion

The temperature increases because of the friction action during the process and strain involved in the material.

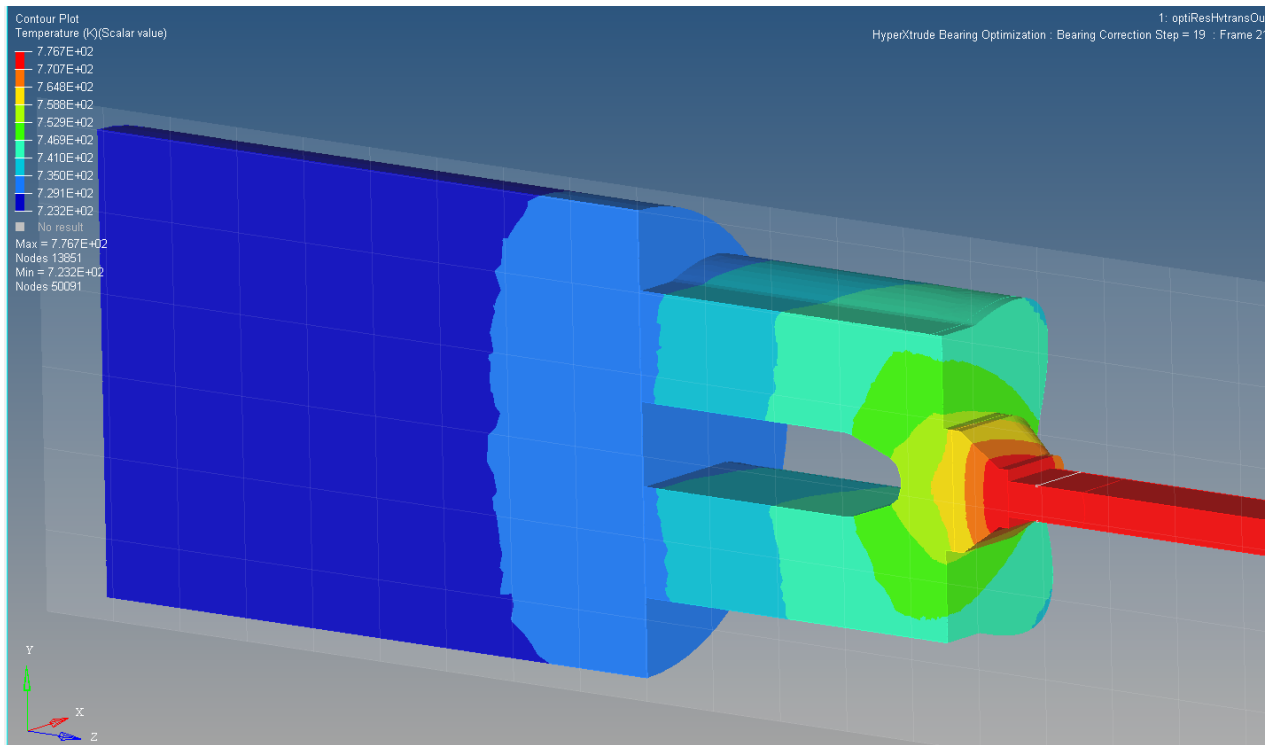


Fig. 3.3.38 The temperature in the material during extrusion

The strain is maximum at the end of the path. It results lower in the core than the external zones.

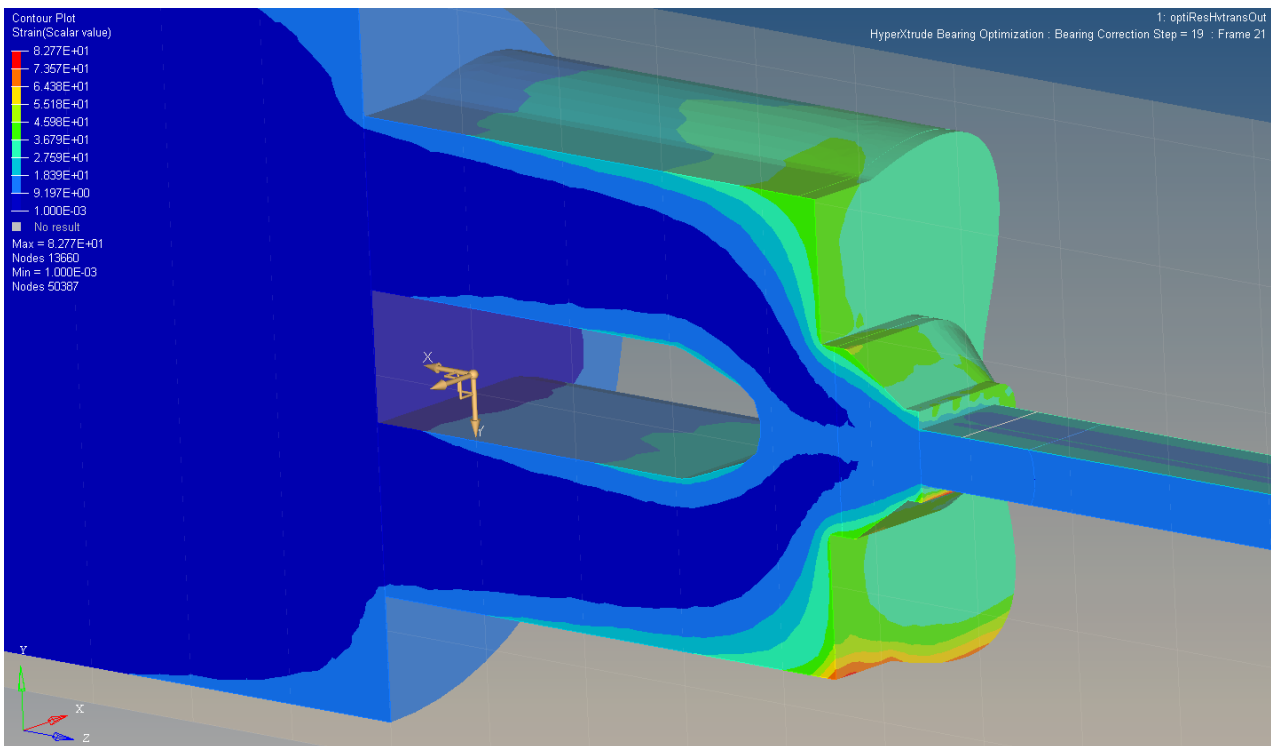


Fig. 3.3.39 The strain affecting the material during extrusion

The stress involved in the process is higher in the point where the deformation of the material is bigger. In fact, in the bearing path it is highest value.

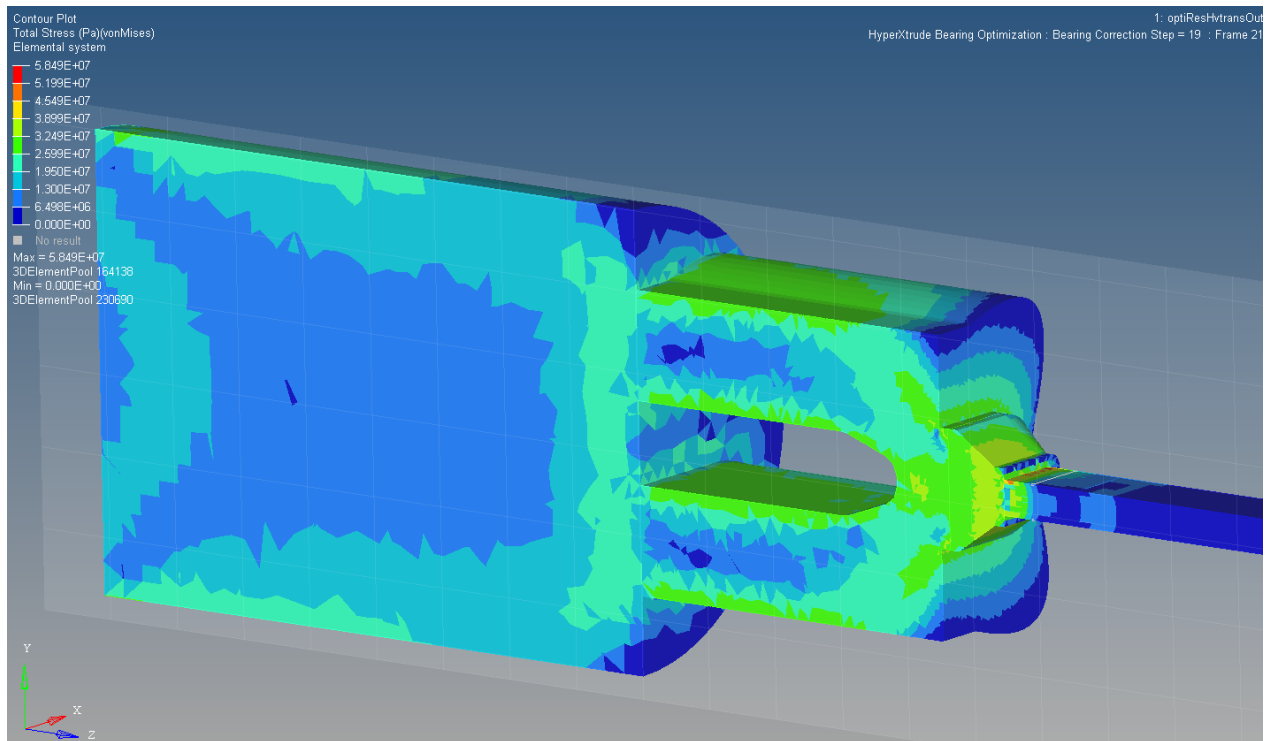


Fig. 3.3.40 The stress in the material during extrusion

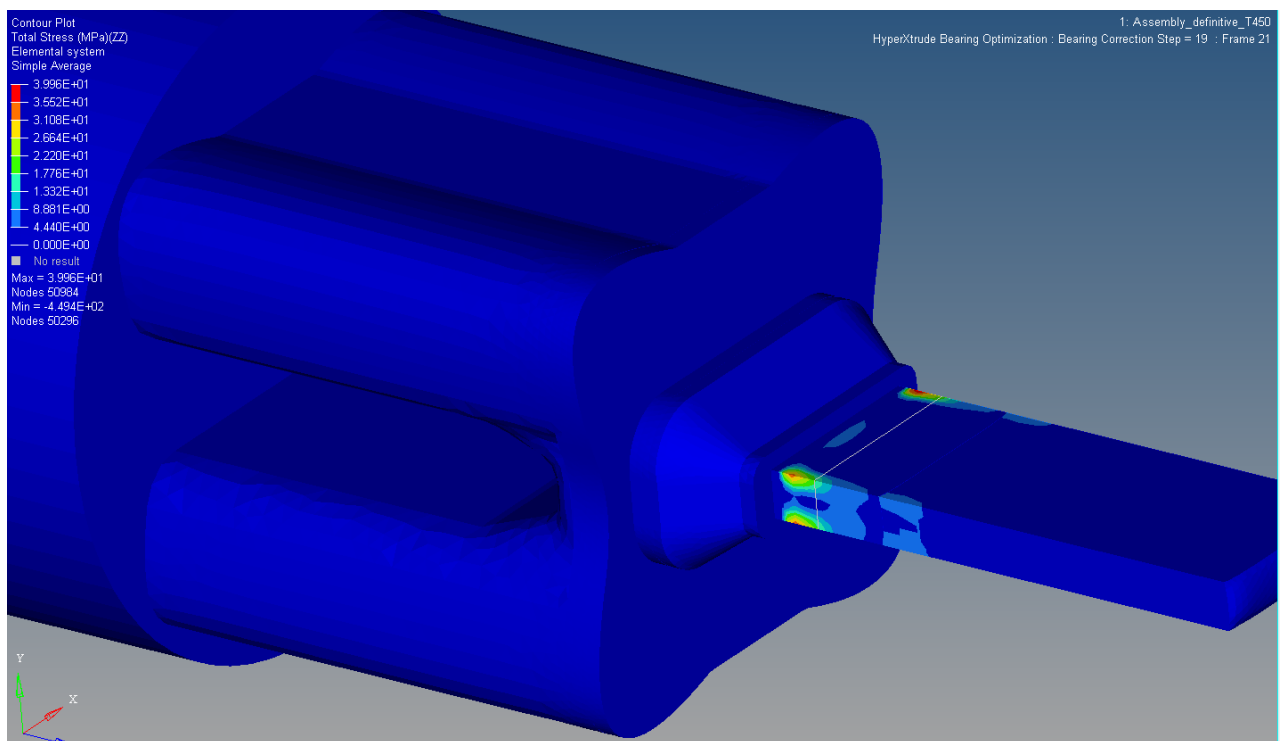


Fig. 3.3.41 The stress affecting the material, focused on the positive values (tensile)

From these tree pictures is possible to see that the stress assumes positive values in the edges of the bearing path. This could be the effect that caused delamination in some profiles, according to experimental trials.

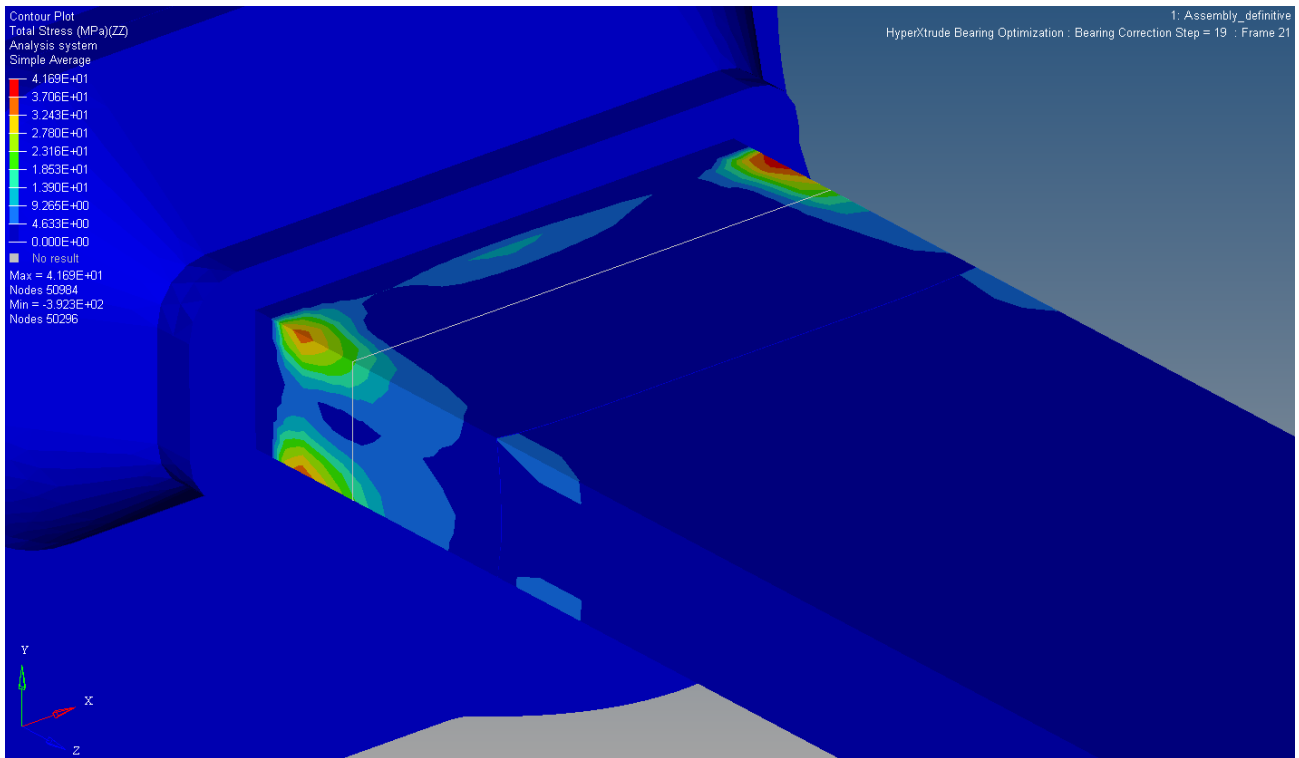


Fig. 3.3.42 The stress affecting the material, focused on the positive values (tensile)

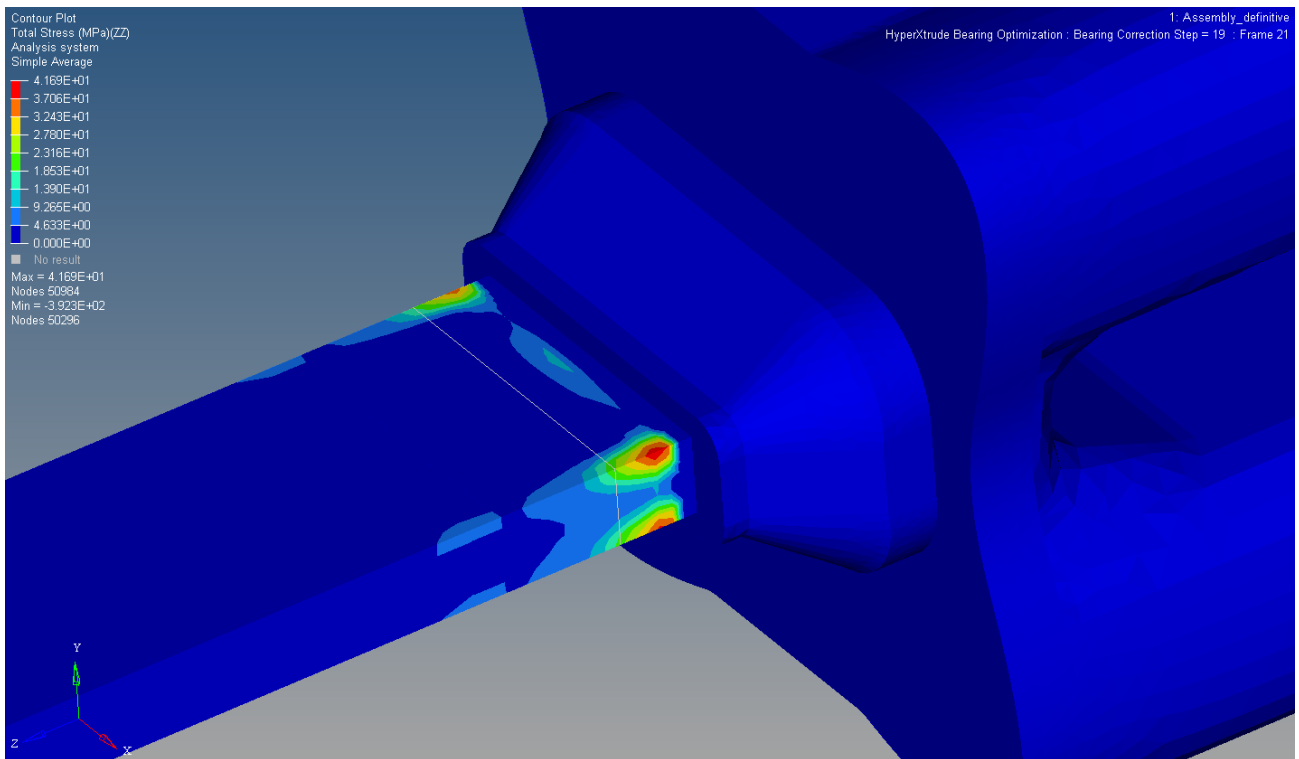


Fig. 3.3.43 The stress affecting the material, focused on the positive values (tensile)

Once run the simulation, we proceeded with a post-processing of the information to validate the criterion required to achieve good sound chip bounding.

We used the Donati and Tomesani longitudinal welding line criterion. It consists in:

$$\frac{1}{m} \sum_{i=1}^l \sum_{j=1}^m \frac{P_{ij}}{\sigma_{ij}} \geq Cost$$

Where:

- m: elements
- l: path from the back side of the die leg up to the die exit
- P: contact pressure
- σ : effective stress

We used a MatLab code which examines the values coming from HyperExtrude simulations to validate the numerical model. The program starts the research from the end of the extruded profile and goes backward trying to find the way where each selected point comes from. It evaluates, point by point, the numerical model proposed with a given step.

We have chosen some significant point from the cross section to make the calculation faster.

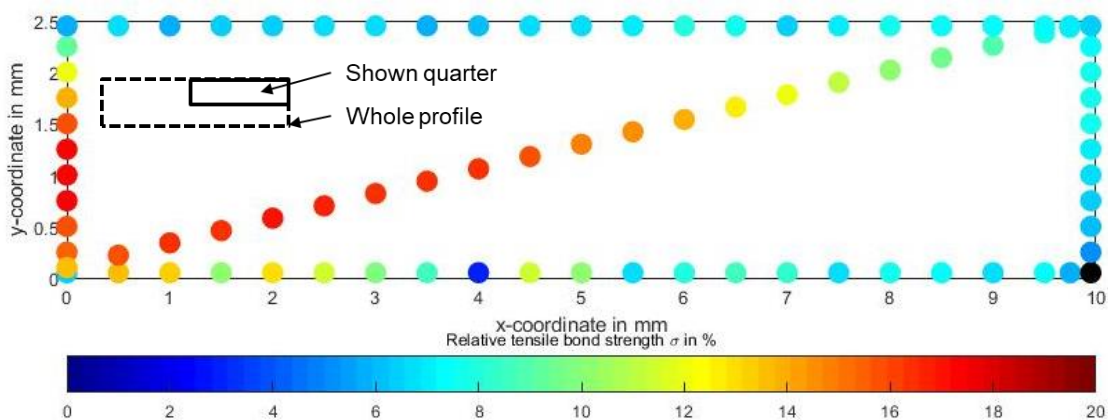


Fig. 3.3.44 The cross-section points chosen for estimation and their results on the final plan

In this plane is visible that the values coming from the numerical model are comparable with the experimental ones, where on the surface the values go down leading to lower quality.

We obtained the outcomes in the following images:

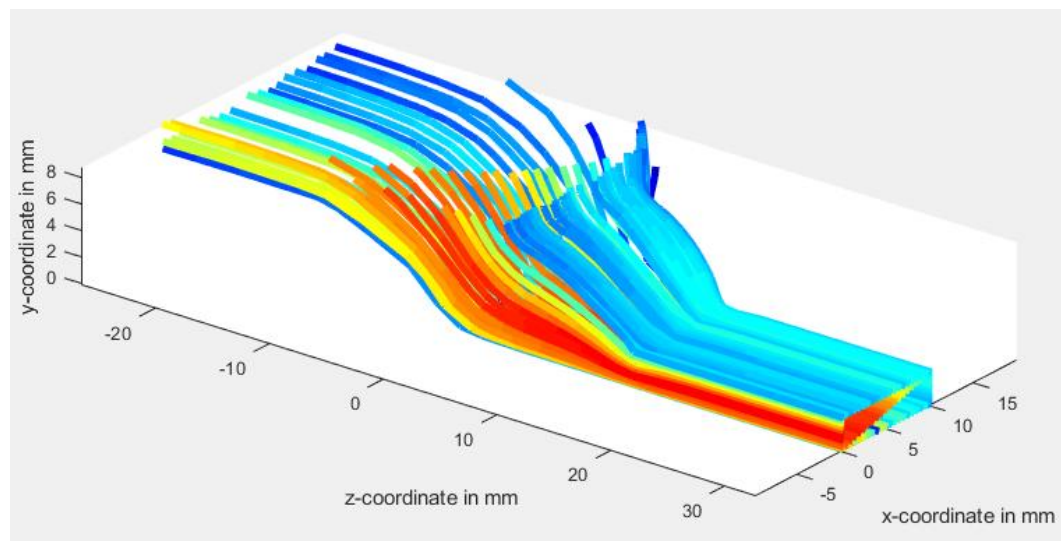
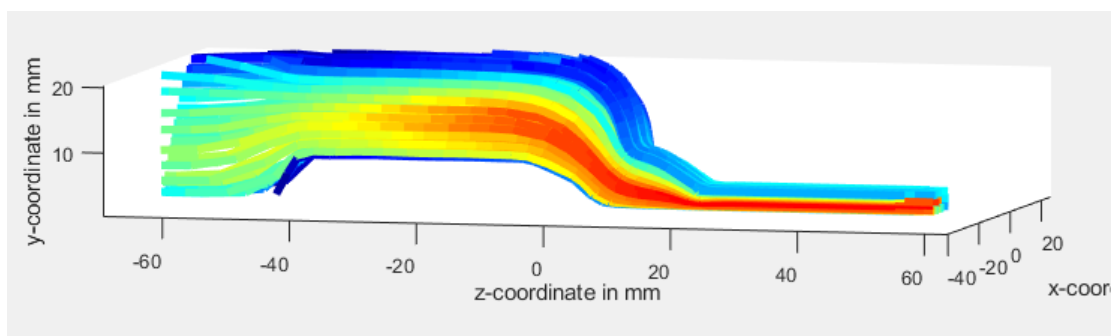
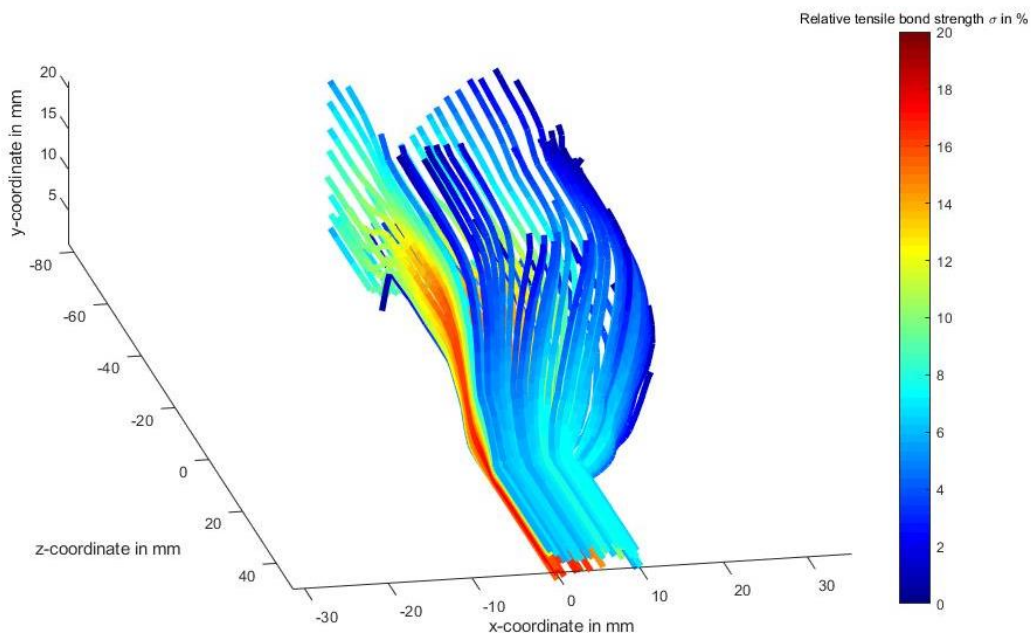


Fig. 3.3.45 MatLab 3D plots with the values of numerical model

After the port-hole die simulation, we implemented the flat-face die FE-Analysis to evaluate the effect of the die design on the extrusion results. We advanced in same way, finding comparable results.

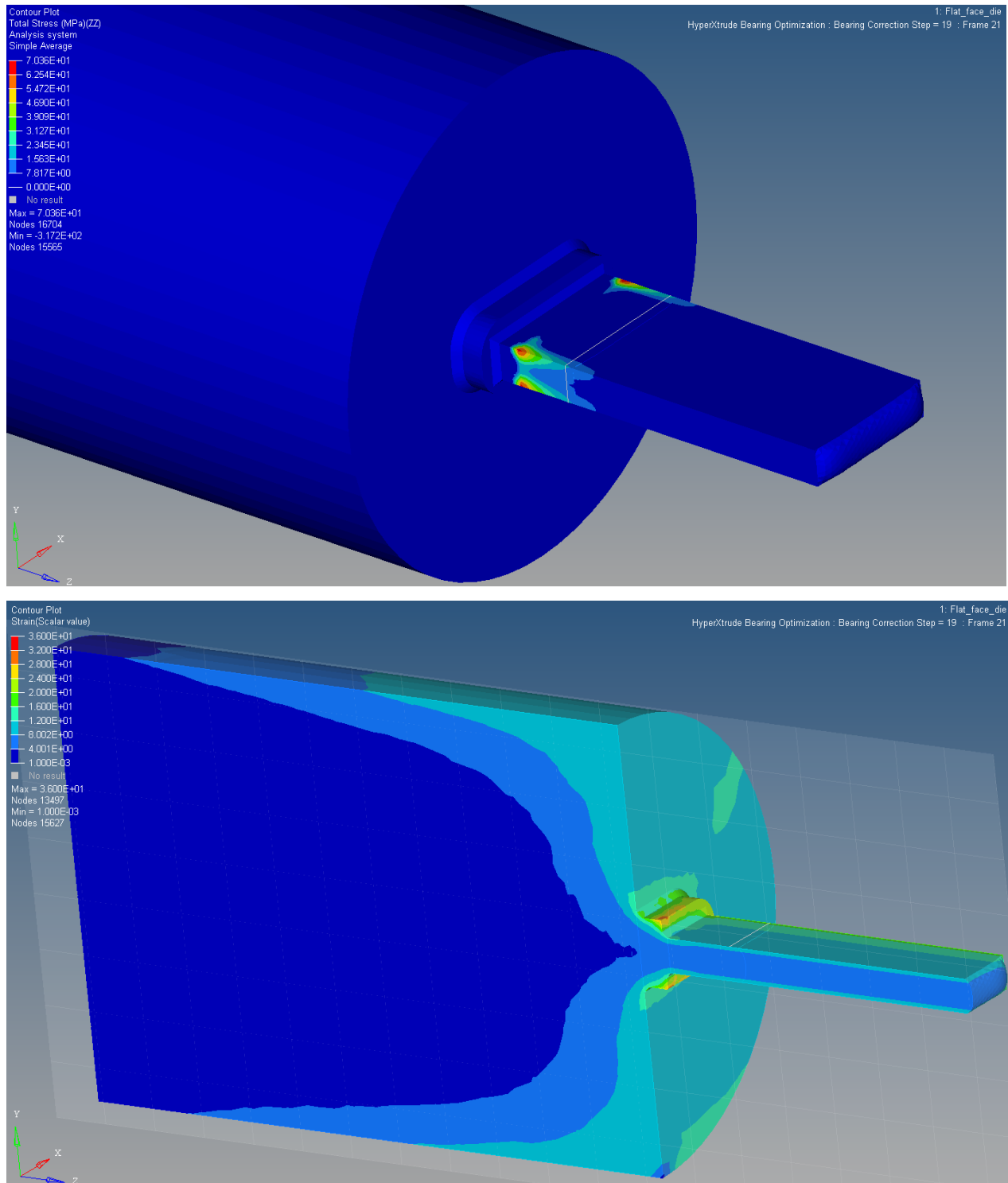


Fig. 3.3.46 HyperExtrude flat-face die simulation

The black dots in the numerical simulation are points where the code was not

able to evaluate a definite path where the material was coming from. It could be because the program crashes in proximity of the edge.

The values are lower than pothole die ones.

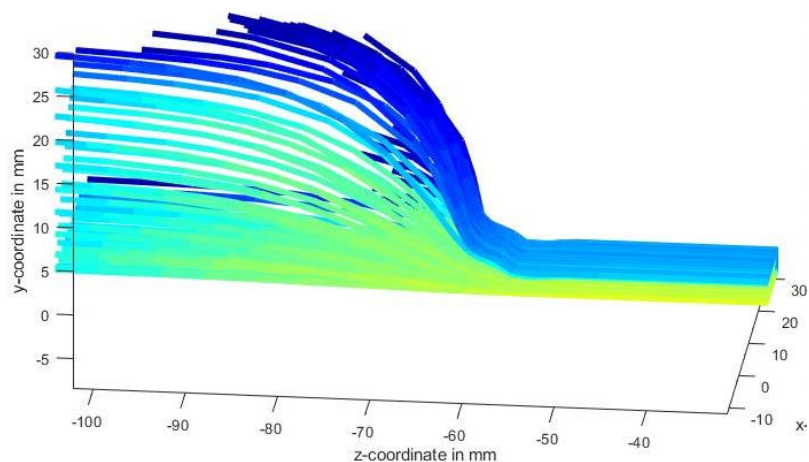
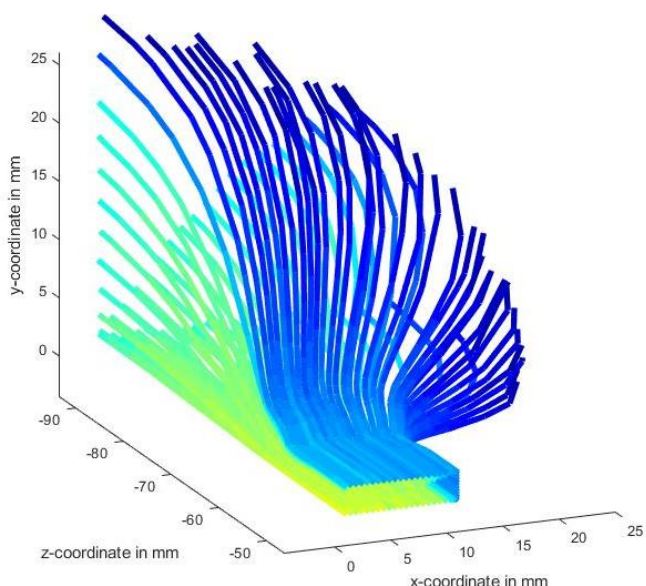
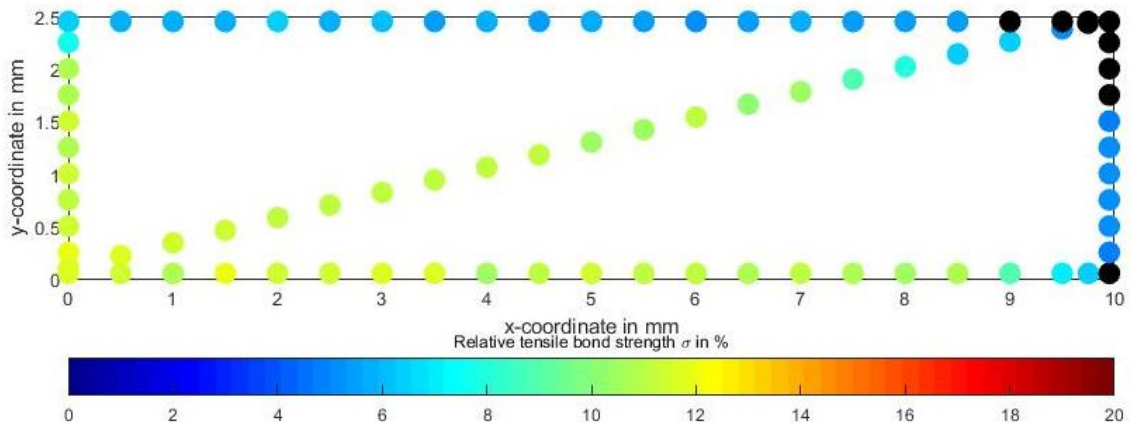


Fig. 3.3.47 MatLab 3D plots with the values of numerical model for the flat-face die

4.1 Outcomes analysis & Conclusions

In conclusion we can assume that is possible to extrude billets composed by different chips, concerning shape and alloy, obtaining useful components. Mixing different alloys and chips with different size, thus various amount of oxides, lead to intermediate values if the materials are mixed in the same proportion.

In the diagram below, is observable one stress-strain median curve for every kind of billets processed. Curves of mixed materials have average values both in stress and in strain direction, consequently average elongation and maximum stress involved during the tensile test.

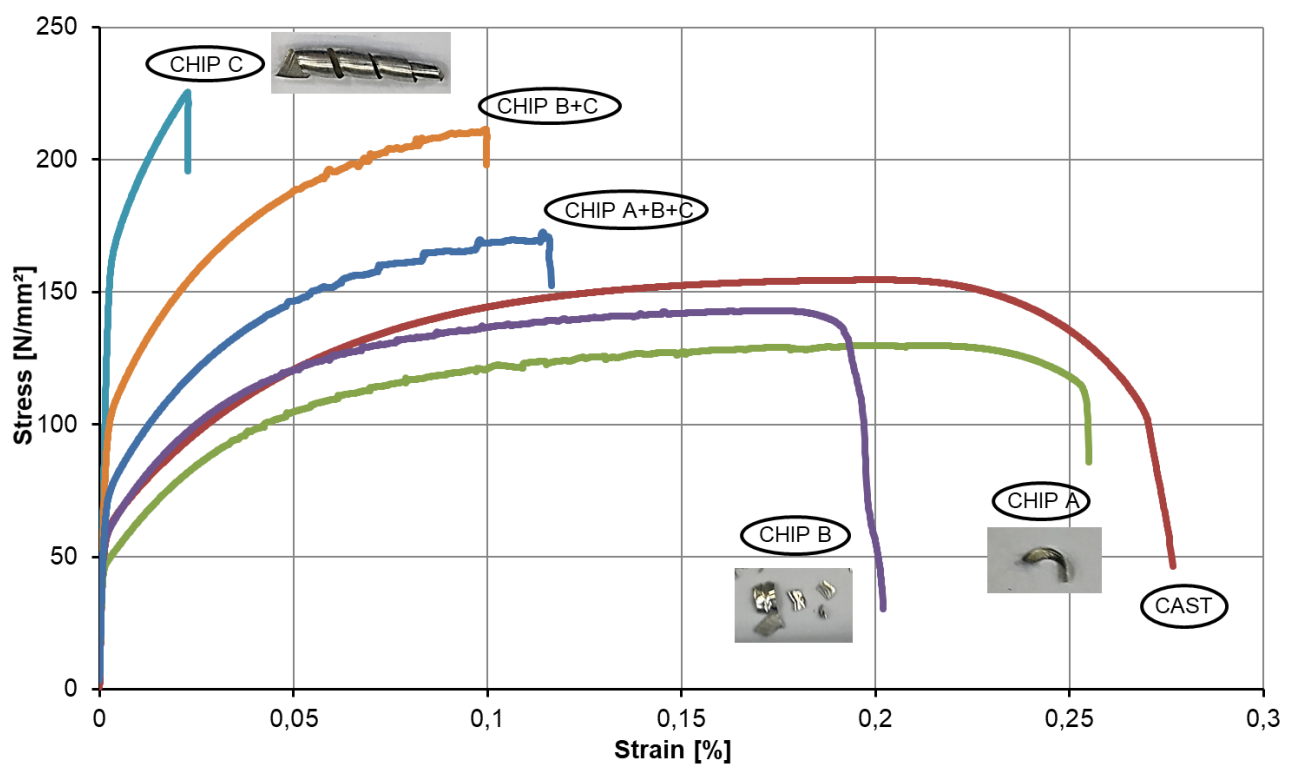


Fig. 4.1.1 Engineering stress-strain curves compared

In the following page is possible to see some average values, and their diffusion. Is noticeable that the hardness values follow the strength trend of the tensile test, with a high scattering due to the discontinuous characteristics on the surface and the mixed chips inside.

From the Young Modulus (E) diagram appears that the mixed profiles have lower E modulus compared to both the materials which they are composed by. This is

a consequence of the lower chip bounding between chips which leads to porosities, thus lower E modulus.

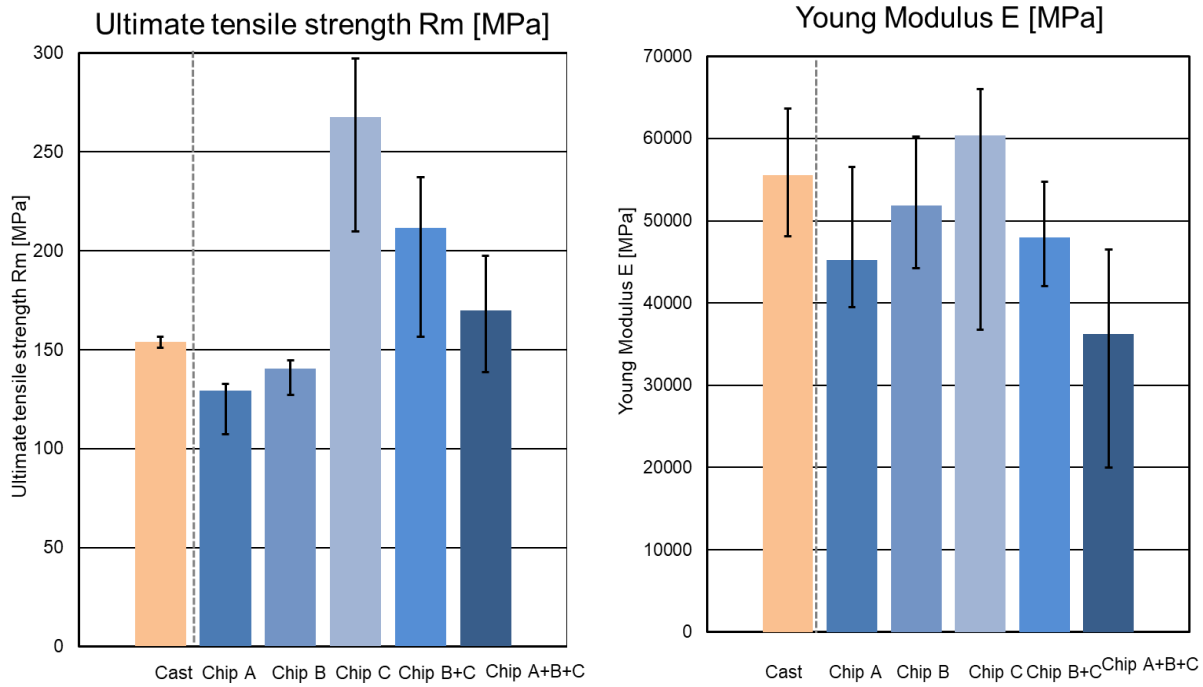


Fig. 4.1.2 Ultimate tensile strength and Young Modulus diagrams

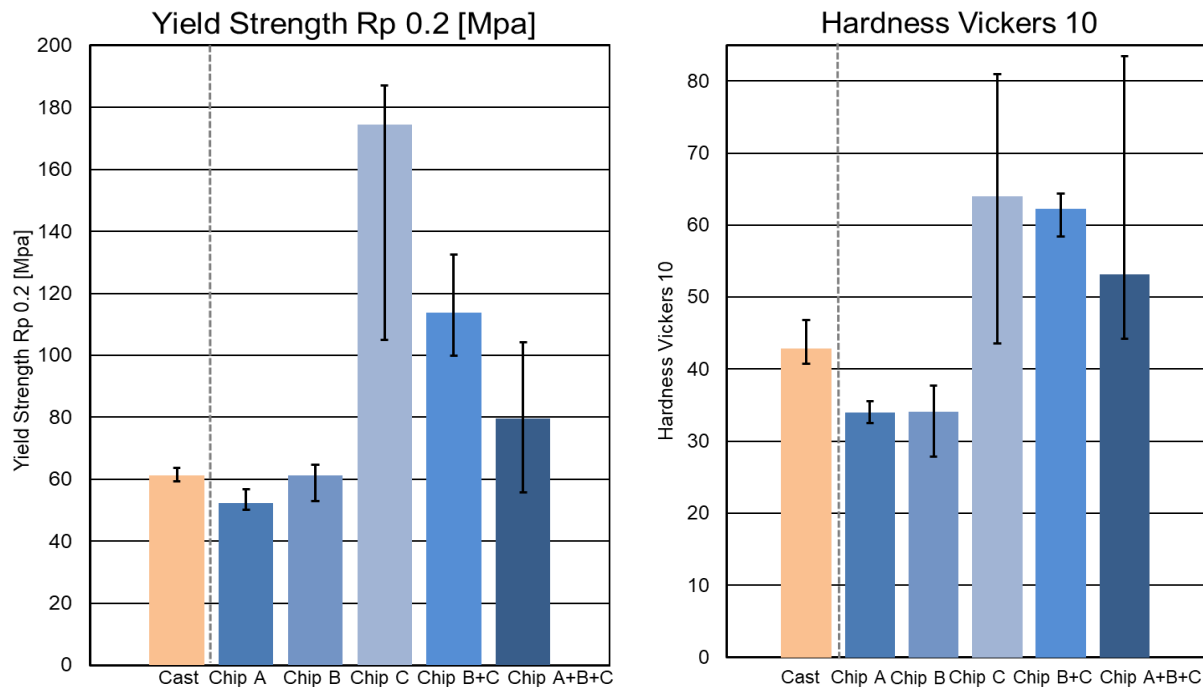


Fig. 4.1.3 Yield strength 0.2 and Hardness Vickers 10

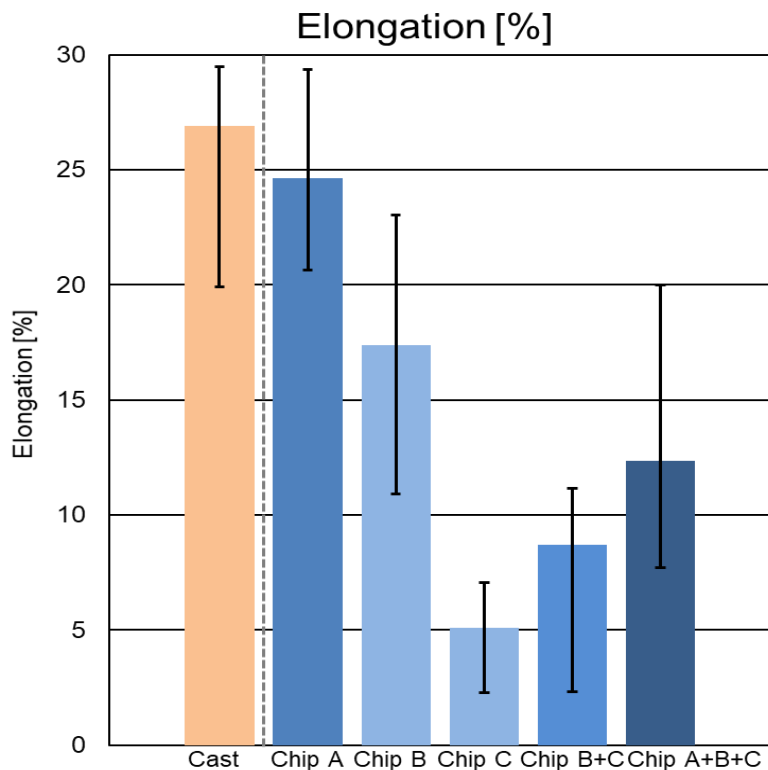


Fig. 4.1.4 Elongation in percentual

We advanced extrusion with the flat-face die, with the same process parameters used in the previous testing, and the results were comparable to the port-hole die ones in term of aesthetic quality, unless some part where appeared peeling effect (Fig. 4.1.5).



Fig. 4.1.5 The peeling effect appeared in profile extruded by flat-face die

The extrudates quality was also affected by the Stick-slip effect. It was appeared because the velocity of the ram was too slow, and the aluminium attached on the bearing path influencing the surface quality as shown in figure 4.1.6. This

demonstrate that the process parameters influence considerably the results and they have to be optimized for every kind of material processed.



Fig. 4.1.6 The imprint on some profiles of the bearing part of the die

5.1 Outlooks

The are several prospective for this research.

First, we should complete the analysis of the flat-face die extrudates with tensile, hardness and microstructure tests.

Overall, there are different ways to be undertaken:

- Prepare chips by cast material optimized for direct extrusion and compare results with industrial chips.
- Investigate the parameters which leads to low quality profiles.
- Change the process parameters to improve outcomes.
- Try second-stage manufacturing process to improve the profiles quality.
- Evaluate the effect of the contact of different materials extruded together (i.e. steel and aluminium).
- Evaluate the effect of the pressure at high temperature on the air inside the profiles.
- Evaluate the chips welding by electronic microscope investigation.

References

- [1] Ma, Xiao, *Surface quality of aluminium extrusion products*, PhD Thesis, University of Twente, Enschede, the Netherlands, February 2011
- [2] <https://www.admet.com/effect-specimen-geometry-tensile-testing-results/>
- [3] <http://www.juancorp.com/aluminium-bar-be-bd-extrusion.html>
- [4] https://www.bonlalum.com/education/aluminum_extrusion_process.shtml
- [5] *Guide to Nickel Aluminium Bronze for Engineers*, Ivan Richardson, edited by Carol Powell, Copper Development Association Publication No 222, January 2016.
- [6] *Manufacturing, Engineering & Technology*, Fifth Edition, by Serope Kalpakjian and Steven R. Schmid. ISBN 0-13-148965-8. © 2006 Pearson Education, Inc., Upper Saddle River, NJ.
- [7] *J. Eng. Mater. Technol* 136(2), 021002 (Jan 17, 2014) (8 pages), *Effect of Cooling Rate on Mechanical Properties of 7075 Aluminum Rods Extruded in Semisolid State*.
- [8] Pradip K. Saha, *Aluminum extrusion technology*, ASM international.
- [9] <https://medium.com/@roger87smith/extruded-aluminium-is-much-better-alternative-to-copper-and-steel-19624bd58850>
- [10] S. Kalpakjian, S. R. Schmid, *Manufacturing engineering and technology*, sixth edition.
- [11] ASTM international, *Standard Test Methods for Tension Testing of Metallic Materials*.
- [12] L. Donati, L. Tomesani, B. Reggiani, C. Bandini, *Microstructure Evolution and Streak Formation Mechanisms*, University of Bologna, DiN Department of Engineering for Industry
- [13] <https://pocketdentistry.com/17-wrought-metals/>
- [14] <http://practicalmaintenance.net/?p=1164>
- [15] A.E. Tekkaya, M. Schikorra, D. Beckera, D. Biermannb, N. Hammerb, K. Pantkeb, *Hot profile extrusion of AA-6060 aluminum chips*, *journal of materials processing technology* 209 (2009) 3343–3350.
- [16] M. Haasea, N. Ben Khalifaa, A.E. Tekkaya, W.Z. Misiolek, *Improving mechanical properties of chip-based aluminum extrudates by integrated extrusion and equal channel angular pressing (iECAP)*, *Materials Science and Engineering A* 539 (2012) 194–204.
- [17] V. Güley a,n, A.Güzel a, A.Jäger a, N.BenKhalifa a, A.E.Tekkaya a, W.Z.Misiolek

- b, *Effect of die design on the welding quality during solid state recycling of AA6060 chips by hot extrusion*, *Materials Science&Engineering A* 574 (2013) 163–175.
- [18] A. GÜZEL, *Microstructure evolution during thermomechanical multi-step processing of extruded aluminium profiles*, Institut für Umformtechnik und Leichtbau, Technische Universität Dortmund.
- [19] Matthias Haase, *Mechanical properties improvement in chip extrusion with integrated equal channel angular pressing*, Institut für Umformtechnik und Leichtbau, Technische Universität Dortmund.
- [20] Harald U. Sverdrup, Kristin Vala Ragnarsdottir, DenizKoca, *Aluminium for the future: Modelling the global production, market supply, demand, price and long term development of the global reserves*. *Resources, Conservation and recycling* 103 (2015) 139–154.
- [21] Wojciech Z. Misiolek, Matthias Haase, Nooman Ben Khalifa, A. Erman Tekkaya, Matthias Kleiner, *High quality extrudates from aluminum chips by new billet compaction and deformation routes*, *CIRP Annals – Manufacturing Technology* 61 (2012) 239–242.
- [22] Marco D'Ascenzo, *analisi del comportamento a caldo dell'acciaio AISI-H11 per la stima della vita utile di matrici per estrusione*, DIEM - Dipartimento di Ingegneria delle Costruzioni Meccaniche, Nucleari, Aeronautiche e di Metallurgia, Alma Mater Studiorum, Universita' di Bologna.
- [23] Siti nor azila binti khalid, *mechanical strength of as-compacted aluminium alloy waste chips*, Faculty of Mechanical and Manufacturing Engineering Universiti Tun Hussein Onn Malaysia.
- [24] T. Kloppenborg, M. Schwane, N. Ben Khalifa, A. E. Tekkaya, A. Brosius, *Experimental and numerical analysis of material flow in porthole die extrusion*, 2012 Trans Tech Publications, Switzerland.
- [25] Diego Colombo, Francesco Zanatta, alluminio, processi di produzione innovativi e tecnologie meccaniche, Corso di Metallurgia dei Metalli non Ferrosi.
- [26] Emanuele Di Giacomo, *implementazione di routine per la previsione dell'evoluzione della dimensione del grano durante l'estruzione di profili in lega leggera*, Università di Bologna.
- [27] M. Cavallini, V. Di Cocco, F. Iacoviello, *Materiali Metallici terza edizione*.
- [28] L. Donati, *L'alluminio e le sue leghe*.
- [29] L. Donati, *lucidi corsi di tecnologia meccanica*, a.a. 2016/2017 UniBo.

- [30] Matteo P., *Elementi di meccanica dei materiali e metallurgia*, settembre 2005.
- [31] Luigi Mitrovich, *Lubrificanti Esso-Mobil*, 08/04/2010.
- [32] Lecture from Master of Science in Manufacturing Technology (MMT),
Technical University of Dortmund.
- [33] Aleris, *Aluminum extrusion plant overview*.
- [34] V. Güley, *Recycling of Aluminium Chips by Hot Extrusion*, Dortmund, 2013.
- [35] Ryoichi Chibaa, Tamon Nakamurab,1, Mitsutoshi Kurodac, *Solid-state recycling of aluminium alloy swarf through cold profile extrusion and cold rolling*, a Department of Mechanical Systems Engineering, Asahikawa National College of Technology, 2-2-1-6 Shunkodai, Asahikawa, Hokkaido 071-8142, Japan.
- [36] V. Güley, N. Ben Khalifa, A.E. Tekkaya, *Direct recycling of 1050 aluminium alloy scrap material mixed with 6060 aluminium alloy chips by hot extrusion*, Institute of Forming Technology and Lightweight Construction (IUL), TU-Dortmund.